Practical Electroencephalography (EEG) Applications in Stroke Rehabilitation: towards brain-computer interface (BCI) setup and motor function assessment

By

Xin Zhang

M.Sc.Eng., Southeast University, China, 2013
B.Eng., Shandong University, China, 2009

Thesis Submitted in Partial Fulfillment of
the Requirements for the Degree of
Doctor of Philosophy

in the
School of Engineering Science
Faculty of Applied Sciences

© Xin Zhang 2019

SIMON FRASER UNIVERSITY

Fall 2019

All rights reserved.
However, in accordance with the *Copyright Act of Canada*, this work may be reproduced, without authorization, under the conditions for "Fair Dealing." Therefore, limited reproduction of this work for the purposes of private study, research, criticism, review and news reporting is likely to be in accordance with the law, particularly if cited appropriately.

Approval

Name:	**Xin Zhang**
Degree:	**Doctor of Philosophy (Engineering Science)**
Title:	**Practical Electroencephalography (EEG) Applications in Stroke Rehabilitation: towards brain-computer interface (BCI) setup and motor function assessment**
Examining Committee:	**Chair: Zoë Druick** Professor, School of Communication
	Carlo Menon Senior Supervisor Professor
	Ryan D'Arcy Supervisor Professor
	Sylvain Moreno Supervisor Associate Professor of Professional Practice, School of Interactive Arts and Technology
	Jie Liang Internal Examiner Professor
	Erik Scheme External Examiner Associate Professor, Electrical and Computer Engineering, University of New Brunswick
Date Defended/Approved:	November 4th, 2019

Ethics Statement

The author, whose name appears on the title page of this work, has obtained, for the research described in this work, either:

a. human research ethics approval from the Simon Fraser University Office of Research Ethics

or

b. advance approval of the animal care protocol from the University Animal Care Committee of Simon Fraser University

or has conducted the research

c. as a co-investigator, collaborator, or research assistant in a research project approved in advance.

A copy of the approval letter has been filed with the Theses Office of the University Library at the time of submission of this thesis or project.

The original application for approval and letter of approval are filed with the relevant offices. Inquiries may be directed to those authorities.

Simon Fraser University Library
Burnaby, British Columbia, Canada

Update Spring 2016

Abstract

Electroencephalography (EEG) records electrical brain activity typically in a non-invasive manner. Recent literature has shown its potential in stroke rehabilitation, to actively engage stroke survivors in rehabilitation. In Chapter 3 of this thesis, the problems of EEG applications in stroke rehabilitation were firstly identified with a pilot study. Two main challenges were identified, hindering further application of EEG in stroke rehabilitation training.

One of the challenges is that the BCI involved rehabilitation process is unsatisfying. Three objectives were derived from this challenge. Firstly, at the beginning of all EEG related stroke rehabilitation training, it is both time and effort consuming to go through data collection and model training for every rehabilitation task. Therefore, in Chapter 4 of the thesis, the possibility of using an EEG model from one type of motor imagery (e.g.: elbow extension and flexion) to classify EEG from other types of motor imagery activities (e.g.: open a drawer) was investigated. Secondly, a novel training method was introduced together with a rehabilitation platform in Chapter 5. The results suggested that the proposed methods in this thesis are feasible and potentially effective. Thirdly, the transition of the offline analysis method to an online control method is one of the major factors that affect BCI performance. However, research particularly focused on the method of filtering the prediction of an online classification is scarce. In Chapter 6, two methods of filtering online classification predictions were proposed and evaluated in a pseudo-online classification paradigm, with the EEG data collected from Chapter 5.

The other challenge is related to motor function assessments in rehabilitation. Motor function is generally assessed with standard questionnaire-based assessments. In these assessments, the rater requires the ratee to perform pre-defined movements and gives scores based on the quality of the movements. Therefore, those motor function assessments have inevitable subjective influences on the functional scores. In Chapter 7 of the thesis, the author investigated the possibility of using EEG data to assess motor function. As a preliminary investigation, EEG-based motor function assessments were only investigated for upper-extremity among participants with stroke. The results suggested that EEG data can be used to assess motor function accurately.

Keywords: EEG; stroke rehabilitation; motor imagery; functionality score; online classification

Acknowledgment

I would like to express my gratitude to my senior supervisor, Dr. Carlo Menon, for his support and guidance throughout my Ph.D.

I would also like to thank the members of the MENRVA lab for their help. It's a wonderful experience to work with all of you.

Finally, I would thank my wife and my son, for their unconditional support and accompaniment. Life and research come as a long journey of unrelenting pursuing. I'm lucky to have you on this trip, and you made this secluded adventure colorful.

Table of Contents

List of Tables

List of Figures

List of Acronyms

ANN----------Artificial Neural Network
BCI----------Brain-computer interface
BF control--------BCI and force control
BSI----------Brain Symmetry Index
CNN----------Convolution Neural Network
DAR----------Delta to Alpha Ratio
EEG----------Electroencephalography
ERP----------Event Related Potential
FES----------Functional Electrical Stimulation
FIM----------Functional Independence Measurement
FMA----------Fugl Meyer Assessment
FMMA----------Fugl Meyer Motor Assessment
GM----------General Model
LDA----------Linear Discriminant Analysis
LPS----------Large-scale Phase Synchrony
MI----------Motor Imagery
NI----------National Instrument
NN----------Neural Network
SVM----------Support Vector Machine
VI----------Virtual Instrument
WMFT----------Wolf Motor Function Test

Chapter 1.

Introduction

Stroke has become one of the leading causes of death worldwide, and has also been the main cause of disability for adults [1], [2]. In clinical practice, rehabilitation training has been the primary treatment for motor function loss in stroke survivors [3]–[6]. Currently, rehabilitation training is generally administered in one-to-one sessions between the healthcare professionals and the patients. Therefore, the throughput of the rehabilitation training is limited by the number of healthcare professionals in the facility. Additionally, the full-time involvement of healthcare professionals becomes a big financial burden to the patients [1]. In order to decrease the involvement of healthcare professionals, some research groups have proposed rehabilitation devices, like robots or functional electrical stimulation (FES) devices, that are capable of delivering automated repetitive rehabilitation training for the stroke survivors [7]–[13]. However, some papers suggested that rehabilitation training with passive movements of individual joints was not efficient [4], [6], [14]. The engagement of the patients during the training has been reported to be crucial for better rehabilitation outcomes. Therefore, some studies have introduced EEG into rehabilitation training to investigate the possibility of ensuring the patients' engagement with the rehabilitation protocol [15]–[17]. In addition, some other papers also reported that EEG has the potential to indicate motor function [18], [19], [28], [20]–[27], which implies it might be feasible to use EEG as a bio-marker of motor function recovery for patients with stroke.

Research on EEG and its clinical applications have been going on for decades. However, the application of EEG during rehabilitation still seems preliminary despite its great potential [29]–[31]. In this thesis, two primary obstacles of EEG applications in rehabilitation training were identified. Possible solutions were also proposed and validated with several preliminary studies.

1.1. Motivation

This thesis starts with a pilot study to identify the challenges in EEG applications for stroke rehabilitation. In this pilot study, a rehabilitation training platform is presented with a portable EEG acquisition system based BCI, controlling a lightweight exoskeleton. To use the proposed platform, the user is required to perform motor imagery on the designated protocol, and a BCI system classifies the EEG data to check if the user is focused on the training protocol. If true, assistance from the exoskeleton is activated to help the user complete the protocol. From this pilot study, the author identifies two challenges in the rehabilitation applications for EEG technologies.

One of the challenges is that the current BCI involved rehabilitation is still unsatisfactory. Three objectives are proposed to overcome this challenge.

Firstly, the BCI application setup process consumes a great portion of time in BCI involved rehabilitation training. Typical rehabilitation protocols may contain several training tasks, for example, the Graded Repetitive Arm Supplementary Program (GRASP) [32]. With multiple tasks in one rehabilitation protocol, the BCI setup process in BCI involved rehabilitation training would require data acquisition for every task of the training protocol, which is labor intensive and time-consuming. In order to solve the problem, it is necessary to investigate if there are certain types of motor imageries (MIs) that generate BCI models with higher testing accuracy in other MIs. This is referred to as higher versatility of MIs in this thesis. Using MIs with higher versatility in the BCI setup, the time EEG data acquisition could be minimized. However, to the best of our knowledge, no study has been reported to investigate the versatility of MIs in the literature, and no study has been reported on investigating guidelines for choosing MIs in BCI related rehabilitation applications.

Secondly, the rehabilitation training is still a long, painful and expensive process for most patients with chronic stroke. Some recent papers suggested the utilization of BCI systems in stroke rehabilitation training resulted in better rehabilitation outcomes than passive rehabilitation training, as the active training brought by the BCI systems might have potentially reinforced the motor learning/re-relearning processes [33]–[37]. However, with the utilization of the BCI systems, it is still possible that the patient could have learned to control the BCI system fluently during the rehabilitation training instead

of gaining motor function recovery [38]. In order to lay emphasis on the rehabilitation training and motor function recovery, some researchers suggested combining motor imagery training (provided by BCI) and active physical training (provided by active minimal movement from the patient) in the rehabilitation training protocol [38]. In the combined rehabilitation training, the patients were required to activate BCI control and move to the designated direction at the same time, which internally connects the mental task and physical task together. Therefore, the combined method could potentially further boost motor function recovery [38]. Although there is a need for such a complex rehabilitation training system, no such system has been reported in the literature.

Thirdly, offline EEG analysis methods have been investigated extensively for decades [39]–[43]. The latest EEG offline analysis algorithm was able to distinguish eight class of MIs with very high accuracy (<80%) [44]. Many BCI applications have also been reported in the literature to investigate the performance of BCI control as an extension of the offline analysis [45]–[51]. In the previous literature on actual BCI online applications, the control signal was based on the predictions generated by directly applying the BCI models on the buffered EEG data. The accuracy of those proposed systems was still not satisfactory. Considering the predictions generated by the BCI model directly affects the performance of the BCI application, filtering those predictions has the potential to improve the performance of the BCI systems.

The other challenge is with the motor function assessment process, which is difficult to perform for people without prior experience. One objective is proposed to overcome the motor function assessment challenge in this thesis. The traditional way of motor function assessment is done in one-to-one sessions between the patients and health care professionals. Usually, the examiner requires the examinee to perform designated movements in the assessment protocol and gives scores based on the quality of the movements. The Medical Research Council (MRC) 0-to-5 scale muscle power assessment tool is the common motor function assessment in clinical practice. Other motor function assessments like Fugl-Meyer Assessment (FMA) [52], Wolf Motor Function Test (WMFT) [53], Functional Independent Measure(FIM) [54] and National Institutes of Health Stroke Scale (NIHSS) [55] are common motor function assessments used in the research field. The one-to-one motor function assessments between the healthcare professionals and patients are not completely objective. The proper

administration of those motor function assessments requires experience and professional skills. In the literature, several objective scores calculated from EEG have been reported to correlate with motor function performance. For example, brain symmetry index (BSI) has been reported to correlate with NIHSS score in patients with acute stroke [23]. Delta to alpha ratio (DAR) has been reported to correlate with FIM score in patients with post-acute stroke [26]. Large-scale phase synchrony(LPS) has been reported to correlate with FIM score in patients with post-acute ischemic stroke [28]. These pieces of evidence suggest there is a great potential for translating EEG data into a motor function assessment method. However, there are several limitations of the previous studies. Firstly, the previous studies were done with acute or post-acute populations, it is unknown if those findings could be transferred to a population with chronic stroke. Secondly, the EEG scores for motor function proposed in the literature (like BSI) were not accurate enough to be used to assess motor function. The correlations reported in the literature were still low ($\rho < 0.8$). A more reliable and accurate method is need for EEG to be used as a motor function assessment. Additionally, all the previous EEG scores were either calculated from power spectrum changes in the EEG or calculated from phase information from EEG. With the development of modern artificial neural network (ANN) methods, there is a great potential to combine those inputs from EEG and create a score for accurate and reliable motor function assessment [56], [57].

1.2. Goal and Objectives

In this thesis, the author firstly identifies the potential challenges of EEG applications in stroke rehabilitation through a pilot study. Two challenges are identified about the BCI involved rehabilitation training and motor function assessment. A total number of four objectives are identified:

- Objective 1: Reduce the time for repetitive raw data acquisition by investigating the possibility of using one MI to generate the BCI model and classify other MIs.
- Objective 2: Design and develop a rehabilitation training platform, which assists the user when both mental and physical engagement were detected. The feasibility of the proposed platform with multiple sessions will be investigated.

- Objective 3: Investigate methods of improving online classification performance using biased-classification and moving-average.
- Objective 4: Investigate the feasibility of translating EEG data into an accurate and reliable motor function assessment.

1.3. Outline of the Dissertation

Chapter 2 covers the literature review about the etiology of stroke and stroke rehabilitation. The current role of EEG in stroke rehabilitation is discussed. The common EEG processing methods are also introduced.

In order to identify the challenges of EEG application in stroke rehabilitation, this thesis starts with a pilot rehabilitation study among eight participants with chronic stroke. In this part, a portable BCI controlled exoskeleton system for rehabilitation is designed and developed. The feasibility of a complex portable BCI controlled rehabilitation platform for chronic stroke is investigated in Chapter 3 of this thesis. Two challenges are identified, which are related to the BCI involved rehabilitation and motor function assessment, respectively. In total, four objectives are identified from this pilot study to overcome the challenges identified in Chapter 3. Figure 1.1 summarized the logic flow of this thesis.

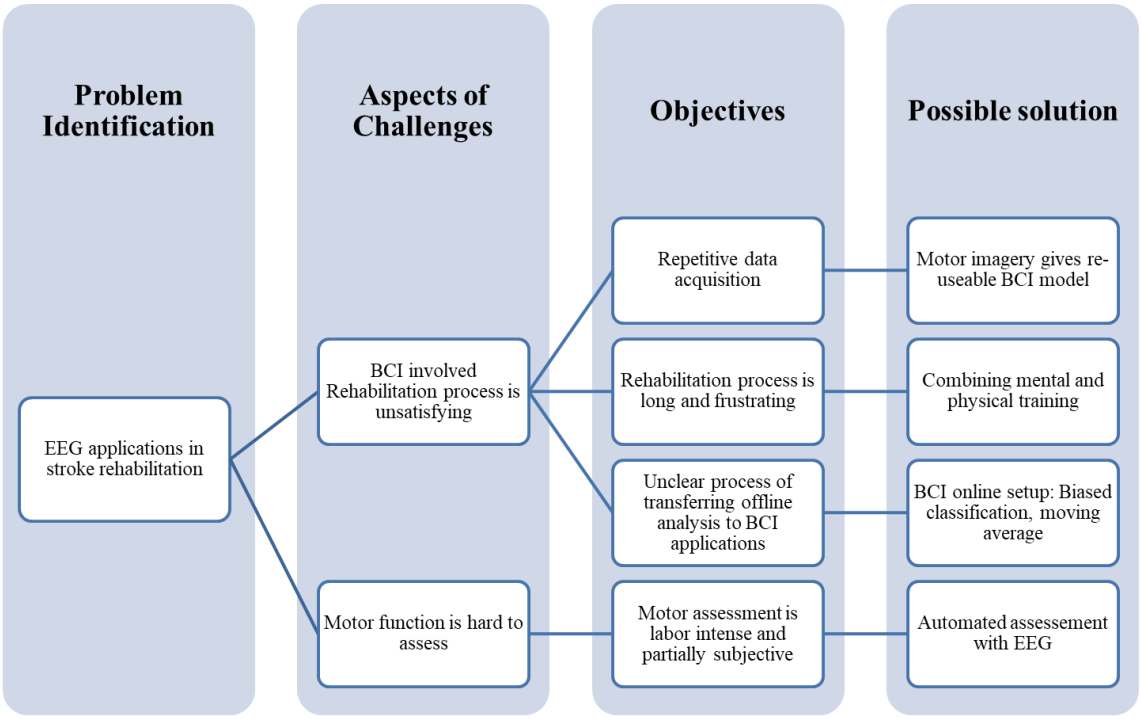

Figure 1.1 The logic flow of this thesis

In Chapter 4 of this thesis, the goal is to investigate which MI task is the most suitable for BCI involved rehabilitation applications. The problem is summarized as an investigation on the guidelines for identifying MI tasks with the highest versatility. In this context, versatility refers to EEG model generated from one specific MI task with high test accuracy for other MI tasks. Twelve healthy participants are recruited for this study. Nine MI tasks centered around the elbow joint are selected. BCI models were tested with intra-task testing and inter-task testing. MIs with higher versatility are identified and possible guidelines for selecting MI tasks in BCI applications in stroke rehabilitation are also summarized. Chapter 4 addresses Objective 1.

In Chapter 5, a portable rehabilitation training platform is designed and fabricated. The proposed platform includes an EEG based BCI system for active training and a robotic/FES device for physical training. A load cell is integrated into the robotic exoskeleton to measure the interactive force between the user and the robotic orthosis. This training platform is designed to combine mental and physical training in rehabilitation for patients with chronic stroke. For the proposed platform, the user is required not only to focus on motor imagery, but to also move to the designated direction, to activate the assistance from the proposed system. A three-level,

progressive training protocol is also designed to support the training platform. One participant with chronic stroke is recruited to participate in this study and go through six weeks of rehabilitation training with the proposed platform. The chapter is included in this thesis to address Objective 2.

In Chapter 6, the author proposes two methods of filtering the predictions from a BCI application (biased-classification method and moving average method). This chapter focuses on binary online BCI classification applications. The proposed methods are validated in a pseudo-online paradigm with EEG data collected from Chapter 5. Performance measures such as accuracy and response delays are summarized. The chapter is included in this thesis to address Objective 3.

In Chapter 7, a configuration of an artificial neural network model is proposed and validated for generating scores to assess motor function with EEG data. The calculated scores are validated with both within-participant test and cross participant test. The proposed method is able to predict the motor function of the participants with chronic stroke, using only EEG data. With the proposed method, the motor function assessment procedures could potentially be automated with minimal intervention from health care professionals. The chapter is included in this thesis to address Objective 4.

A conclusion and future work sections are presented in Chapter 8. The conclusions and scientific findings of the previous chapters are discussed, as well as limitations and possible future work.

Chapter 2.

Literature review

2.1. Stroke etiology

Stroke is caused by either blockage or rupture of brain vessels, which results in low blood supply to certain regions of the brain, and subsequently brain cell death [58]. Based on the cause of the stroke, stroke is categorized into two main categories: ischemic stroke, which is caused by blockage of the brain blood vessels, or hemorrhagic stroke, which is caused by rupture of the brain blood vessels. According to the literature, the majority of strokes are ischemic (about 87%), the rest are hemorrhagic [59] [60]. An illustration figure for the cause of the two stroke categories is shown in Figure 2.1.

Stroke causes damage directly to brain cells. Therefore, the consequences of stroke are usually severe. Stroke has been one of the most common causes of death. When patients survive, they usually suffer from permanent impairments, such as problems with controlling or sensing one side of the body, impaired cognition and language abilities, or sometimes impaired vision on one side [59] [59]. Therefore, stroke has also been reported to be one of the most common causes of disability for adults [1], [2], [61]–[63]. Among all disabilities caused by stroke, motor function impairment is the most common one, which greatly deteriorates the stroke survivors' quality of life [64]. According to the literature, the severity of the stroke does not necessarily correlate with the severity of motor function impairment [65], [66].

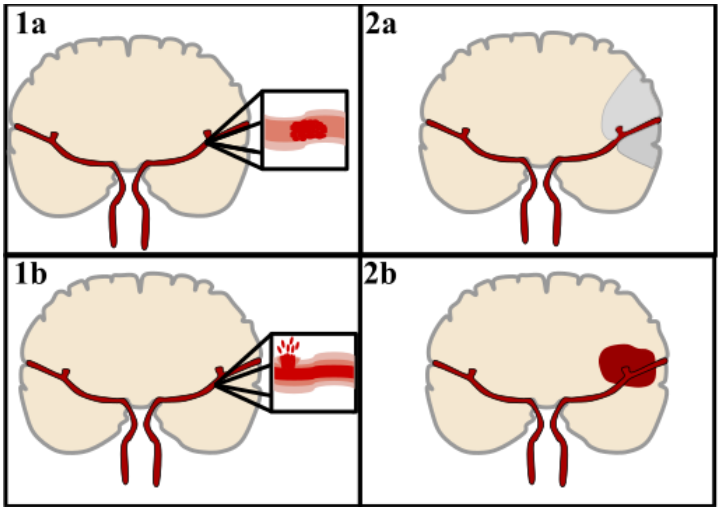

Figure 2.1 **An Illustration of ischemic stroke (top), and hemorrhagic stroke (bottom). This picture was reproduced from Elinor Hunt** [67] **with permission.**

2.2. Stroke rehabilitation for motor function

Stroke has become one of the leading healthcare problems for modern society [1], [2]. Even if patients managed to survive the stroke, they usually suffer from permanent disabilities for the rest of their lives [1], [2], which subsequently affects the patients' ability to live independently [68]. Motor function impairments usually persist, but motor function, even in chronic stroke survivors, may improve through intervention [68]. Rehabilitation training is currently the common option for motor function recovery, which is labor intensive and expensive. A hypothetical pattern of motor function recovery is shown in Figure 2.2. The rehabilitation training and motor function recovery process are usually long and frustrating for stroke survivors, which limits the patients from actively participating.

In clinical practice, rehabilitation of motor function in stroke survivors requires healthcare professionals to assist the patients with designated training protocols with a high number of repetitions. More recent literature suggests that rehabilitation training has better outcomes if those designated training protocols are goal oriented (context specific) [65], [66], [69]. Although the patients may gain some motor function improvement through rehabilitation training, there is no solid evidence to support that rehabilitation training results in neural repair in the brain for human subjects. [70]

Instead, the majority of papers in the rehabilitation field support the fact that functional recovery is based on compensatory mechanisms [70].

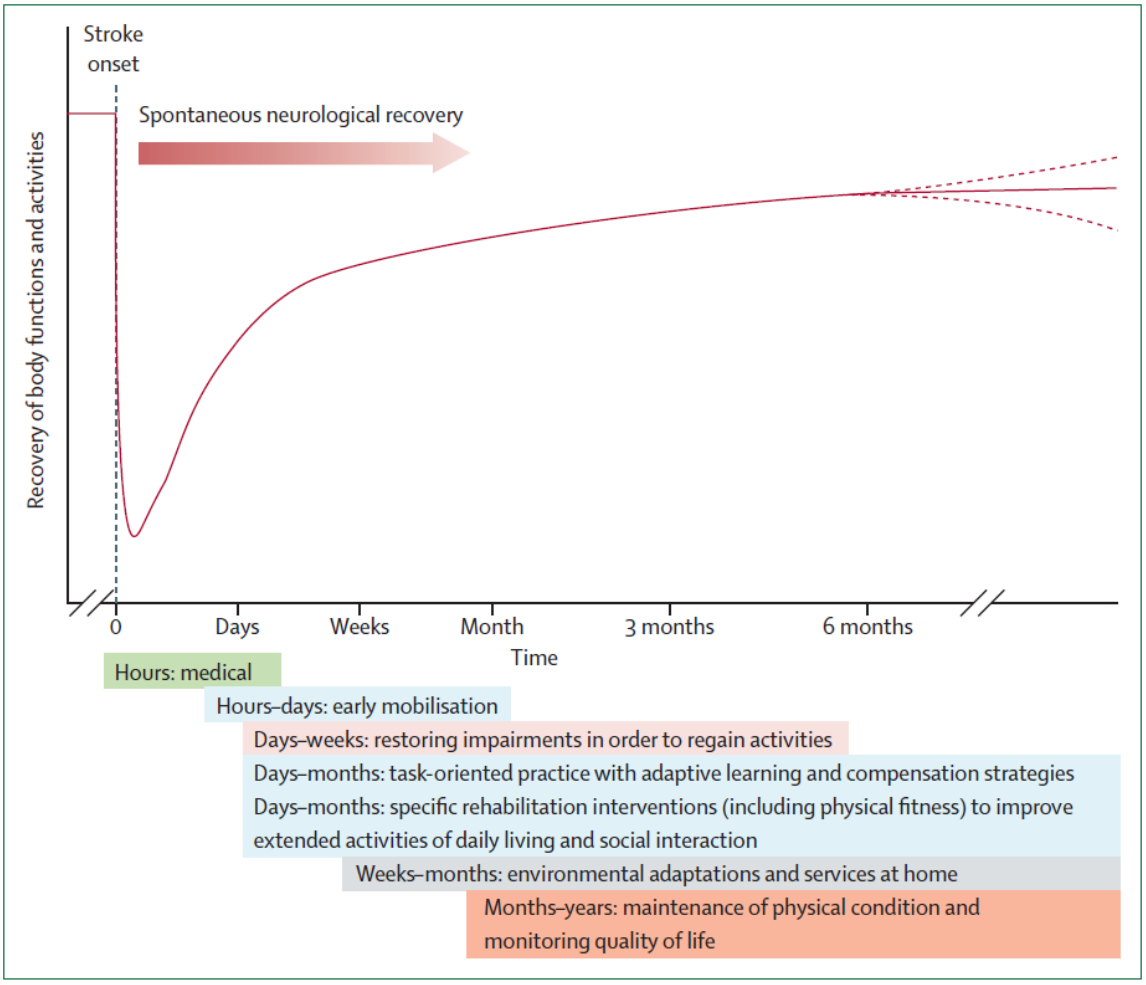

Figure 2.2 The hypothetical pattern of recovery after stroke with the timing of intervention strategies [70]**, this picture was reproduced with permission from the publisher.**

2.3. EEG and its characteristics

EEG was firstly discovered by Richard Carton in 1875, on exposed brains of rabbits and monkeys [71]. Later in 1890, an investigation on the spontaneous electrical activities of rabbits and dogs were reported by Adolf Beck, who is believed to be the founder of the modern brain wave research [72]. The evoked potential was discovered in 1912, by Vladimir Vladimirovich Pravdich-Neminsky, through EEG recordings on intact dogs [73]. The first human EEG was recorded by Hans Berger in 1924 [74]. The

beginning of clinical applications for EEG is believed to be research on the pattern of epileptic spike waves and interictal spike waves, which was reported by F.A. Gibbs, H. Davis, and W.G. Lennox in 1935 [75]. The first application of EEG based BCI was reported in 1988, by Bozinovski et al. [76].

EEG commonly refers to the signal which measures the electrical activity caused by brain cell excitation, propagated through tissues and structures, and captured on the scalp [77]. Therefore, EEG correlates directly with the activity of groups of brain cells, reflecting their excitation/inhibition. Due to its acquisition method, EEG is low in spatial resolution and extremely sensitive to environmental noise. EEG is used extensively both in clinical applications and scientific research. Generally, EEG signals measure the potential difference between an active electrode and a reference electrode over time. For better data quality, an extra third electrode is commonly used to minimize the impact of the external noise signal to the active and the reference electrodes. The third electrode usually defines a virtual zero potential point and separates the signal ground from the power ground, is commonly referred to as the ground electrode. Therefore, the minimal configuration for EEG acquisition should include three electrodes: one active electrode for actual EEG signal recording, one reference electrode, and one ground electrode.

In the fields of EEG related applications and research, EEG is generally investigated in the frequency domain and the time domain. Those two domains reflect the two major types of characteristics in EEG analysis: rhythmic activity and transient activity. For rhythmic activity analysis, EEG is usually divided into frequency bands. In clinical applications and scientific research, EEG is conventionally divided into frequency bands like alpha, beta, theta, and delta [78]. The division and detailed characteristics of the frequency bands are shown in Table 2.1. EEG rhythmic activity within a certain frequency band has been found to correlate with designated distribution on the scalp (i.e. mu band with motor imagery or motor execution) or with the biological state (i.e. alpha band with eye closure). As shown in Table 2.1, the Delta band (<4Hz) activity correlates with slow-wave sleep for adults which is normally seen in frontal areas. The Theta band activity usually refers to the frequency components between 4-7 Hz, which relates to drowsiness and idling. The Alpha activity (8-15 Hz) can be found in posterior regions of the brain, and relates to relaxation. The Beta activity usually refers to a

frequency component around 16 to 31 Hz. Literature suggests that Beta activity is seen in the frontal lobe and often relates to active thinking. The Gamma activity usually refers to the frequency component greater than 32 Hz, which is primarily found in the somatosensory cortex and related with sensory processes. The majority of the EEG frequency power can be observed between 1-20 Hz. The time domain EEG analysis generally includes certain signal pattern extraction and analysis. For example, the event-related potential (ERP) analysis is a typical time domain EEG analysis. The time domain analysis reflects the true electrical activities around EEG recording regions, which was widely used in clinical and research applications, such as hearing test (N80 signal) and cognitive function (P300 signal).

In this thesis, the author's research primarily focused on ERD/ERS related Mu band changes, which is related to motor imagery/action [79]–[81].

Table 2.1 Summary of EEG frequency bands, modified from Table 3.1 in [82].

Band name	Delta	Theta	Alpha	Beta	Gamma
Frequency (Hz)	Less than4	4 to 7	8 to 15	16 to 31	Greater than 32
Location	Frontal for adults, posterior for children;	No region specific	Posterior regions of the head; C3-C4 at rest;	Frontal lobe	Somatosen-sory cortex
Representation	Slow-wave sleep for adults; Continuous-attention for babies	Drowsiness; Idling; inhibition	Relaxed; Eyes closed;	Mild obsessive; Thinking; Alerted, Anxious	Sensory processing; Short-term memory

2.4. EEG applications in stroke rehabilitation

Literature shows that conventional rehabilitation training is usually a long process requiring extensive labor from healthcare professionals with financial strain for the patients' family [1]. In the literature, rehabilitation protocols usually require six months of repetitive training in the acute phase and one to two months of repetitive training in the sub-acute/chronic phase, depending on the protocol [70]. Therefore, in order to minimize

human labor and decrease the rehabilitation cost, rehabilitation devices have been developed with pre-programmed rehabilitation training protocols, targeting for a high number of passive rehabilitation training repetitions [10]–[13]. For example, Sanchez et al. proposed a pneumatic robot for goal-oriented movement training of the arm and hand for stroke survivors based on the Wilmington Robotic Exoskeleton (WREX) [8]. Freeman et al. developed an experimental test facility for use by stroke patients in order to improve sensory-motor function of their upper limb [12]. Herrnstadt et al. developed a bimanual training robot, which consists of two wearable robotic exoskeletons for elbow joint matching training [7].

Due to the fact that EEG directly correlates with brain cell activity, incorporating EEG based BCI into traditional training can be used to indicate the engagement level of the patient [17]. There have been several preliminary studies in the literature suggesting that using EEG based BCI has the potential to improve motor function rehabilitation training outcomes [29]–[31].

However, some papers have pointed out that using BCI aided rehabilitation training may not be the best for motor function rehabilitation training.[38]. The combination of motor imagery training (facilitated by the EEG based BCIs) and physical training (facilitated by other physiological signals or other external systems) might be necessary for the users to get the most out of the training [33]–[37].

2.4.1. Brain-computer interfaces (BCIs) and data acquisition protocol in the BCI model generation

The inherent connection between EEG and brain activity [77] resulted in the concept of using thoughts to control devices, i.e. EEG based BCIs. In the past few decades, research on BCI has been particularly active [40], [43], [83]–[85]. BCI systems have found their applications in communication [86] or assisting mobility for different types of patient populations. For example, BCI controlled lower-limb neuroprostheses [87]–[89] and wheelchairs [90] have been developed to assist patients with lower-limb disabilities. Due to the characteristics of EEG signals, EEG based BCIs are relatively low in control accuracy with a limited number of control signal classes. It is challenging for BCIs to deal with complex assistance situations in daily living [84]. However, with predefined rehabilitation training protocols, the BCI technology is more suitable for

applications in rehabilitation[91], which also facilitates the active training in the rehabilitation[40], [92].

Motor imagery (MI) is a common control method for BCIs [84], [93]. The MI tasks can be goal-oriented/context-specific, which are meaningful or have a goal in daily life [94]. For example, reaching out and grasping a cup of water, or eating with a spoon are both goal-oriented. Opposite to the goal-oriented MIs, some other MI tasks are joint specific, which is not meaningful or doesn't have a specific goal [94]. For example, elbow extension/flexion, wrist extension/flexion or figure flexion/extension are all non-goal-oriented.

Both goal-oriented and non-goal-oriented MI tasks have been used in BCI applications. Table 2.2 summarizes some of the MI tasks and BCI setup methods in the literature. The MI tasks selected in the literature were mainly selected based on the training protocol. In fact, the MI tasks selection affects the outcomes of rehabilitation training. Some researchers have suggested that goal-oriented rehabilitation training tasks tend to show longer effects with larger areas in the brain even after the training [3], [6], [94], [95]. However, as shown in Table 2.2, goal-oriented MI tasks were, in fact, not widely used. Only studies reported by Frisoli et al. [30], Royer et al.[96] and Min et al. [97] used goal-oriented MI tasks. The majority of other studies were using non-goal-oriented MI tasks.

Table 2.2 Examples of different EEG control setup and tasks used in the literature. This table was reproduced with permission [98]**.**

Bibliography	Feedback	EEG Classes
[99]	EEG+Visual	8-Class: By combining Vertical and Horizontal control to select 8 targets
[100]	EEG + Visual + FES	2-Class: MI (Wrist/Hand) vs Rest
[101]	EEG + Visual + Orthosis	2-Class: MI (Grasp) vs MI (Open)
[102]	EEG + Visual + FES	2-Class: MI/AT (Finger Extension) vs Relax
[103]	EEG	4-Class: MI of finger/wrist with different moving speed
[104]	EEG + Visual	2-Class: MI Left vs MI Right (Arm/Hand)
[105]	EEG + Visual + NES	2-Class: MI (Hand) vs Rest
[106]	EEG + Visual + Robot	2-Class: MI/AT (Grasp) vs Rest
[107]	EEG + Visual + Orthosis	2-Class: MI/AT (Grasp) vs MI/AT (Open)
[108]	EEG + Visual + FES	2-Class: MI (Wrist) vs Rest
[109]	EEG + Visual + Robot	2-Class: MI (Elbow Flexion/Extension) vs Rest
[110]	EEG + Visual + Orthosis	2-Class: MI (Open Hand) vs Rest
[111]	EEG + Visual	2-Class: MI Left vs MI Right (Hand)
[112]	EEG + Visual	2-Class: MI/AT (Grasp) vs Rest
[113]	EEG + EMG + FES	2-Class: MI/AT (Grasp/Finger Extension) vs Relax
[30]	EEG + Arm Exoskeleton + Kinect + Eye-Tracker	2-Class: MI (Right Arm) vs Rest
[114]	EEG	4-Class: MI on both wrist movement
[115]	EEG + Orthosis	2-Class: AT (Reach & Grasp) vs Rest
[116]	EEG + Visual + FES + TS	2-Class: AT (Open + Close Hand) vs Rest
[117]	EEG + Visual + Robot	2-Class: MI (Grasp) vs Rest
[118]	EEG	2-Class: Action vs Rest; 4-Class: L-R motor, L-R MI
[119]	EEG+FES	2-Class: AT(Elbow) vs Rest
[91]	EEG Offline Analysis	4-Class: MI(Grasp, Elbow, Reach&Grasp) vs Rest
[29]	EEG + Exoskeleton + FES	2-Class: MI (Grasp) vs Rest
[44]	EEG	4-Class: MI on one hand movement

MI: motor imagery; AT: attempted movement; NES: neuromuscular electrical stimulation; TS: tongue stimulation; S: stroke volunteers; H: healthy individuals; sess: session(s)

In terms of reliability, BCIs generated based on goal-oriented and non-goal-oriented MI tasks have different performances as well. Yong et al. reported an EEG based BCI study investigating the BCI model accuracy with four MI tasks within the same limb in healthy participants [91]. They claimed that the goal-oriented MI tasks showed higher testing accuracy [91].

Although goal-oriented tasks have advantages both in the BCI control accuracy and the rehabilitation training outcomes, selection of an appropriate MI task for rehabilitation training with BCIs is still unclear and largely depends on the arbitrary

choice of the authors. One problem is related to the BCI setup time. During rehabilitation training for clinical applications, it is common for the actual rehabilitation training protocol to consist of several relevant training exercises. It requires a lot of time and effort, from both the participants and the examiners, to go through repetitive EEG data acquisition sessions for each MI task involved in the training. The feasibility of using only one BCI model from one specific MI task for the entire rehabilitation training (which involve other types of MI tasks) is unknown. Specific guidelines for selecting such MI tasks are also needed to decrease the setup time of rehabilitation training involving EEG based BCI.

2.4.2. Offline EEG analysis to BCI application

The research on offline EEG analysis is well established in the literature. Many methods and algorithms have been developed to analyze the target EEG signal in an offline paradigm [41]. From a machine learning point of view, there are a lot of well-established features and classification algorithms investigating how to build a model with relatively high offline test accuracy [41], [120]–[122]. In a recent publication, EEG offline analysis algorithms can reach 8-class classification with high accuracy (>80%) [44]. In addition to the development of the offline analysis method, many studies have also pushed one step further to investigate online classification process of EEG based BCI to control external devices [123]–[126]. The performance of those BCI applications was still not satisfactory. The methods used to set up the BCI application are still preliminary. Most of the reported BCI applications apply the offline BCI model directly to buffered EEG data. Extra analysis effort could be put on the predictions of the BCI models, which may improve the online classification performance. For example, filtering or thresholding the probability prediction from the BCI model has the potential to minimize false positives and inter-trial variation. However, to the author's knowledge, no paper has been published on analyzing the online prediction of a BCI model to improve the performance of BCI applications.

2.4.3. EEG based assessment for motor function

Motor function assessments play an important role in the field of stroke rehabilitation, as they quantify motor function improvements and contribute to decision making during the intervention [27]. In healthcare facilities, motor function is usually

assessed with standardized questionnaires which require the examinees to perform pre-defined standard tasks and the examiners to give scores based on the examinees' performance. Therefore, those assessments are partially subjective and require prior training of the examiner.

Some papers have shown that some EEG features could be related to the motor function recovery of stroke survivors [24], [127]. Therefore, various scores were proposed in the literature, which claimed to correlate directly with motor function. For example, event-related desynchronization/synchronization (ERD/ERS) signal [22], [128]–[130], Delta-alpha ratio (DAR) [26], Brain symmetry indexes (BSI) [23], [25] and recently, Large-Scale Phase Synchrony (LPS) [28] were the scores proposed in the literature. Those scores are basically band power shifts or phase information from the EEG signal. Most of these scores were tested with acute/subacute stroke populations. It is not known if the results could be extended to the chronic stroke population. The scores proposed in the literature are neither accurate nor reliable enough to be used as motor function assessments. However, considering that the algorithms proposed in the literature are still preliminary, as they only utilize preliminary features like band power or phase information, there is a great potential of using EEG to accurately assess motor function for chronic stroke survivors, with the help of advanced machine learning technology like artificial neural networks.

2.5. Feature extraction/dimension reduction and machine learning

With the development of electronic devices, EEG data recording systems are able to record EEG with a large number of channels at a high sampling frequency. For example, EGI acquisition station (Geodesic Inc.) is able to record EEG for 256 channels at 1 kHz sampling rate. Therefore, the amount of data collected from EEG can be abundant. The simple time/frequency domain features from EEG are not able to satisfy the need of EEG applications like BCI systems. General feature extraction and dimension reduction processes are always needed in EEG analysis. Specifically, in applications like BCIs, a typical EEG data process should consist of pre-processing (filtering), feature extraction/dimension reduction, machine learning model generation and classification.

For feature extraction methods, common spatial pattern (CSP) was used in Chapter 3, Chapter 4 and Chapter 7. For classifiers, linear discrete analysis (LDA) was used in Chapter 4, support vector machine (SVM) was used in Chapter 3 and Chapter 7. Artificial neural networks were used in Chapter 6. Therefore, the author is briefly introducing those algorithms in the following sections.

2.5.1. Common spatial pattern

The derivatives and equations of this section were modified from [131], [132] and [133].

Various feature extraction methods have been developed for various applications of EEG signals [41]. Considering that the BCI application within this thesis is mainly related to motor imagery or actual finger movement, ERD/ERS is the main focus of this thesis. In the literature, common spatial pattern (CSP)/filter bank CSP has been proven to be very efficient in extracting features related to ERD/ERS [134]–[138].

The common spatial pattern (CSP) algorithm is a very useful feature algorithm in decomposing multiple-channel recording signals into a number of independent subset virtual channels, whose variance differences are maximized according to the selected windows[139]. The algorithm returns a subset of vectors which are referred to as the spatial pattern.

Let's assume X_1 and X_2 of size (n, t) are two windows of a multiple-channel signal recording. Here, n stands for the channel numbers of the signal, and t stands for the number of samples along the time. The CSP algorithm calculates a subset of w, for $V_1 = wX_1$ and $V_2 = wX_2$ the variance is maximized.

As introduced in [140], the variance of X1 and X2 can be represented as their covariance matrix respectively as follows:

$$V_1 = \frac{X_1 {X_1}^T}{t} \qquad \text{Equation 2.1}$$

$$V_2 = \frac{X_2 {X_2}^T}{t}$$ Equation 2.2

As introduced in [140], the variance maximization between V_1 and V_2 can be written as:

$$w = \text{argmax}_w \frac{wV_1w^T}{wV_2w^T}$$ Equation 2.3

Several approaches and methods can be used to solve Equation 2.3. In this section, the generalized eigenvalue decomposition is used, which is a simultaneous diagonalization of V_1 and V_2. As suggested in [140]:

$$\mathrm{U}^{-1}\mathrm{V}_1\mathrm{U} = D$$ Equation 2.4

$$\mathrm{U}^{-1}V_2\mathrm{U} = I_n$$ Equation 2.5

where $I_n$is the identity matrix. The matrix U is composed by the eigen vectors and the resulted diagonal matrix D is a diagonal matrix of eigenvalues. Note that the eigenvalues are sorted by decreasing order. Higher eigenvalues represent higher difference in variance.

The general eigendecomposition of S_1 and S_2 is equivalent to the eigendecomposition of $S_2^{-1}S_1$, as mentioned in [140]:

$$V_2^{-1}\mathrm{V}_1 = \mathrm{UDU}^{-1}$$ Equation 2.6

where w^T will correspond to the columns of U.

2.5.2. Fisher's linear discriminant analysis

The derivations and equations of this section were modified from [141], Chapter 4, Section 4.1.

Linear discriminant analysis (LDA) or Fisher's linear discriminant analysis is a machine learning and pattern recognition method to find a linear combination of the input

features and separate them into a designated number of classes. The LDA is a very efficient classification method in the machine learning and pattern recognition field [141]. The goal of LDA is to identify a linear discriminant function that separates two classes with a hyperplane. Therefore, LDA can only have very good performance when the feature distribution of the dataset is linearly separable. In practical applications, it is very common to use LDA to assess the feature and perform feature dimension reduction for later processes. For two-class classification, the discriminant function, y($\boldsymbol{x}$), has the following form [141]:

$$y(x) = w^T x + w_0 \qquad \text{Equation 2.7}$$

where $\boldsymbol{w}$ is a vector that weights the input $\boldsymbol{x}$ and b is the bias. The input features are columns of $\boldsymbol{x}$, who will be assigned to C1, if y(x) ≥0 and C2 if y(x)<0. The decision surface is defined as the separating hyperplane between classes, which is actually y(x) = 0. By taking y(x) = 0 back into Equation 2.7, we can see that the orientation of the decision surface is determined by w, and the displacement of the decision surface is determined by w_0.

Originally, LDA only applies to two class problems. For multiple class problems, the discriminant function is slightly different from the two-class discriminant function. If we assume K is the number of classes, in this case, K discriminant functions need to be set up, with the following form [141]:

$$y_k(x) = w_k^T x_k + w_{0k} \qquad \text{Equation 2.8}$$

where for input x_k will be assigned to class K (C_k) if the output $y_k(\boldsymbol{x})$ has the greatest value among all the other discriminant functions. As mentioned in equation 4.10 in [141] (reproduced with permission), with the same property from the two class problem, the decision surface between class i and j is calculated as the following equation [141]:

$$(w_i - w_j)^T x + (w_{0i} - w_{0j}) = 0 \qquad \text{Equation 2.9}$$

To compute the w_{0i} and w_{0j} for class i, we can consider LDA as a dimensional reduction method, by projecting input x into y dimension. Therefore, adjusting w is able

to maximize the class separation between C_i and C_j. Through this point of view, the objective function of LDA is defined as mentioned in equation 4.26 in [141]:

$$w = argmax_w \frac{w^T S_B w}{w^T S_w w} \qquad \text{Equation 2.10}$$

Similar to the objective function in the CSP algorithm, the solution of Equation 2.10 is the eigenvectors of, and the separation between these two classes will be equal to the eigenvalue of $S_w^{-1}S_B$. In Equation 2.10, S_B is defined as the "between classes covariance matrix" and S_w is defined as the "within classes covariance matrix". The two covariance matrixes are defined as mentioned in [141]:

$$S_B = \sum_{i \in C} (\mu_{ci} - \bar{X})(\mu_{ci} - \bar{X})^T \qquad \text{Equation 2.11}$$

$$S_w = \sum_{c \in C} \sum_{i \in C} (x_{ci} - \mu_{ci})(x_{ci} - \mu_{ci})^T \qquad \text{Equation 2.12}$$

where C is the number of classes in the classification problem, $\bar{X}$ is the overall mean of all the data points, $\boldsymbol{\mu}_{ci}$ is the mean of data points in class i, x_i is the input x from class i.

2.5.3. Support vector machine

The derivations and equations of this section were modified from [142] and [141], Chapter 7, Section 7.1

Support vector machine (SVM) is a kernel method in the supervised machine learning field. Different from LDA, which can only have good performance on linearly separable datasets, SVM is able to process a dataset with arbitrary distribution with various kernels. SVM was also originally designed to tackle two-class classification problems. The SVM model is designed to map a margin between the two-class data points on the feature domain to separate the two-class data points apart from each other. The classification result depends on which side of the SVM model that input data point is located.

Given a set of n points (X_1, y_1)...(X_n, y_n) as training data for two-class classification problem, the y_i is either +1 or -1, which indicates the class that X_i belongs to. The SVM is designed to find a hyperplane that separates X_i into two groups accordingly and maximize the distance between the hyperplane and nearest data points from either class. The above-mentioned hyperplane is called the “maximum-margin hyperplane”. To simplify the derivatives, we only talk about linear kernels in the following. Therefore, the maximum-margin hyperplane can be defined as mentioned in [142]:

$$wx_i - w_0 = 0 \qquad \text{Equation 2.13}$$

where w is the vector to the maximum-margin hyperplane. Similar to the LDA analysis, $\frac{w_0}{\|w\|}$ is the basis of the maximum-margin hyperplane, and $\frac{w}{\|w\|}$ is the orientation of the maximum-margin hyperplane.

Considering the training data points and their distribution, since the maximum-margin hyperplane is in the middle of the data points of two classes, the possible distance between the two classes can be considered as twice the distance to the maximum-margin hyperplane, which is defined as$\frac{2}{\|w\|}$. This is defined as the margin of the SVM model. If we want to maximize the margin to prevent misclassification, we need to minimize the norm of the weight vector.

To prevent the data points from falling into the margin, we add the following two constraint conditions as mentioned in [142], to the original SVM model:

$$wx - w_0 \geq 1, if\ y_i = 1 \qquad \text{Equation 2.14}$$

and

$$wx - w_0 \leq -1, if\ y_i = -1 \qquad \text{Equation 2.15}$$

The constraint conditions stated in Equation 2.14 and Equation 2.15 can also prevent the data points from falling into the wrong side of the SVM model. If we multiply y_i on both sides of the constraint conditions, as mentioned in [142], Equation 2.14 and Equation 2.15 can be re-written into the following equation:

$$y_i(wx_i - w_0) \geq 1, for\ 1 \leq i \leq n \qquad \text{Equation 2.16}$$

Therefore, to summarize all the derivations we have, the SVM problem transfers into an optimization problem, which is to minimize $\|w\|$ subject to $y_i(wx_i - w_0) \geq 1, for\ 1 \leq i \leq n$. The solution of this optimization algorithm returns the maximum-margin hyperplane for the SVM. Maximizing the margin of the two-class data points will result in a particular choice of decision boundaries, which was determined by the closest data points to the maximum-margin hyperplane. These decision related data points are known as the support vectors.

In order to solve the w and w_0 from the SVM model, the hinge loss function was the common loss function in the SVM model generation. The hinge loss function, as mentioned in [142], has the following form:

$$\max(0,1 - y_i p_i) \qquad \text{Equation 2.17}$$

where the y_i is the class label and p_i are the predicted class from the SVM model. The output of the hinge function is related to the constraint function in Equation 2.16. If the constraint function in Equation 2.16 is met, the hinge function will output zero. If not, that means the X_i is classified on the wrong side of the maximum-margin hyperplane, and the hinge function will output a distance related value to the maximum-margin hyperplane. Therefore, in the SVM algorithm, the loss function is designed as mentioned in [142]:

$$\left[\frac{1}{n}\sum_{i=1}^{n}\max(0,1 - y_i \mathrm{p}_i)\right] + \lambda\|w\|^2 \qquad \text{Equation 2.18}$$

The first half of Equation 2.18 describes the classification accuracy and the second half relates to the margin of the SVM model. λ is an arbitrary value describing the weight between the classification accuracy and the margin size of the SVM model. With a fairly small λ value, the second half of the SVM model will be neglectable, and the SVM model will only value the accuracy of the prediction.

Combining Equation 2.16 and Equation 2.18, the optimization problem can be simplified as mentioned in [142],:

$$argmin(\frac{1}{n}\sum_{i=1}^{n}\zeta_i + \lambda\|w\|^2) \qquad \text{Equation 2.19}$$

$$Subject\ to\ y_i \mathrm{p}_i \geq 1 - \zeta_i\ and\ \zeta_i \geq 0$$

where ζ is the hinge loss function output. This equation can be solved through the Lagrangian dual method. As mentioned in [141], for an arbitrary kernel $\Phi(\boldsymbol{x})$, we can get

$$w = \frac{1}{n}\sum_{i=1}^{n} a_i y_i\, \Phi(\mathrm{x}_i)$$

$$\sum_{i=1}^{n} a_i y_i = 0 \qquad \text{Equation 2.20}$$

$$a_i = \frac{1}{2\lambda} - \mu_i$$

where a_i and μ_i are the Lagarangian multipliers. As mentioned in [141], in order to solve the Lagrange multiplier a_i, the following equation is introduced:

$$f(a_i) = argmax[\sum_{i=1}^{n} a_i - \frac{1}{2}\sum_{i=1}^{n}\sum_{j=1}^{n} y_i\, y_j a_i\, a_j \Phi(\mathrm{x}_i)\Phi(\mathrm{x}_j)^T] \qquad \text{Equation 2.21}$$

$$Subject\ to\ \sum_{i=1}^{n} a_i y_i = 0\ and\ 0 \leq a_i \leq \frac{1}{2\lambda}$$

The parameter a_i can be solved with quadratic programming algorithms. With the optimal a_i, the data point $\boldsymbol{x}_n$ which has non-zero a_i is the support vector mentioned before. The rest of a_i does not contribute to the maximum-margin hyperplane. Therefore, they can be removed from the calculation.

Once the a_i is calculated, the weight parameter can be solved based on Equation 2.20. As mentioned in [141], the bias w_0 can be calculated on the following equation:

$$w_0 = \frac{1}{M} \sum_{i \in M} \left(y_i - \sum_{j \in N} a_j y_j \, \Phi(\mathrm{x}_i)^T \Phi(\mathrm{x}_j) \right) \qquad \text{Equation 2.22}$$

where M is the length of a_i, which is $0 \leq a_i \leq \frac{1}{2\lambda}$, M is the number of support vectors.

2.5.4. Artificial neural network (ANN)

Artificial neural networks (ANN) are algorithm frameworks inspired by actual biological neural networks. The ANN consists of neuron nodes that are controlled by the activation function, which has a similar mechanism as biological neural systems. ANN was referred to as cybernetics in the 1940s-1960s, or connectionism system in the 1980s-1990s [143]. ANN and related research have generated more and more interest all around the world.

ANN is able to learn features and patterns automatically. Therefore, ANN is very suitable for machine learning and pattern recognition applications with large and complex data input.

ANN is defined as a special data managing architecture rather than an algorithm, the actual algorithm is referring to the special method designed to update the weights for the artificial neural nodes. Figure 2.3 shows a simple three-layer ANN architecture. For this ANN architecture example, the data input is a three-dimensional vector $\boldsymbol{x}$ = (x_1, x_2 x_3). Starting from the second layer, for each neural node in this layer, a weight factor $w_{i,j}^{(k)}$ is multiplied with each previous layer's neural node output $h_i^{(k-1)}$, where k is the layer numbering and i is the neural node numbering of the neural nodes from the previous layer (connected from), j is the numbering of the neural nodes in the current layer (connected to). The output $h_i^{(k-1)}$ is calculated with a pre-defined activation function f(x), which regulates the output in a predefined way. Figure 2.4 shows several common activation functions. An activation function is chosen on an empirical basis with consideration on the current function of the neural node layer and the general application of the ANN.

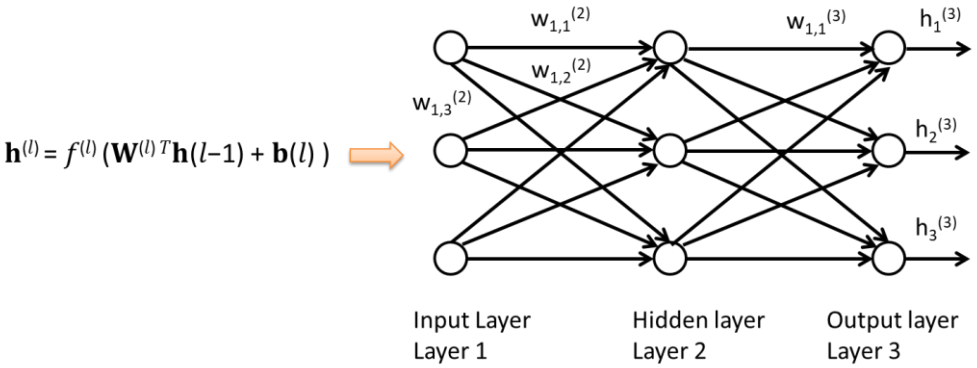

Figure 2.3 A typical three-layer ANN configuration. In the equation on the left of the figure, $w_{j,}^{(l)}$ is the weight of the connection between neuron j in layer $l-1$ and neuron k in layer l. $h^{(l)}$ is the output of neuron k in layer l. $b^{(l)}$ is the bias term of neuron k in layer l. $_{(l)}$ (x) will be the activation function used in the neurons in layer l.

With the architecture of the ANN setup, the next step is to train the weights based on the training data set, which is obtaining the optimal value for weights and biases. A general method called backpropagation is commonly used to obtain the weights and biases. Reference [143] has a detailed explanation of backpropagation, therefore only the basic mechanism will be explained in this part of the thesis.

With the example in Figure 2.3, the values of weights and biases are updated by going through several iterations of the training dataset. Each iteration is called epoch in the ANN field. If the training dataset is too big, it can be further divided into batches. Firstly, the ANN is initialized with random values of weights and biases. The training data is passed through the initialized ANN and output $h^{(3)}$ is calculated. Errors are calculated based on the true values and the output $h^{(3)}$. The gradient of layer 3 is computed as well. The weight values and bases values of layer 3 are then updated according to the gradient. The next step is to calculate the errors in layer 2. The error values in layer 3 are passed to layer 2, proportionally to the weight values between the neural nodes of the two layers ($h^{(3)}$ to $h^{(2)}$). Gradients of layer 2 are also calculated and the weight and base values of layer 2 are also updated. Based on the same method, the weight and base values are updated for the whole ANN. A maximum error value and a maximum number of epochs have to be pre-defined to break the ANN training process if the ANN training process achieves either of the two constraint conditions.

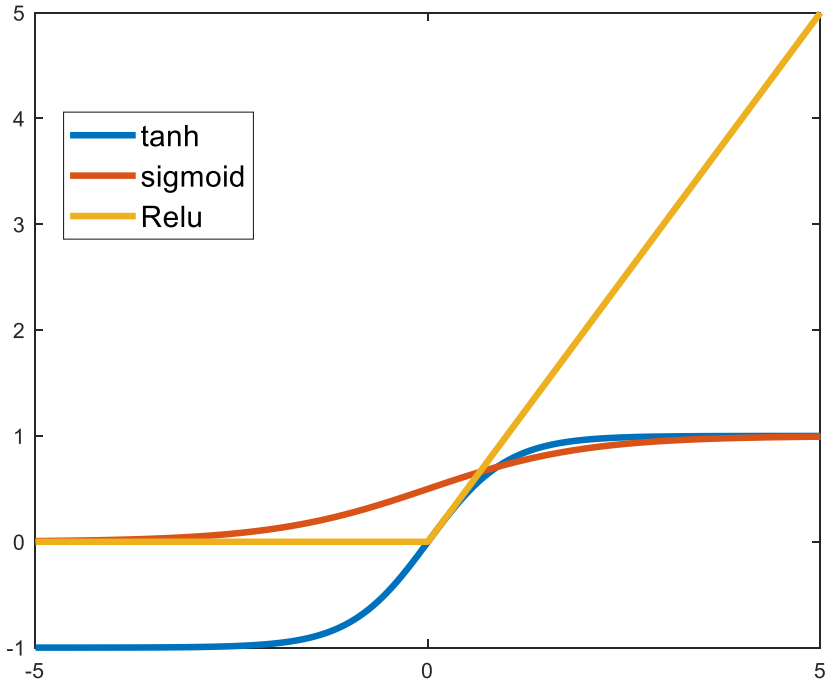

Figure 2.4 Some common activation function used in ANN.

Special layers of ANN were also developed recently to serve for special needs, for example, convolutional neural network (CNN). CNN was inspired by mammal visual cortex structure [144]. CNN is very suitable to find locally related features and patterns [145]. CNN has shown its wide applications in computer vision and video recognition fields. A typical CNN usually combines convolutional layers and fully connected layers (sometimes referred to as the hidden layer) as a complete network. Recently, deep CNN architectures have been proposed to deal with object recognition problems, and the results are promising. For example, CNN based Inception-ResNet has been reported to have very good performance on the ImageNet classification challenge, which is now one of the most accurate methods in the object recognition field [146].

Convolution layer is the key component layer of CNN. The convolutional layer is designed to compute convolution with the adjacent input and send the output to the next-layer input. The convolution computation can be done with arbitrary dimension. Since the major applications of CNN are for image recognition, an illustration of a 2D convolutional layer algorithm is shown in Figure 2.5. Based on the calculation procedure shown in Figure 2.5, each input element has a limited field of influence on the output of

the convolutional layer. Compared to same-size fully connected neural network configuration, CNN has a lower number of parameters to learn and the resulted features are more locally relevant [143].

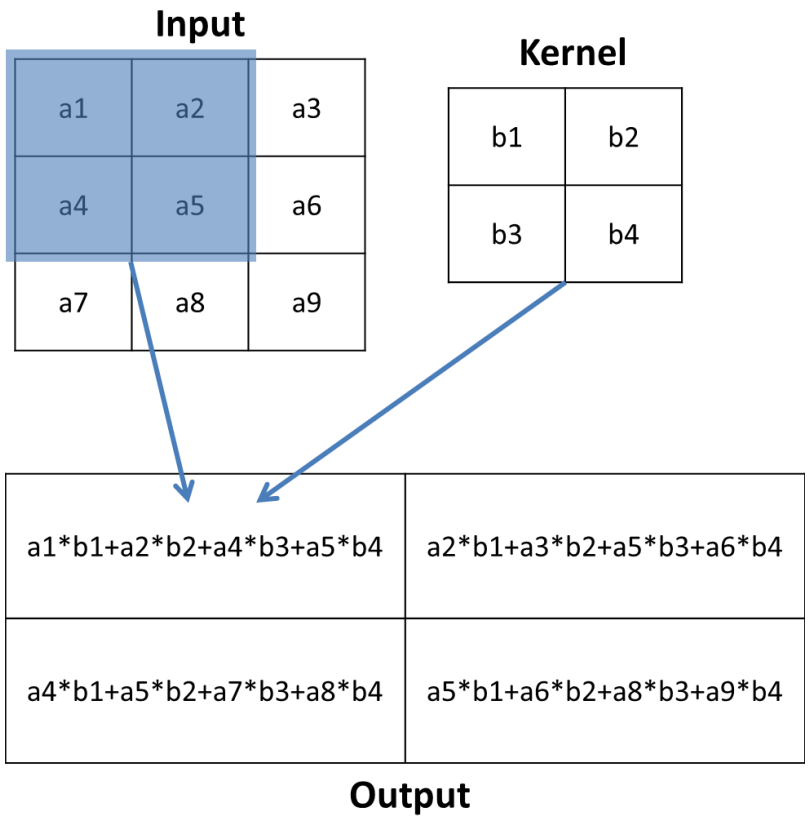

Figure 2.5 Illustration of a 2D convolutional layer algorithm [143]**.**

2.6. Chapter summary

In this chapter of the thesis, the literature related to EEG applications in stroke rehabilitation has been reviewed. This chapter started with the etiology of stroke and the significance of stroke rehabilitation. Characteristics and possible fields of EEG application were also reviewed to investigate the possible research direction for the following chapters. At the end of this chapter, several popular EEG feature algorithms and machine learning methods were also reviewed to further clarify the research methodologies in the following study.

In the next chapter, a pilot study will be introduced to address the specific challenges of BCI applications in stroke rehabilitation.

Chapter 3.

A pilot study to identify the challenges of EEG applications in stroke rehabilitation

This chapter is reproduced with permission from the following paper I co-authored:

Elnady, A. M., Zhang, X., Xiao, Z. G., Yong, X., Randhawa, B. K., Boyd, L., & Menon, C. (2015). A Single-Session Preliminary Evaluation of an Affordable BCI-Controlled Arm Exoskeleton and Motor-Proprioception Platform. *Frontiers in Human Neuroscience*, *9*. https://doi.org/10.3389/fnhum.2015.00168

Some sections are adapted to fit within the scope and comply with the format of the thesis.

In the study introduced in this chapter, the author's major contribution is in EEG acquisition, BCI realization, and FES unit programming. The training protocol design and programming are done in collaboration with the first author. This chapter is included in the thesis to identify the potential challenges with respect to EEG applications in rehabilitation.

3.1. Introduction

The general changes after rehabilitation training are the result of learning effects, as learning has been shown to create new pathways on how the brain processes information, suggesting that the brain is plastic [147], [148]. In order to consolidate the changes brought by learning effects, repetitive training is necessary. Based on this hypothesis, exercises using the unimpaired part of the brain may enhance brain plasticity and subsequently improve the motor performance of the patients with stroke [149], [150].

Traditional rehabilitation training protocols consist of one-to-one training sessions between healthcare professionals and patients. In these training sessions, the healthcare professional manually assists the patient, which is labor intensive for healthcare professionals and costly for patients [1]. Robotic-assisted rehabilitation training was proposed to minimize interventions from healthcare professionals and

reduce the cost for patients [10], [13], [151]–[154]. Those devices have the advantage of delivering a high dose of training repetitions without full supervision from healthcare professionals. However, some papers have pointed out that therapeutic training with only passive robotic-assisted joint movements is not efficient, as those training protocols do not need the patients' active participation in rehabilitation training [14], [155]. Therefore, BCI controlled robotic-assisted rehabilitation devices were developed to ensure the users' focus in rehabilitation training [156]–[160]. In this specific application, the BCI system interprets the user's intention of moving to control commands for the robotic-assisted rehabilitation device, which assists the user in the rehabilitation training [15]. Misinterpretation of the users' intention would deteriorate the training efficiency and the stability of the BCI system, as the users may be misled by the misclassification.

Most BCI controlled robotic-assisted rehabilitation devices reported in the literature used motor imagery to trigger the assistance. The utilization of BCI and robotic rehabilitation creates a feedback loop that includes active training and somatosensory feedback at the same time. This feedback loop may have a strong and positive influence on rehabilitation outcomes.[107], [161], [162].

The objective of this chapter is to use an experimental design of BCI-exoskeleton rehabilitation training platform to identify the challenges of EEG applications in stroke rehabilitation. In this chapter, the author proposed a rehabilitation training platform combining BCI, robotic exoskeleton and FES. The author contributed in the design and coding of the BCI system, the FES control component, and partially with the training protocol, which was designed in collaboration with the first author. The robotic exoskeleton was designed and fabricated by colleagues in the lab [29].

3.2. Methods

3.2.1. BCI Setup

EEG technology has many advantages like non-invasiveness and direct relation to brain cell activation. EEG-based BCI technologies were extensively investigated in the literature [38], [40], [41], [84], [120], [121], [163], [164]. Recently, BCI has been used in applications like assistive devices [92], communication and rehabilitation [11], [15], [38], [85]. Current BCI technologies still suffer from low reliability and performance, which

limited their application in daily lives. Rehabilitation seems to be a good match for BCI technologies, as rehabilitation applications generally deal with less complex situations and have less requirement on the accuracy, compared to assistive applications in daily-living [84].

A typical EEG based BCI is usually set up following these steps: 1) time/frequency domain filter, 2) spatial filter, 3) feature extraction/selection, 4) classification/regression, 5) testing/using [165]. In the past decade, most research focused on the spatial filters, feature extraction/selection and the classification process (i.e. classifiers) [165]. For example, principal component analysis (PCA), independent component analysis (ICA) [166] and common spatial pattern (CSP) [132] were the basic spatial filters proposed in the literature. Some other variants of spatial filters were also reported to have positive effects on classification accuracy, such as filter bank common spatial pattern (FBCSP) [167]. In order to select the relevant features in the BCI model generation, the feature extraction/selection process was included in the BCI setup. The correlation-based feature selection, information gain, and 1R ranking methods were the top feature extraction/selection methods as reported in [168]. With the development of modern machine learning technologies, the boundary between feature selection and classification has become unclear, such as in the modern artificial neural network technologies. The modern artificial neural network is a data processing framework designed to learn features and classify directly and jointly from the data (i.e. convolutional neural networks (CNNs), restricted Boltzmann machines (RBMs)) [165]. However, modern artificial neural networks usually require a large amount of system computational resources, which is a big challenge for online BCI applications.

Despite many papers published in the field of BCI, spatial filtering the EEG signals and utilizing frequency band power or time domain features are still common practice, especially for real-time BCI applications [165]. For the purpose of reducing the computation complexity and improving the portability of the entire system, a wireless Emotiv headset (Emotiv SDK Research Edition Specifications, 2010), which was designed for gaming, was used to record the EEG data for the online BCI application in this chapter. The EEG data were sampled at 128Hz. The EEG recording headset was originally designed as 14 channels of the 10-20 EEG system [169]. The channels

include: AF3, AF4, F7, F8, F3, F4 FC5, FC6, T7, T8, P7, P8, O1, and the reference channels are located at the P3/P4 locations.

In order to calibrate the EEG model for the BCI, the Stimulus Presentation mode of BCI2000 was used to record the EEG data [170]. BCI2000 is an open source software written in C++, co-developed by Brain-Computer Interface R&D Program at the Wadsworth Center of the New York State Department of Health in Albany, the Institute of Medical Psychology and Behavioral Neurobiology at the University of Tübingen, the BrainLab at Georgia State University, and Fodazione Santa Lucia in Rome and other research institutions. In this part of the session, the participant was required to sit comfortably in front of a screen. On the screen, two pictures (rest and motor imagery) were shown consecutively, one at a time. The participant was required to follow the picture on the screen and react correspondingly. When the rest picture was on the screen, the participant was required to look at the screen and stay at rest. When the motor imagery picture was shown on the screen, the participant was required to imagine hand grasping with his/her stroke-impaired hand. The sequence of the two pictures was randomized. Each picture was shown for a random time between 4 to 6 seconds on the screen, in order to minimize adaption. Each of the stimulus presentation consisted of two runs, the total session lasted for about 15 mins. In total 20 trials of EEG data were recorded, for each participant and each visual stimulation. The participants were encouraged to take breaks when needed.

The EEG acquired from the Emotiv was firstly filtered with a finite impulse response (FIR) bandpass filter, whose passband was set to 1-45 Hz. The influence of artifacts on the EEG data was minimized. The mu band power of the EEG data was extracted as the main feature input for the BCI. A classifier was trained to distinguish between the rest and motor imagery states of the user. The output of the classifier was then sent to the exoskeleton and the FES unit.

Then, the collected EEG data of the two states were processed to generate the BCI models for each participant, which were used in the rehabilitation training. A MATLAB based toolbox (BCILAB) was used to generate the BCI model [171]. To generate a BCI model, a spatial filter algorithm was first applied to the EEG data. In this chapter, Common Spatial Pattern (CSP) algorithm [132], [134] was used to filter the

EEG signals. The standard deviations of the filtered signals were used as features for the model generation. Linear Discriminant Analysis (LDA) was used as classifiers to classify the EEG data [141]. To evaluate the performance of the BCI, the 10 x 10 cross-validation method was used [141]. In the 10 x 10 cross-validation, the entire data set was randomly shuffled and divided into ten subsets. Nine of the subsets were used to train the classifier and the remaining one subset was used to test the prediction accuracy of the obtained model. This procedure was repeated for ten times, with the ten subsets in turn. Then, the average BCI cross-validation classification accuracy was computed by averaging the validation accuracy in the ten folds. Among the ten folds, the BCI model with the highest test accuracy in the cross-validation was saved for later online application.

For online testing, the EEG data were streamed to the classifier with a two-second data buffer (256 data samples of 14 channels). The output of the classifier was either “0” or “1”. The classifiers were configured to produce classification decision output every 0.5 seconds. The classification output was used to control the exoskeleton arm or the FES unit, depending on the process of the rehabilitation protocol. The classifier “0” output represented the resting state of the user. The classifier “1” output represented the motor imagery state (or active state) of the user. During the rehabilitation training, the motor imagery state was used to activate assistance of the exoskeleton or to turn on the output of the FES unit. The resting state was used to indicate that the user did not intend to activate the device.

3.2.2. System Integration

The robotic exoskeleton used in this chapter was designed and fabricated in the lab, not by the author [29]. The exoskeleton is shown in Figure 3.1

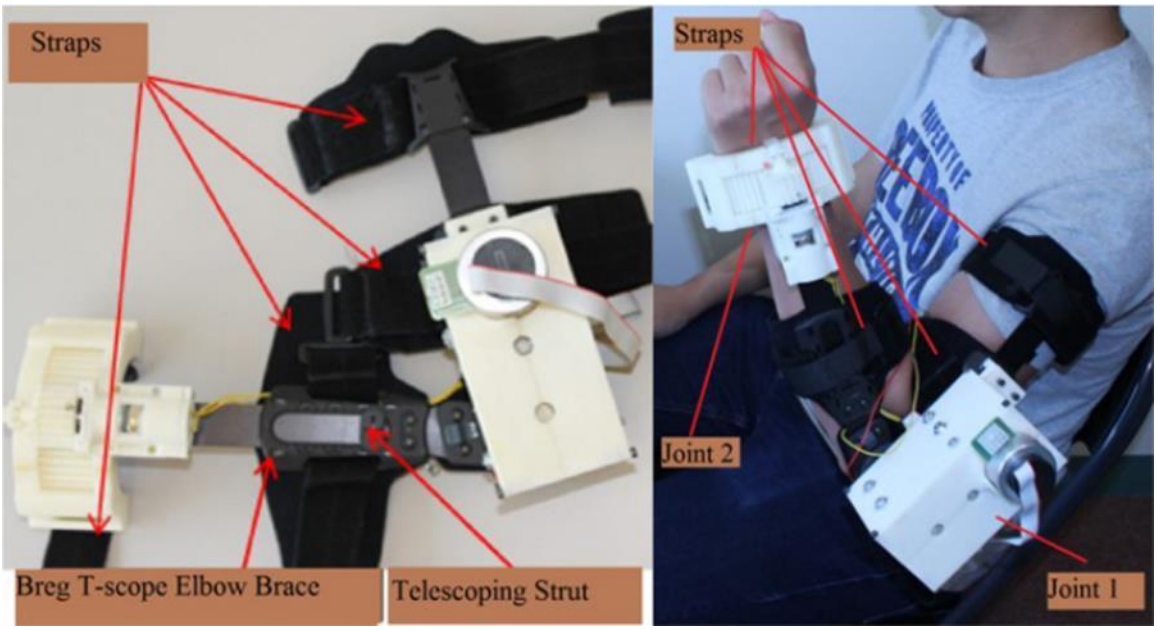

Figure 3.1 The exoskeleton used in this study [29]

RehaStim I (Hasomed, Magdeburg, Germany) was the FES unit used in this chapter. The FES unit was configured to output biphasic rectangle pulses with 35 Hz of frequency and 150us of pulse width. The output peak-to-peak amplitude was adjusted accordingly for each participant.

Figure 3.2 shows the main components of the proposed BCI-controlled exoskeleton training system. The BCI system was set up using MATLAB. The FES unit and the exoskeleton were programmed and controlled via LabVIEW. The EEG data were streamed in real time via Bluetooth from Emotiv, to the processing terminal. The processing terminal was a laptop in this study. The EEG data were then processed and classified into classification decision output (either “0” or “1”). In the proposed rehabilitation training platform, the classification output was transmitted internally in the laptop via UDP protocol. A LabVIEW virtual instrument (VI) was created to handle the data exchange between the classifier and the rehabilitation training protocol. The rehabilitation training protocol was programmed separately with another LabVIEW VI. The rehabilitation training protocol program was designed to control the exoskeleton and the FES unit directly. The exoskeleton was controlled through a National Instrument (NI) data acquisition card. The angular position of the exoskeleton’s elbow joint was monitored in real time with the same NI data acquisition card, which acted as feedback

control for the motor of the exoskeleton. The FES unit was controlled using byte control directly via USB.

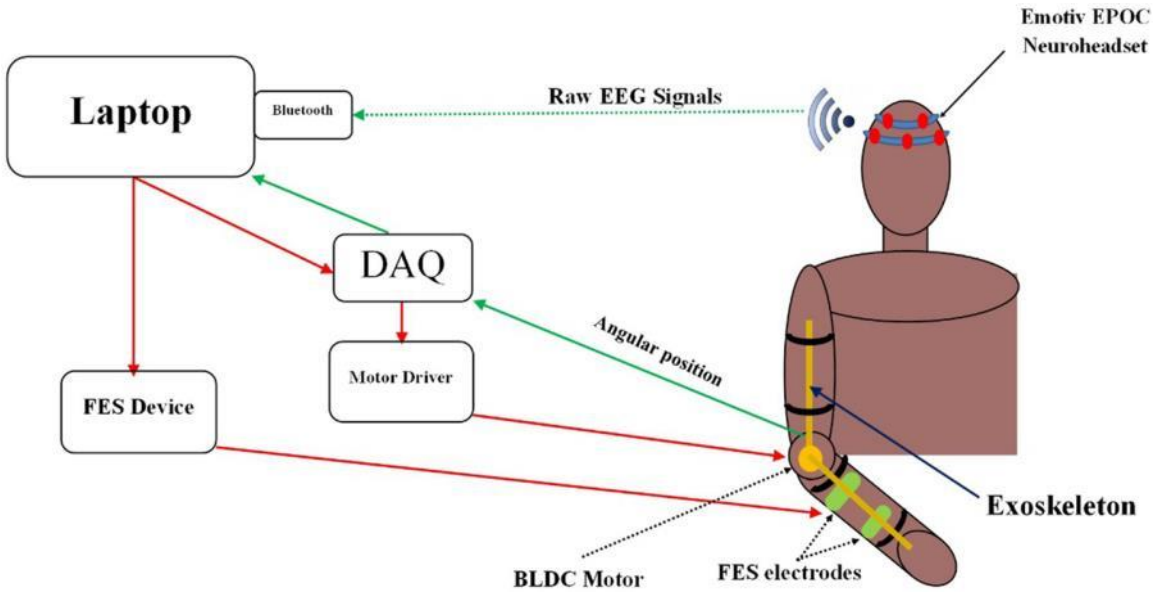

Figure 3.2 Schematic drawing for the rehabilitation training system used in this study [29]

The rehabilitation training platform was designed in a pre-programmed movement sequence with a goal-directed motor task. The overall training protocol involved training on the hand, elbow joint and shoulder joint. The training protocol was divided into 11 phases. These 11 training phases were shown in Figure 3.3. Moving from one phase to the following phase, the user was required to perform the same motor imagery in the stimulus presentation part. The BCI model ("rest" vs "motor imagery") obtained from the previous model training procedure was used to determine the users' mental status ("rest" or "active") based on the users' EEG data. The classification decision "0" did not have any influence on the system control. If the classification decision "1" was detected during the phase transition, the training protocol would move to the next phase of the assistive protocol for the rehabilitation training.

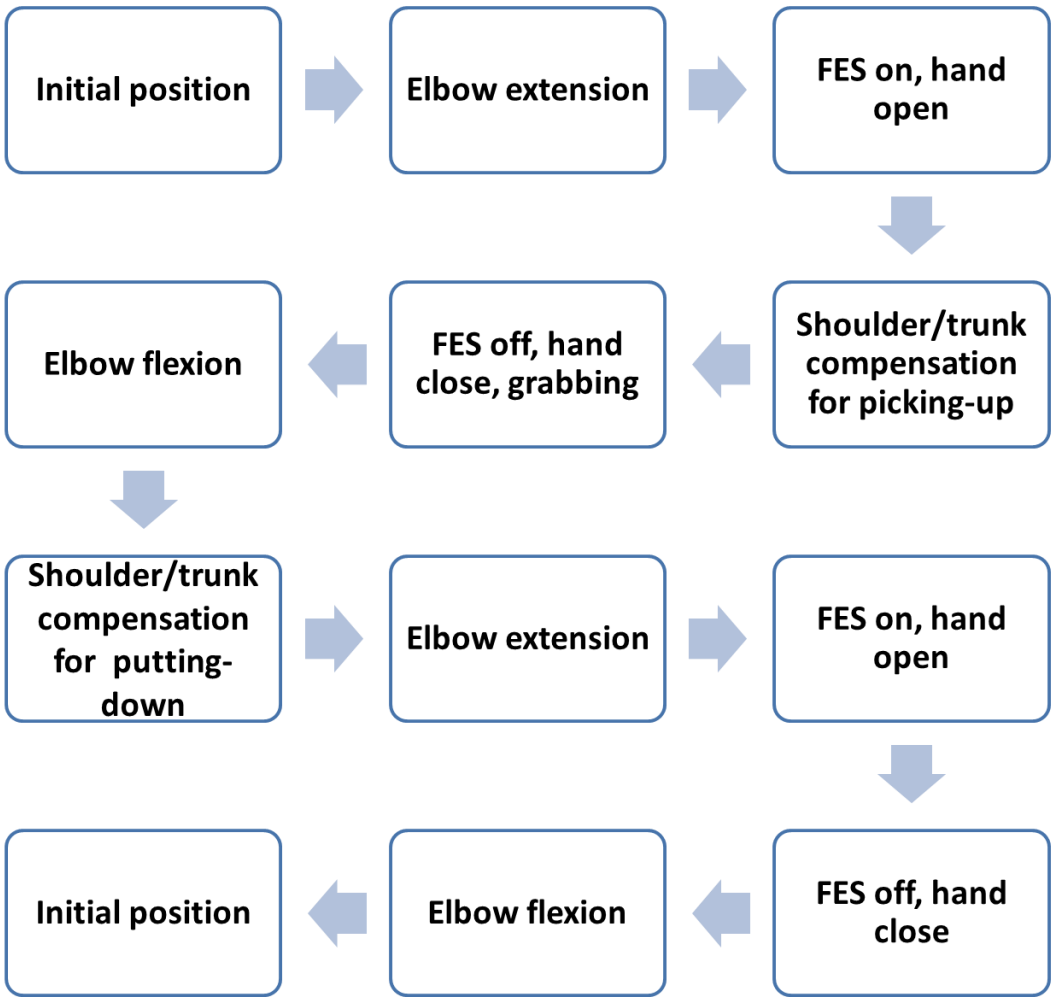

Figure 3.3 Flowchart of the training protocol [29]**.**

3.2.3. Participants

Participants with chronic stroke (> 6 months post) were recruited through local rehabilitation hospitals and stroke clubs. All potential participants were screened to meet the following inclusion criteria: (a) age range from 35 to 85 years, (b) post-stroke duration ≥ 6 months, (c) Montreal Cognitive Assessment (MoCA) ≥ 25 [172], or pass any other cognitive assessment test, (d) shoulder active range of motion (ROM) in all directions of 10˚-15˚, (e) elbow passive extension and flexion ROM of 0˚-130˚, (f) wrist passive extension ROM of 0˚-15˚, and (g) fingers full passive extension. The exclusion criteria included: a) any other neurological conditions in addition to stroke, b) unstable cardiovascular disease, c) contraindications to FES or d) other conditions (e.g. poor sitting balance) that precluded them from undergoing the study. Nine male stroke

participants (mean age 66 ±11.9 years) agreed to participate in this study. The protocol of this study was approved by the Office of Research Ethics at Simon Fraser University and all the participants gave informed consent before participating.

3.2.4. Training Protocol

Participants were instructed to learn how to use the training device to perform a pre-defined goal-directed motor task. The training platform required to be calibrated individually for each participant, which consisted of two main steps: the setup of the BCI and the setup of the FES unit.

The Emotiv EEG acquisition system requires to soak its EEG contacts in an electrolyte solution in advance to ensure good contact between the device and the user's scalp. Then the Emotiv system was applied to the participant. The contact resistance for each channel was adjusted until the resistance was below 10kΩ, as suggested by the Emotiv manual. The BCI system was then set up as described in the previous section.

The RehaStim FES unit was used to assist the participants in grasping and releasing an object. For each participant, two self-adhesive rectangular electrodes were attached to the arm surface of the stroke-affected side, close to the extensor digitorum. The peak-to-peak amplitude of the FES was incrementally tuned, and the electrode positions were adjusted until the participants' impaired hand was open (enough to grasp the designated cup). For the FES used in this study, symmetrical biphasic square pulses, with a fixed frequency of 35Hz and signal duration of 150μs, were used to open the hand of the participants [173]. In the training protocol, the participants were required to adjust hand/shoulder position to grasp a cup. Then, the FES unit was deactivated so that the participants were able to flex their fingers and grasp the object.

After setting up the BCI and the FES unit, the participants were required to wear the exoskeleton. Straps were used to fasten the exoskeleton arm on the participant's impaired side.

An introduction was then given to each participant on how to use the training device to perform a pre-defined goal-directed motor task, with assistance from the

proposed training platform. The pre-programmed rehabilitation training protocol required the participants to move a cup from an initial position to a new position. It was divided into 11 phases, as shown in Figure 3.3.

At the beginning of the rehabilitation training, participants were required to place their arm in an elbow-flexed initial position that is comfortable for them.

During phase 1, participants were required to perform motor imagery to activate the BCI. If the classification result changed from “0” to “1”, the BCI system would then activate the assistance from the exoskeleton to extend the participants’ elbow to the designated elbow position.

During phase 2, participants were required to perform the same motor imagery as the one used during the EEG data acquisition session, to activate the BCI. If the classification result changed from “0” to “1”, the BCI system would turn on the assistance from the FES unit to open the participants’ hand.

During phase 3, participants were required to adjust their shoulder and trunk to aim at a target cup on the table with the hand on the impaired side.

During phase 4, when the hand was placed beside the cup, participants were required to use BCI to deactivate the FES unit. The FES unit would remain on during phase 3 and phase 4 until it received an “1” output from the BCI system. With the FES unit deactivated, the participants were able to grasp with the hand on the impaired side to hold the cup.

During phase 5, participants were required to lift the cup up with elbow flexion. In order to perform this movement, the participant was required to perform motor imagery to activate the BCI again, and the BCI would activate the assistance from the exoskeleton. The exoskeleton helped the participant perform elbow flexion with a small angle (approximately 15°) to lift the cup.

During phase 6, participants were required to move their shoulder and trunk to aim for the designated new location for the cup.

During phase 7, participants were required to place the cup in a new position. In order to perform this movement, the participants were required to perform motor imagery to activate the BCI. The BCI system would activate the assistance from the exoskeleton. Then, the exoskeleton would assist the participants to perform elbow flexion to put the cup on the table again.

During phase 8, participants were required to release the cup at the target location. The participants were required to perform motor imagery to activate the BCI. The BCI system would activate the FES Unit. Then, the participants were able to release the cup.

During phase 9, participants were required to use their shoulder and trunk, to move the impaired hand away from the target cup. In this phase, the participants do not need to maintain the MI state to maintain the elbow extension state of the exoskeleton.

During phase 10, participants were required to perform motor imagery to deactivate the FES unit using the BCI.

During phase 11, participants were required to flex their elbow and return to the initial position using the exoskeleton. The participants were required to perform motor imagery again and activate the BCI. The BCI system would activate the assistance from the exoskeleton, and the exoskeleton would help the participants flex the impaired arm to return to the initial position.

The sequence of the training protocol was repeated during one hour of training. The participants were able to pause or terminate the rehabilitation training on their own volition.

3.3. Result

Table 3.1 presents the BCI validation accuracy for each stroke participant. Considering that this is a single session training, no standard variation was obtained. For all nine participants, the average cross-validation accuracy achieved 68.8%, with a standard deviation of 9.0%. The accuracy of the BCI in this chapter is similar to the performance of the BCI systems reported in the literature [174].

Table 3.1 BCI Cross validation accuracy

Participant ID	P01	P02	P03	P04	P05	P06	P07	P08	P09
Accuracy (%)	81.10	65.20	83.20	69.26	62.87	64.25	55.78	63.31	73.90
Mean ± Standard Deviation	68.76 ± 9.03								

During the one-hour training, all participants with chronic stroke (n = 9) were able to complete the training exercises for at least two repetitions. The average number of training repetitions was 3 ± 0.7 (ranged from 2 to 5).

For each trial of the training exercises, the following data were recorded in real-time: the BCI output: rest ('0') or activate ('1'); the FES status: deactivate ('0') or activate ('1'); the angular position of the exoskeleton; and the time to complete a trial (Tc). In Figure 3.4, an example time course response of the BCI output (rest ('0') or activate ('1')), the FES status, and the angular position of the exoskeleton for participant P05 is presented. This example shows the typical behavior of the system output in real-time when the participant was in good control of the training device. As shown in Figure 3.4, the participant successfully generated positive BCI output (classification output '1') that triggered the exoskeleton and the FES. However, not all positive BCI predictions in the figure are true positives. Three of the positive BCI output labeled as 'PO' did not trigger any device. These 'PO' occurred at 1.52s, 0.55s, and 5.65s respectively after a true positive. The first and the last POs were very likely false positives because they took place more than 1s after a true positive. The undesired positive output, however, did not affect the overall system performance. This was caused by the system design that, when the exoskeleton was in operation, no other devices could be triggered.

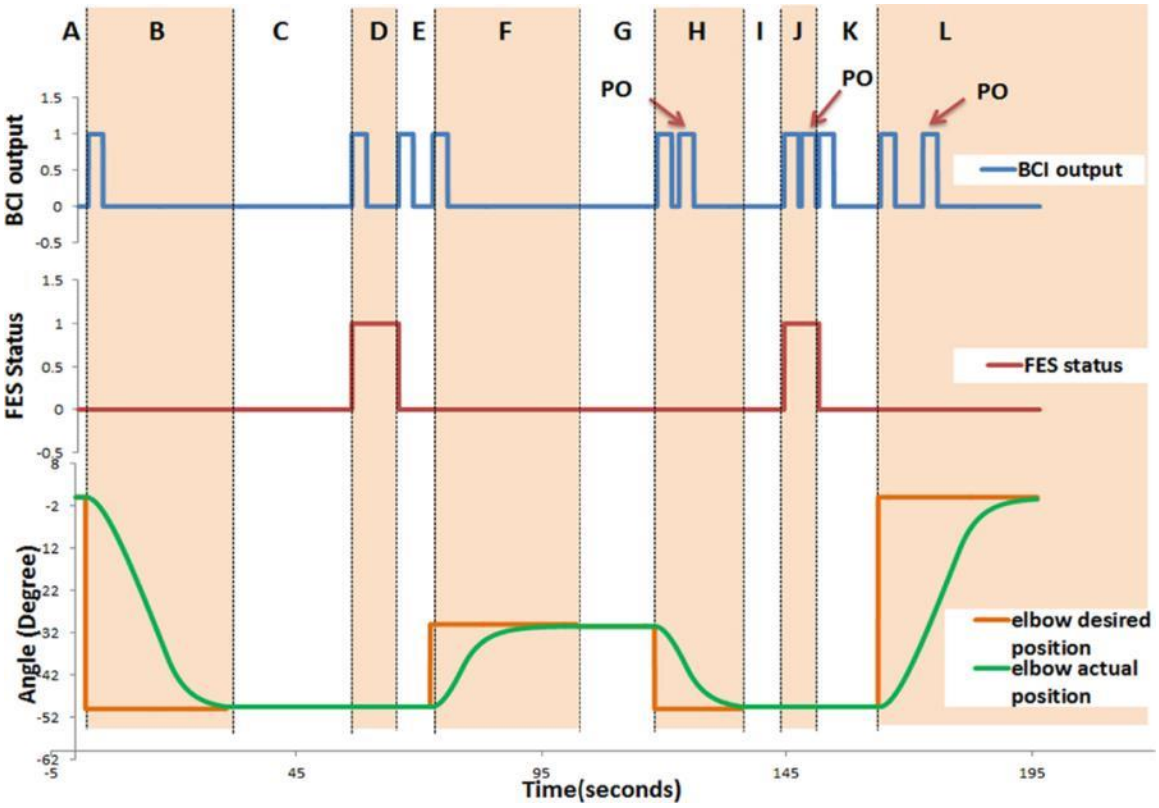

Figure 3.4 **Time course of the system response from one of the participants** [29]**.**

3.4. Discussion

The BCI cross-validation accuracy is an important metric that has been widely used to assess the performance of the BCI model generated offline. The results showed that the BCI cross-validation accuracy was in a range between 55.78% and 83.20%, which was within the same range compared to the BCI applications reported in the literature [174]. The BCI accuracy for some of the participants (P02, P04, P05, P06, P07, and P08) was not very high (<70%). Some of these participants reported that they were not able to focus when performing motor imagery due to their age and stroke-related problems. Also, the configuration of electrodes placed around the motor cortex area for the Emotiv system was sparse, which may also result in the relatively low accuracy in these participants. To improve the performance of the BCI system, dense EEG acquisition montage could be used, with more electrodes around the motor cortex area. Also, EEG signals are generally considered to have a low signal-to-noise ratio and are frequently contaminated by artifacts. These types of unwanted noise originate either

from the user (e.g. ocular and adjacent muscle activity) or from other non-physiological sources, such as power line interference. These artifacts could affect the quality of the EEG signals and subsequently deteriorate the BCI classification performance.

During this study, the author noticed four potential problems with EEG applications in stroke rehabilitation.

Firstly, a rest-vs-MI BCI model was generated from the model generation process. The rising edge of the BCI output (output switching from “0” to “1”) was configured as the triggering signal to move from one phase of the training protocol to the next phase. One type of MI was used consistently throughout the training. According to the literature, goal-oriented tasks are generally preferred in rehabilitation training protocols [65], [66], [69]. However, with the EEG based BCI involved in the protocol, it takes time and effort to go through EEG data acquisition and model training for every rehabilitation training task. Therefore, a general model, which is reusable for different rehabilitation training tasks, would drastically reduce the training time as the data acquisition would be done with only one single motor task. However, no study has investigated whether an EEG model trained using the EEG signals from motor imagery of a single upper extremity movement (e.g. elbow flexion and extension) could be used to classify the motor imagery from other similar motor imagery (e.g. motor imagery of opening a door, combing hair, placing a ball into a basket, etc.).

Secondly, for this preliminary pilot study, the participants were able to learn to control the proposed portable EEG based BCI system within a few trials. However, based on the feedback from the participants, they were expecting substantial motor function improvement with less effort. Some papers suggested that combining motor imagery training and physical training would further boost the rehabilitation outcome. With major hardware and software modifications, the proposed platform could facilitate such sophisticated rehabilitation training protocols. The feasibility and possible efficacy of such rehabilitation training platforms should be investigated with a relatively long-term rehabilitation training protocol.

Thirdly, although many methods and algorithms have been developed to analyze the target EEG signals, the transition of the offline analysis method to an online BCI application is another major factor that affects the BCI performance. Potentially, filtering

the prediction/classification output of the BCI system could supress the false positives and improve the sensitivity. However, no papers have investigated how to improve the performance of the online BCI application by filtering the prediction output of the classifier.

Fourthly, in order to quantify the rehabilitation outcomes, motor function is generally monitored through standardized clinical motor ability assessments during or after the rehabilitation. However, those standard motor assessments are neither efficient nor completely objective. According to the literature, EEG has shown its potential as a motor function indicator (BSI, DAR, LPS). However, in previous studies, the correlation between the EEG-based motor function scores and questionnaire-based motor function assessment scores were low. Those scores proposed in the literature are not accurate enough to be used as motor assessments. New methods of calculating motor function scores from EEG data should be investigated, in order to assess motor function automatically and reliably.

3.5. Chapter Summary

In this chapter, a portable BCI controlled exoskeleton system for rehabilitation was designed and developed in the lab. The feasibility of a complex portable BCI-controlled rehabilitation platform was proven. Four possible challenges of EEG applications in stroke rehabilitation were identified from this pilot study. In the following chapters, different methods and approaches were proposed and investigated according to the challenges identified in this chapter. These four challenges were addressed separately in Chapters 4 to 7.

Chapter 4.

Re-using EEG models generated with different motor imageries

This chapter is reproduced with permission from the following paper I co-authored:

Zhang, X., Yong, X., & Menon, C. (2017). Evaluating the versatility of EEG models generated from motor imagery tasks: An exploratory investigation on upper-limb elbow-centered motor imagery tasks. *PLoS ONE*, *12*(11). https://doi.org/10.1371/journal.pone.0188293

Some sections are adapted to fit within the scope and comply with the format of the thesis.

This chapter is included to address Objective 1, which is related to the investigation of using one MI to generate the BCI model and classify other MIs.

4.1. Introduction

Electroencephalography (EEG) has recently been considered for applications in the rehabilitation for people with motor deficits [84][93]. EEG data from the motor imagery of different body movements have been used, for instance, as an EEG-based control method to send commands to rehabilitation devices that assist people to perform a variety of rehabilitation training tasks. Motor imagery can be either goal-oriented or be related to a single joint. Goal-oriented motor imagery refers to imagery on context-specific movements, such as grasping a glass of water for drinking or eating with a spoon [94]. On the other hand, single joint motor imagery refers to imagining a single joint movement that is not goal-oriented or has a specific meaningful purpose. Examples of single joint motor imagery include imagining flexing or extending the elbow, the wrist, or another joint without grasping an object or any specific function [94]. However, it is both time and effort consuming to go through data collection and model training for every rehabilitation training task.

The use of a general model approach (GM) could potentially avoid repetitive data acquisition and model generation process. Here, general model means EEG

classification model acquired while the participant is performing certain motor imagery and being used for classification of another motor imagery. However, it is not known whether an EEG model trained using the EEG signals of the motor imagery of a single upper extremity movement (e.g. elbow flexion and extension) could be used to classify the motor imagery of similar other movements (e.g. opening a door, combing hair, placing a ball into a basket, etc.). To the best of the authors' knowledge, it is also not known which movement would work best to generate the GM. The investigation of whether a model can be reused in different training tasks is an important problem to be addressed especially in EEG controlled rehabilitation applications, where each goal-oriented movement is functionally different from the others.

The objective of this chapter was to avoid the repetitive EEG data acquisition and model training in BCI setups by re-using one BCI model for multiple MI tasks. In this chapter, the author investigated the versatility of motor imagery, by using an EEG model from one type of motor imagery (e.g.: elbow extension and flexion) to classify EEG from other types of motor imagery activities (e.g.: open a drawer). In this chapter, versatility refers to EEG model generated from one specific MI task with high test accuracy for other MI tasks (higher inter-task testing accuracy). Given the complexity of the problem, this exploratory study focuses only on upper-extremity movements to simplify the investigation. Specifically, all the tasks were selected to be centered on the elbow joint. And the general rules of selecting these types of motor imagery tasks was also investigated in this chapter.

4.2. Methods

In this chapter, 12 able-bodied participants (aged 20-33 years old, 10 males and 2 females) agreed to join the study. The protocol was approved by the Office of Research Ethics at Simon Fraser University. All participants signed informed consent forms before taking part in the experiment. Each individual was seated in front of a computer monitor, which provided a simple Graphical User Interface (GUI) that displayed pictures or cues to the participant.

4.2.1. Experimental protocol

A 32-channel, EGI Geodesic N400 system (Electrical Geodesics Inc., Eugene, OR, USA) was used to acquire the EEG data from the participants. EEG data were amplified and recorded at a sampling rate of 1 kHz. The electrode contact sites are shown in Figure 4.1. 17 channels were used in this study, as the remaining channels were located on the face (the EGI cap does not allow to re-position the electrodes). All participants were requested to wear the EGI sensor net for approximately 40 minutes during this experiment. During the experiment, the participants could take a break if desired. The impedance of the EEG contacts was measured every 30 minutes to maintain signal quality.

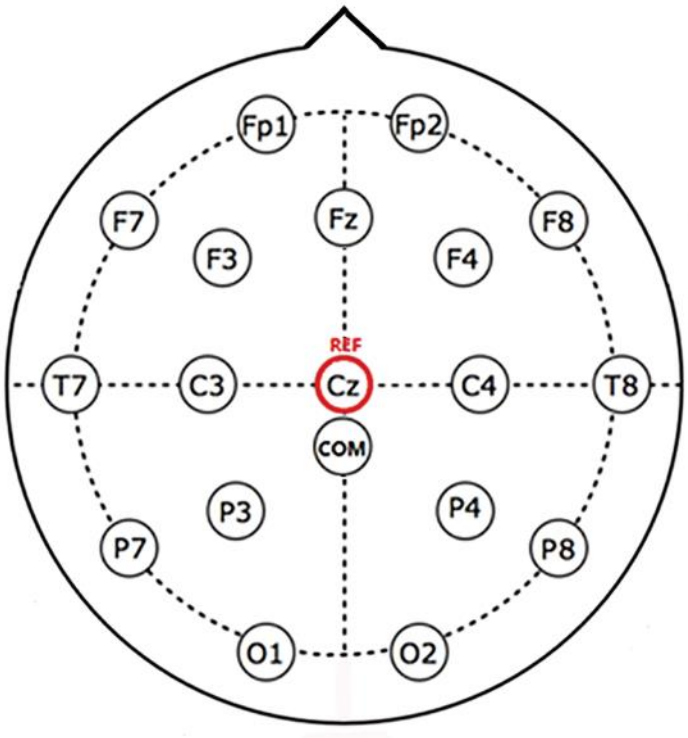

Figure 4.1 Contact montage of the EEG system in the experiment, 17 channels were used. Cz was defined as the reference contact by the EGI system, COM was the common ground contact.

EEG data were collected using the Stimulus Presentation mode in BCI2000 [170]. During Stimulus Presentation, customized pictures were shown on the screen while the EEG signals were recorded and filtered with a bandpass filter of 0.1-40 Hz. In

this study, the pictures for ten different tasks were randomly selected and displayed on the screen. These pictures are presented in Figure 4.2. The participants were asked to repetitively perform the kinaesthetic motor imagery task displayed on the screen for 4 seconds without actually moving their limb. The participants were instructed to finish two repetition of MI during the predefined 4 seconds. Kinaesthetic motor imagery means that the participants were required to perform imaginary movement by focusing on imagining the sensation of the movement [175]. The participants were required to perform MI on their dominant hand.

Figure 4.2 **Picture of the tasks that were used in the Stimulus Presentation tasks where: (a)Rest Task, rest and stay alert; (b)Elbow Task, imagine elbow flexion and extension; (c)Drawer Task, imagine opening and closing a drawer; (d)Soup Task, imagine drinking soup with a spoon; (e)Weight Task, imagine lifting and putting down a dumbbell; (f)Door Task, imagine opening and closing a door; (g)Plate Task, imagine cleaning a plate; (h)Comb Task, imagine combing hair; (i)Pizza Task, imagine cutting a pizza with a pizza cutter; and (j) Pick &Place Task, imagine picking up a ball and put it into a basket;**

In this study, nine motor imagery tasks were chosen as upper limb movements. Tasks were selected to primarily involve the elbow joint. These motor imagery tasks can be divided into three main categories: 1) simple joint task that does not have any context meaning. In this chapter, Elbow Task, Drawer Task, and Weight Task were chosen. In these tasks the participants were required to only focus on a simple elbow joint movement. Among the three tasks, the differences were only about the force that were exerted in the imagination; 2) simple elbow joint tasks that are commonly executed in daily life and require a relatively low level of synergy of other joints. In this chapter Door Task, Plate Task, and Comb Task were chosen; and 3) goal-oriented tasks, which require trajectory planning and multiple joint synergies. In this chapter, Soup Task, Pizza Task, and Pick&Place Task were chosen. The specific instructions given to the participants with respect to the ten tasks are summarized below:

1. Rest (Fig 2(a)): rest while looking at the center of the cross;
2. Elbow task (Fig 2(b)): kinaesthetically imagine flexing and extending the elbow of the dominant arm;
3. Drawer task (Fig 2(c)): kinaesthetically imagine opening and closing a drawer with the dominant hand;
4. Soup task (Fig 2(d)): kinaesthetically imagine getting a spoonful of soup and drinking the soup using the dominant hand;
5. Weight task (Fig 2(e)): kinaesthetically imagine lifting and putting down a dumbbell with the dominant hand;
6. Door task (Fig 2(f)): kinaesthetically imagine opening and closing door with the dominant hand on the doorknob;
7. Plate task (Fig 2(g)): kinaesthetically imagine cleaning a plate with only elbow extension and flexion movement;
8. Comb task (Fig 2(h)): kinaesthetically imagine combing hair with the dominant hand.
9. Pizza task (Fig 2(i)): kinaesthetically imagine cutting a pizza with a pizza cutter with the dominant hand;
10. Pick&Place Task (Fig 2(j)): kinaesthetically imagine picking a ball and placing it into a basket with the dominant hand.

During the Stimulus Presentation, each picture was displayed on the screen for 4-6 seconds, followed by 4-6 seconds of rest, and the timing was randomized by the software in order to prevent participants from adapting to the data acquisition sequence. When the picture was displayed on the screen, the participant was requested to perform

motor imagery of the corresponding task repetitively for 1-2 repetitions. For each participant, the test consisted of 15 consecutive runs. Each run consisted of 4 Rest, 4 Elbow Tasks and 16 other tasks (2 for each of the remaining tasks). Each run lasted for approximately 3 minutes. To ensure compliance with the protocol, one observer was assigned to monitor the participants to ensure they were not moving during the task. In the case of the slightest movement, the recorded data were disregarded, and the participant was asked to repeat the experiment.

4.2.2. Feature extraction and classification

The data acquired were analyzed using BCILAB [176], a BCI toolbox based on Matlab. The data were first resampled at 250 Hz to save system resources, so that the system delay caused by the processing could be minimized. Then, a finite impulse response (FIR) bandpass filter was used to filter out the 6–35 Hz frequency band. The FIR bandpass filter used in this part was used to suppress the artifacts and the unwanted frequency components of the recorded EEG data. The FIR filter used here retained the mu (7-13 Hz) and beta (13-30 Hz) rhythms in the EEG signal, which have been reported to exhibit event-related synchronization and desynchronization (ERD/ERS) during motor imagery [130]. The band power changes of the mu and beta rhythms have been used in BCI systems to classify EEG signals related to motor imagery [133], [134], [138]. Therefore, band power (BP) of a certain band frequency can be used as a basic feature for classification [130], [177]. However, ERD/ERS signals could be overlapped in time and space by multiple signals from different brain tasks. For this reason, in some cases, it may not be sufficient to use simple methods such as a bandpass filter to extract the desired band power. The literature suggests that spatial filters, like a common spatial pattern (CSP), could be appropriate [132]. The performance of spatial filters is dependent on its operational frequency band. Therefore, filter bank CSP (FBCSP) was also included in this study to avoid this potential problem [167], [178].

As each participant had a different reaction time to the stimulus, nine different epoch periods were extracted from the EEG data to find out the optimal epoch that led to the best EEG control performance. The different epochs used are presented in Table 4.1

Table 4.1 Epoch periods used in data analysis.

Epoch ID	1	2	3	4	5	6	7	8	9
Epoch Period*	0.5-2.5s	1-3s	1.5-3.5s	2-4s	2.5-4.5s	3-5s	0-3s	1-4s	1-5s

*Refer to the time after the stimulus was shown on the screen

In this chapter, BP [179], CSP [134] and FBCSP [178] were used as feature extraction algorithms to extract features, for each EEG epoch. Detailed information is presented in Table 4.2.

Table 4.2 Feature setting for model training

Algorithm	Frequency Band	Feature Dimension
BP	6-32Hz	17
CSP	6-32Hz	6
FBCSP	6-15Hz; 15-25Hz; 25-32Hz	18

The features were then sent to classifiers. Since the author wanted to evaluate the influence of different motor imageries in this chapter, classifiers were limited with basic classifiers. Linear discriminant analysis (LDA) and dual-augmented lagrangian (DAL) methods [180] [181] were used for classification. All classifiers were regularized during training. For LDA, analytical covariance shrinkage was used to regularize the dimensionality of the model [182]. For DAL, the dual-spectral logistic norm was used for regularization, with grid searching λ from 2^{-15} to 2^{10}, the step size being 2 times that of the previous value [183]. A binary classifier was generated for the EEG features obtained from each combination of the Rest Task data and one of the Tasks (b)-(j) respectively. A 5×5 cross-validation method was used to validate the performance of the classifiers.

Three features (i.e. BP, CSP, and FBCSP) and 2 classifiers (LDA, DAL) were included as a possible combination, which resulted in 6 models per epoch for each participant. On top of the features and classifiers, 9 possible time episodes were included in EEG data epoch extraction, which resulted in 54 different models (3×2×9=54). The best model for each motor imagery task for each participant was selected. Each participant performed 9 different tasks, and 12 participants were included in this study. Through this process, 108 models were generated in total (9×12=108). By

doing this, a uniform objective classification standard was set for all nine different motor imagery tasks. The performance of the models from these motor imagery tasks is presented in the following sections.

4.2.3. Model training and testing

The main goal of the work was to assess the versatility of the EEG models derived from different motor imagery tasks. This problem was studied in the inter-task testing, where the model generated from one type of motor imagery task was tested with data from another motor imagery task. The data were collected to investigate this inter-task problem. Specifically, 30 trials (T) for each of the 9 motor imagery tasks (i.e. T_1 -T_9) were collected. For each task, the data were randomized. Furthermore, 60 trials of rest were recorded. After randomization, they were divided into two groups: training (R_{TR}) and testing (R_{TE}). Therefore, a total number of 330 trials (i.e. 30 trials × 9 motor imagery tasks + 30 rest for training (R_{TR}) + 30 rest for testing (R_{TE})) were recorded.

During training, 9 two-class models were created for each participant. Each model, corresponding to a single task, was trained using the 30 trials of rest (R_{TR}) collected for training purposes (class 1) + the 30 trials related to the single task in question (class 2). Specifically, Model 1 (m_{1_INTER}) was trained using T_1 and R_{TR}, model 2 (m_{2_INTER}) was trained using T_2 and R_{TR}, etc. Table 4.3 shows the training datasets for each model. 5-fold cross-validation was used to generate each of the 9 two-class models, which included: 1) randomly dividing the training set into 5 subsets; 2) training models on 4 subsets, and test models on the remaining one; 3) loop through the 5 subsets and 4) return the model with the highest validation accuracy for later analysis.

Table 4.3 Data usage in training models for inter-task problem

Model Name	m_{1_INTER}	m_{2_INTER}	m_{3_INTER}	m_{4_INTER}	m_{5_INTER}	m_{6_INTER}	m_{7_INTER}	m_{8_INTER}	m_{9_INTER}
Data Used	T_1 and R_{TR}	T_2 and R_{TR}	T_3 and R_{TR}	T_4 and R_{TR}	T_5 and R_{TR}	T_6 and R_{TR}	T_7 and R_{TR}	T_8 and R_{TR}	T_1 and R_{TR}

For testing, each model was tested with data collected for the other models. Specifically, m1 was tested with 8 testing datasets, the first being T2+RTE, the second

being, T3+RTE, the third T4+RTE, etc. Table 4.4 shows the data usage in testing datasets.

Table 4.4 Data usage in the inter-task testing

Model Name	Elbow	Drawer	Spoon	Weight	Door	Plate	Comb	Pizza	Pick& Place
m_{1_INTER}	----	T_2+R_{TE}	T_3+R_{TE}	T_4+R_{TE}	T_5+R_{TE}	T_6+R_{TE}	T_7+R_{TE}	T_8+R_{TE}	T_9+R_{TE}
m_{2_INTER}	T_1+R_{TE}	---	T_3+R_{TE}	T_4+R_{TE}	T_5+R_{TE}	T_6+R_{TE}	T_7+R_{TE}	T_8+R_{TE}	T_9+R_{TE}
m_{3_INTER}	T_1+R_{TE}	T_2+R_{TE}	---	T_4+R_{TE}	T_5+R_{TE}	T_6+R_{TE}	T_7+R_{TE}	T_8+R_{TE}	T_9+R_{TE}
m_{4_INTER}	T_1+R_{TE}	T_2+R_{TE}	T_3+R_{TE}	---	T_5+R_{TE}	T_6+R_{TE}	T_7+R_{TE}	T_8+R_{TE}	T_9+R_{TE}
m_{5_INTER}	T_1+R_{TE}	T_2+R_{TE}	T_3+R_{TE}	T_4+R_{TE}	---	T_6+R_{TE}	T_7+R_{TE}	T_8+R_{TE}	T_9+R_{TE}
m_{6_INTER}	T_1+R_{TE}	T_2+R_{TE}	T_3+R_{TE}	T_4+R_{TE}	T_5+R_{TE}	---	T_7+R_{TE}	T_8+R_{TE}	T_9+R_{TE}
m_{7_INTER}	T_1+R_{TE}	T_2+R_{TE}	T_3+R_{TE}	T_4+R_{TE}	T_5+R_{TE}	T_6+R_{TE}	---	T_8+R_{TE}	T_9+R_{TE}
m_{8_INTER}	T_1+R_{TE}	T_2+R_{TE}	T_3+R_{TE}	T_4+R_{TE}	T_5+R_{TE}	T_6+R_{TE}	T_7+R_{TE}	---	T_9+R_{TE}
m_{9_INTER}	T_1+R_{TE}	T_2+R_{TE}	T_3+R_{TE}	T_4+R_{TE}	T_5+R_{TE}	T_6+R_{TE}	T_7+R_{TE}	T_8+R_{TE}	---

Before running the inter-task problem, the authors wanted to ensure that the considered BP/CSP/FBCSP+LDA/DAL method was a suitable method for the motor imagery tasks considered. Therefore, an intra-task problem was first addressed. In this case, each task had to be tested with data collected from the same motor imagery task (e.g. a model trained with T1 could not be tested with T2 as for the inter-task case as T1 and T1 were datasets related to different tasks, thus not suitable for the intra-task case). For this reason, each of the 30 trials was divided into training and testing datasets for the intra-task case. Specifically, 24 trials of each motor imagery task (e.g. T1_TR) together with 24 trials of Rest Task (Rintra_TR) were used for training. The remaining six trials of the same motor imagery task (e.g. T1_TE) together with 6 trials of Rest Task (Rintra_TE) were used for testing. These trials were randomly selected from the whole dataset, not determined through a cross validation process, as a limitation of computational resources. Table 4.5 shows the training and testing dataset for each model.

Table 4.5 Training and testing datasets for the Intra-task problem.

Model Name	Data used in training	Data used in Testing
m_{1_INTRA}	T_{1_TR} and R_{intra_TR}	T_{1_TE} and R_{intra_TE}
m_{1_INTRA}	T_{2_TR} and R_{intra_TR}	T_{2_TE} and R_{intra_TE}
m_{1_INTRA}	T_{3_TR} and R_{intra_TR}	T_{3_TE} and R_{intra_TE}
m_{1_INTRA}	T_{4_TR} and R_{intra_TR}	T_{4_TE} and R_{intra_TE}
m_{1_INTRA}	T_{5_TR} and R_{intra_TR}	T_{5_TE} and R_{intra_TE}
m_{1_INTRA}	T_{6_TR} and R_{intra_TR}	T_{6_TE} and R_{intra_TE}
m_{1_INTRA}	T_{7_TR} and R_{intra_TR}	T_{7_TE} and R_{intra_TE}
m_{1_INTRA}	T_{8_TR} and R_{intra_TR}	T_{8_TE} and R_{intra_TE}
m_{1_INTRA}	T_{9_TR} and R_{intra_TR}	T_{9_TE} and R_{intra_TE}

4.2.4. The coefficient of determination (R^2 value)

The coefficient of determination (R^2 value) is a common method in BCI research, giving a statistical estimation on the difference of two types of distributions based on the variances of the two [15]. In the field of BCI research, the R^2 value is usually calculated based on certain secondary features of EEG data collected in two conditions (e.g. resting state and MI). By analyzing the R^2 value of such features of the EEG data, EEG analysis methods and BCI applications could be built based on the results.

For the consistency of the R^2 analysis, in this section, EEG data collected from MI of the left hand were flipped between the corresponding channels on the right and left hemisphere. The R^2 value at each electrode location was computed for all participants and all combinations of different tasks in order to investigate the topographical distribution on the scalp of the difference between rest and the other imaginary tasks. The frequency that generated the highest R^2 value was used to generate the topography. The 6-32Hz frequency component was considered for this representation as motor imagery was investigated.

4.2.5. Statistical analysis

The accuracy results were analyzed with statistical tools to investigate the significance of the performance difference with models generated from different MI tasks. Considering that the sample size was relatively low, the accuracy results were first analyzed with Shapiro-Wilk parametric hypothesis test to test the normality of the dataset. Based on the normality of the dataset, either one-way analysis of variance (for

normally distributed dataset) or Kruskal-Wallis test (for non-normally distributed dataset) was used to test if any of the accuracy distribution was statistically different. Then, a post hoc analysis was conducted to identify the MI tasks that had statistically different accuracies compared to the other tasks.

4.3. Results

4.3.1. Intra-task problem: cross-validation results using the training dataset

For the inter-task problem, the models were generated according to Table 4.3. Figure 4.3 summarizes the distribution of the feature algorithms and classifiers used to obtain the model. Among all the features and classifiers, CSP together with LDA was the most common combination: it took 35% of all the 108 models. BP feature with LDA contributed 30% to all the models.

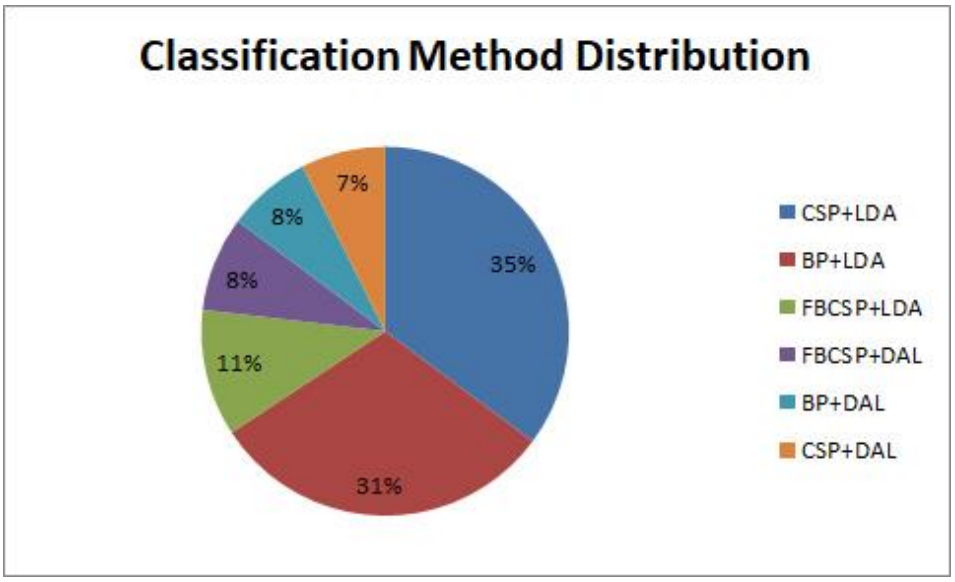

Figure 4.3 Distribution of the classification method of the highest cross-validation accuracy.

The cross-validation accuracy achieved for each of the nine EEG models and participants is shown in Table 4.6. This table reports the cross-validation accuracy with the highest value obtained from the optimal combination of the epoch period, feature extraction method and the classifier discussed earlier.

Table 4.6 Intra-task 5x5 cross-validation accuracy for each participant.

ID*	Elbow	Drawer	Spoon	Weight	Door	Plate	Comb	Pizza	Pick & Place	Mean± SD
H1	0.840	0.757	0.845	0.840	0.817	0.893	0.832	0.893	0.943	0.851±0.053
H2	0.705	0.748	0.752	0.747	0.758	0.723	0.712	0.775	0.740	0.740±0.023
H3	0.783	0.803	0.755	0.788	0.823	0.793	0.772	0.822	0.830	0.797±0.025
H4	0.797	0.743	0.840	0.798	0.802	0.812	0.832	0.905	0.788	0.813±0.044
H5	0.835	0.817	0.883	0.855	0.878	0.820	0.853	0.903	0.825	0.852±0.031
H6	0.670	0.732	0.772	0.708	0.717	0.768	0.792	0.738	0.753	0.739±0.037
H7	0.852	0.848	0.805	0.798	0.850	0.942	0.822	0.907	0.883	0.856±0.047
H8	0.810	0.800	0.890	0.830	0.860	0.883	0.765	0.878	0.837	0.840±0.043
H9	0.777	0.787	0.788	0.847	0.792	0.782	0.823	0.787	0.885	0.807±0.037
H10	0.943	0.952	0.900	0.930	0.928	0.882	0.957	0.930	0.997	0.935±0.033
H11	0.775	0.733	0.728	0.780	0.695	0.755	0.733	0.712	0.870	0.754±0.052
H12	0.842	0.802	0.815	0.855	0.738	0.733	0.820	0.912	0.790	0.812±0.056

*H1-H12 are the IDs for the participants

As shown in Table 4.6, the task with the highest cross-validation accuracy was subject-specific. H10 achieved the highest mean cross-validation accuracy (0.935±0.033) among the participants. This participant achieved the highest cross-validation accuracy for the Pick&Place Task (0.997± 0.023). H6, on the other hand, had the lowest cross-validation accuracy (0.739±0.037). The motor imagery task with the highest average cross-validation accuracy is Comb task (0.792± 0.160). Figure 4.4 shows the 5×5 cross-validation accuracy averaged across participants. The cross-validation accuracy ranges from 0.793±0.062 to 0.847±0.076, with the Pizza Task having the highest cross-validation accuracy and the Drawer Task having the lowest mean cross-validation accuracy. Based on the cross-validation accuracy results, the null hypothesis of Shapiro-Wilk parametric hypothesis test cannot be rejected (p=0.430), and a one-way analysis of variance (ANOVA) was used to check the cross-validation accuracy difference among different tasks No statistical difference was found (p=0.536).

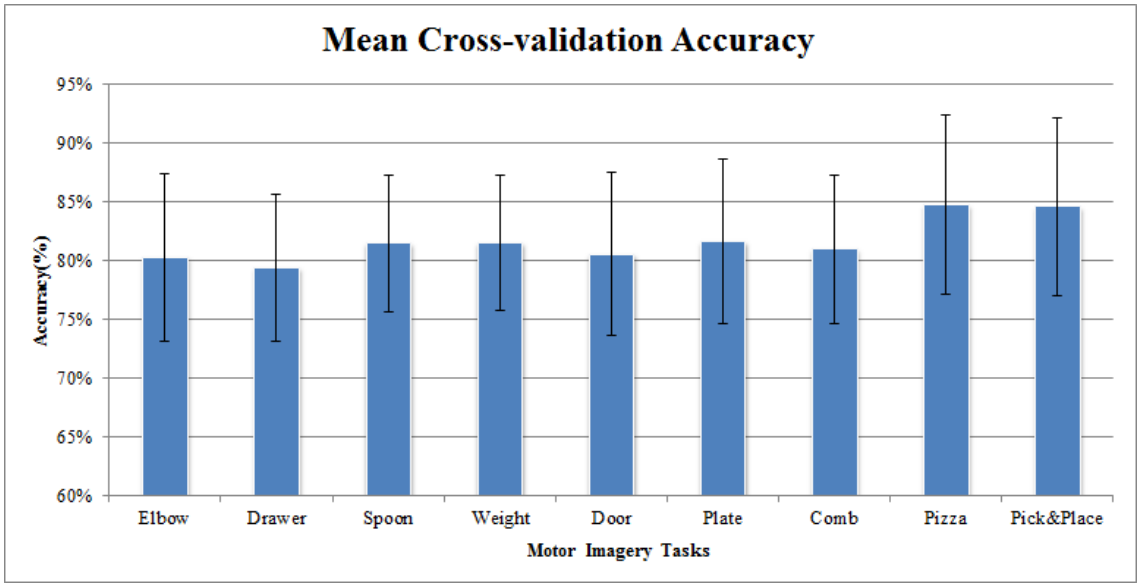

Figure 4.4 Mean 5×5 cross-validation accuracy for different motor imagery tasks

4.3.2. Inter-task problem: testing result

The models were generated and tested as described in Table 4.4 for testing the results of the inter-task problem. The test accuracy obtained from the inter-task test is summarized in Table 4.7. More specifically, the model for each motor imagery task was tested on 30 trials of eight other motor imagery tasks. For example, the model generated from the Elbow Task was tested with EEG data from all the other tasks, but not from Elbow Task. All test accuracies for all EEG models were greater than 0.5. Table 4.7 also shows that Weight Task model has the highest average inter-task test accuracy. More specifically, it has the highest average accuracy when tested on data from other motor imagery tasks.

Table 4.7 Inter-task test accuracy summary

		Test Data (30 trials together with 30trials of Rest Task data)									
		Elbow	Drawer	Spoon	Weight	Door	Plate	Comb	Pizza	Pick& Place	Mean ±SD
Model Name	Elbow	---	0.561	0.583	0.607	0.578	0.597	0.589	0.635	0.603	0.594 ±0.022
	Drawer	0.637	---	0.572	0.571	0.583	0.607	0.578	0.588	0.581	0.589 ±0.022
	Spoon	0.592	0.535	---	0.533	0.538	0.547	0.535	0.549	0.535	0.545 ±0.020
	Weight	0.641	0.604	0.617	---	0.565	0.596	0.588	0.626	0.600	0.605 ±0.024
	Door	0.601	0.561	0.556	0.528	---	0.563	0.533	0.558	0.532	0.554 ±0.024
	Plate	0.597	0.543	0.531	0.539	0.538	---	0.524	0.551	0.519	0.543 ±0.024
	Comb	0.637	0.536	0.565	0.568	0.546	0.557	---	0.588	0.538	0.567 ±0.033
	Pizza	0.615	0.524	0.569	0.536	0.543	0.536	0.540	---	0.532	0.549 ±0.030
	Pick& Place	0.645	0.563	0.567	0.572	0.554	0.565	0.553	0.586	---	0.576 ±0.030
	Mean± SD	0.620± 0.022	0.553± 0.025	0.570± 0.024	0.557± 0.027	0.556± 0.018	0.571± 0.026	0.555± 0.026	0.585± 0.032	0.555± 0.034	---

The mean values reported in the last column of Table 4.7 summarize the averaged inter-task test accuracy for models generated from the nine motor imagery tasks. This indicates the ability of the models to classify EEG data from other motor imagery tasks. The mean values reported in the last row of Table 4.7 summarize the averaged inter-task test accuracy for EEG data from the nine motor imagery tasks, which indicates the versatility of EEG data for the nine motor imagery tasks. The mean model test accuracy ranges from 0.543±0.023 to 0.605±0.022. The model generated from the Weight task data has the highest mean inter-task test accuracy, while the model generated from Plate Task data has the lowest mean test accuracy. The mean data test accuracy ranges from 0.553±0.025 to 0.620±0.022. The data from Elbow Task

has the highest mean inter-task test accuracy and the data from the Drawer Task has the lowest mean inter-task test accuracy.

A Shapiro-Wilk parametric hypothesis test was performed to test the normality of the test accuracies for different task data in Table 4.7. The test accuracies for models Drawer, Spoon, Plate, Pizza, Pick&Place are not normally distributed (their *p* values are 0.030, 0.002, 0.030, 0.012, and 0.006 respectively). Kruskal-Wallis test showed the inter-task test accuracy is statistically different ($p=2.6\times10^{-5}$), see Figure 4.5.

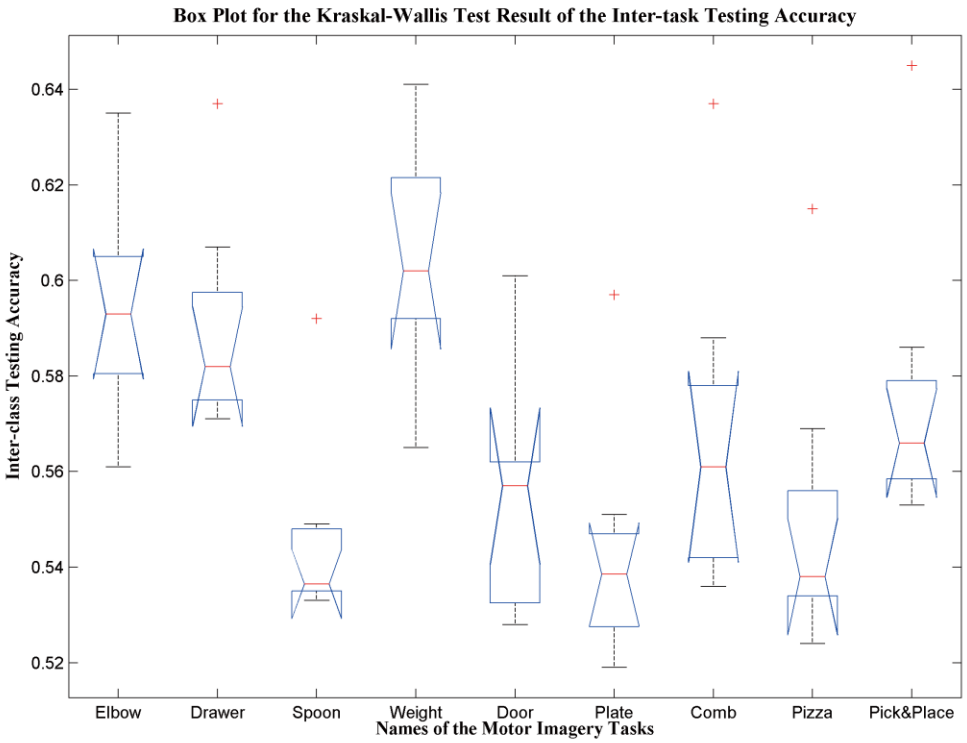

Figure 4.5 Box plot for the Kruskal-Wallis Test result for the inter-task testing accuracy.

In the post-hoc analysis, Dunn & Sidák's approach was used [184]. The model from the Weight Task has statistically higher inter-task test accuracy, compared to the model from the Spoon Task, Door Task, Plate Task, and Pizza Task($p<0.05$). No statistical difference was found among Elbow Task, Drawer Task, and Weight Task ($p>0.05$), see Table 4.8.

Table 4.8 Dunn & Sidák post-hoc analysis of the inter-task testing accuracy. Checkmarks indicate models whose inter-task accuracies are significantly different ($p<0.05$).

Model Names	Elbow	Drawer	Spoon	Weight	Door	Plate	Comb	Pizza	Pick& Place
Elbow			√			√			
Drawer									
Spoon									
Weight			√			√		√	
Door									
Plate	√			√					
Comb									
Pizza				√					
Pick& Place									

4.3.3. The Coefficient of Determination Analysis Result

The averaged R^2 value for different tasks is shown in Figure 4.6. One of the participants (H5) was left handed. The channels of his EEG were therefore flipped between left and right hemisphere in this analysis.

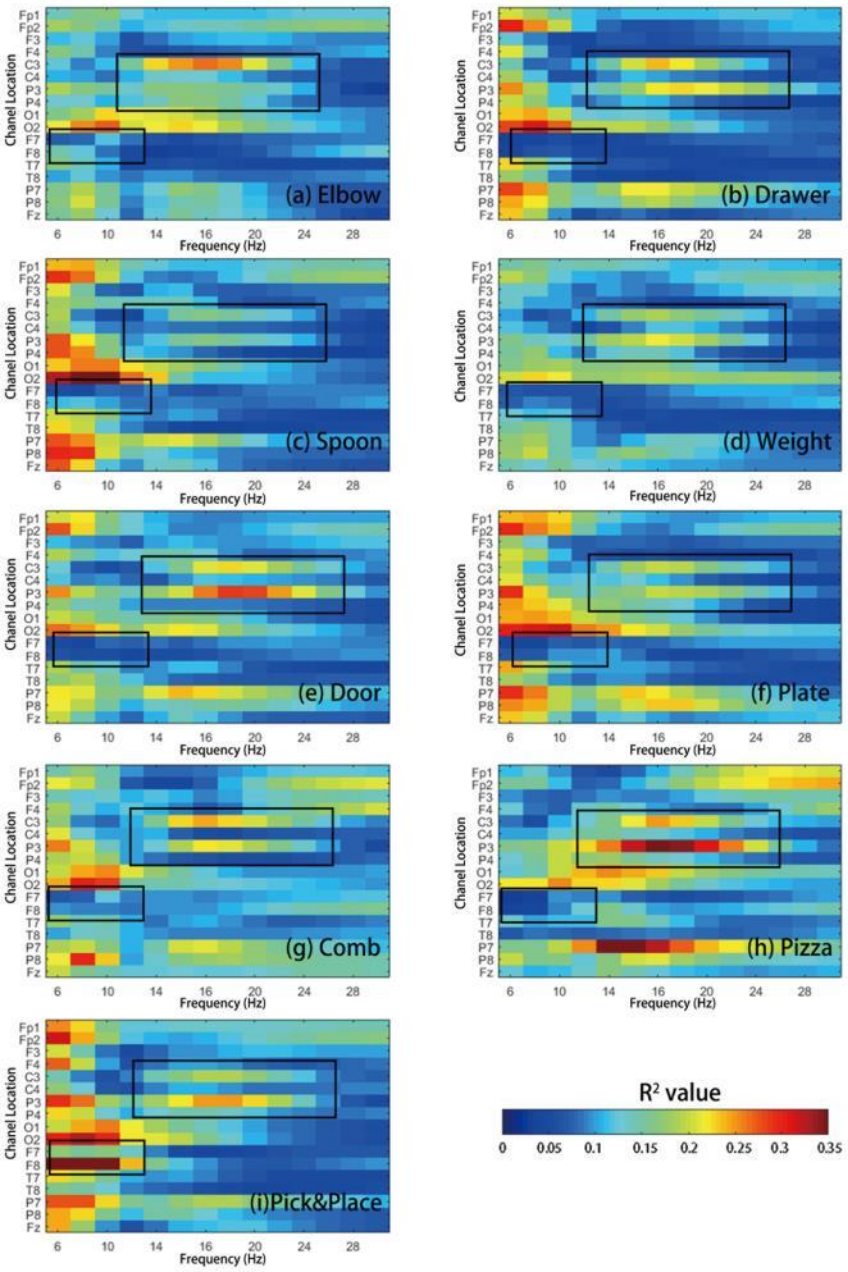

Figure 4.6 **EEG R^2 analysis for different motor imagery tasks, averaged among participants. (a)R^2 value mapping for Rest Task vs Elbow Task; (b) R^2 value mapping for Rest Task vs Drawer Task;(c) R^2 value mapping for Rest Task vs Soup Task;(d) R^2 value mapping for Rest Task vs Weight Task;(e) R^2 value mapping for Rest Task vs Door Task(f) R^2 value mapping for Rest Task vs Plate Task;(g) R^2 value mapping for Rest Task vs Comb Task;(h) R^2 value mapping for Rest Task vs Pizza Task;(i) R^2 value mapping for Rest Task vs Pick&Place Task. Frequency bands with the highest R2 value among the nine MI tasks are outlined with a black box.**

From Figure 4.6, it can be observed that most of the EEG activities are located in the central and parietal lobe area. Most of the EEG activities for different motor imagery tasks (at C3 channel) are located around 12-20Hz. The peak activities for all the motor imagery tasks were always centered around 18Hz in C3 and P3 channel. Also, some activities were found in the F8 channel between 6-16Hz, which might be related to the motor planning [130]. Since all these two activities were both been seen around 16Hz, the topography analysis of 16Hz is shown in Figure 4.7, with H10, who had the highest cross-validation accuracy during the training among the participants. For H10, the data acquisition was performed with MI of the right hand.

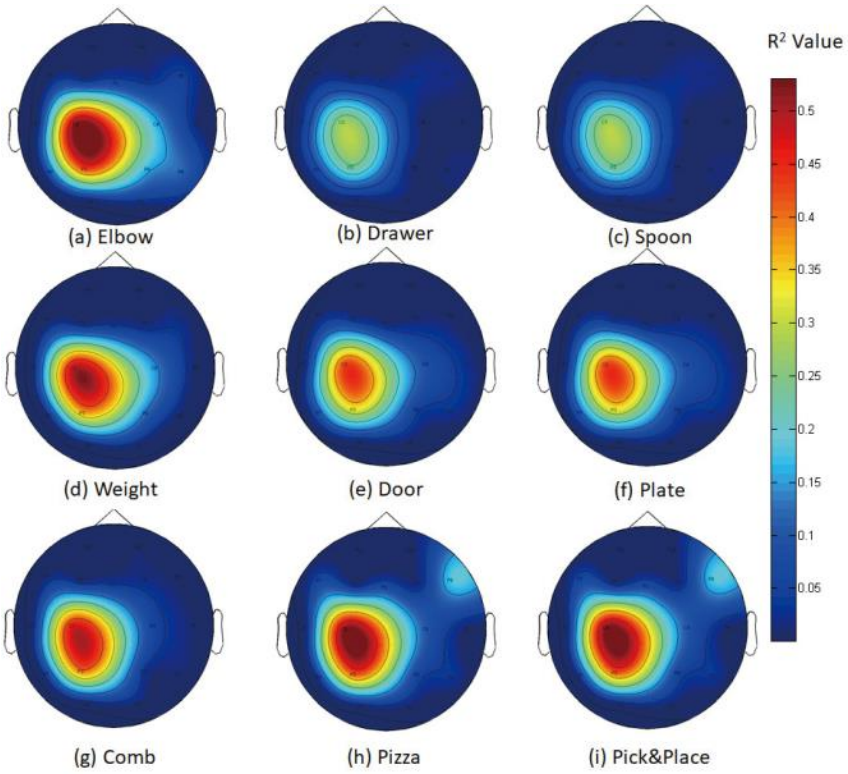

Figure 4.7 Topographical distribution of R^2 value for H10 at 16Hz. (a) R^2 value for Rest vs Elbow Task;(b) R^2 value for Rest vs Drawer Task; (c) R^2 value for Rest vs Soup Task; (d) R^2 value for Rest vs Weight Task; (e) R^2 value for Rest vs Door Task; (f) R^2 value for Rest vs Plate Task; (g) R^2 value for Rest vs Comb Task; (h) R^2 value for Rest vs Pizza Task; (i) R^2 value for Rest vs Pick & Place Task;

In Figure 4.7, large R^2 values are observed at electrode locations near the contralateral motor cortex area in all the motor imagery tasks. This was a result of the event-related desynchronization of the beta rhythms when motor imagery tasks were

executed. The strength of activation and the topographical distribution, however, were different from task to task.

For H10, the topographical distributions for Rest vs Elbow Task and Rest vs Spoon Task are similar (see Figure 4.7 (2) and (3)). Similar topographical distribution was observed in Door Task and Plate Task (Figure 4.7 (5) and (6)), as well as Pizza Task and Pick&Place Task (Figure 4.7 (8) and (9)). Especially, in Figure 4.7 (8) and (9), while imagining to perform the Pizza Task and Pick&Place Task, EEG activity was recorded in the frontal lobe area (F8 channel), which might be related to the motor planning activities in complex motor imaginary tasks. These similarities suggested fundamental brain activity connections in performing some imagination tasks.

4.3.4. Assessing the validity of the BP/CSP/FBCSP+LDA/DAL method during intra-task testing

For the intra-task problem, the models were generated and tested as described in Table 4.3. In addition to the 5-fold cross-validation performed in the previous section, the models generated from Section 4.3.1 were also tested with additional EEG data collected from the same MI tasks, which is referred as “intra-class test accuracy” in the following sections of the thesis. The intra-class test accuracy for each motor imagery task was averaged across participants (see Figure 4.8).

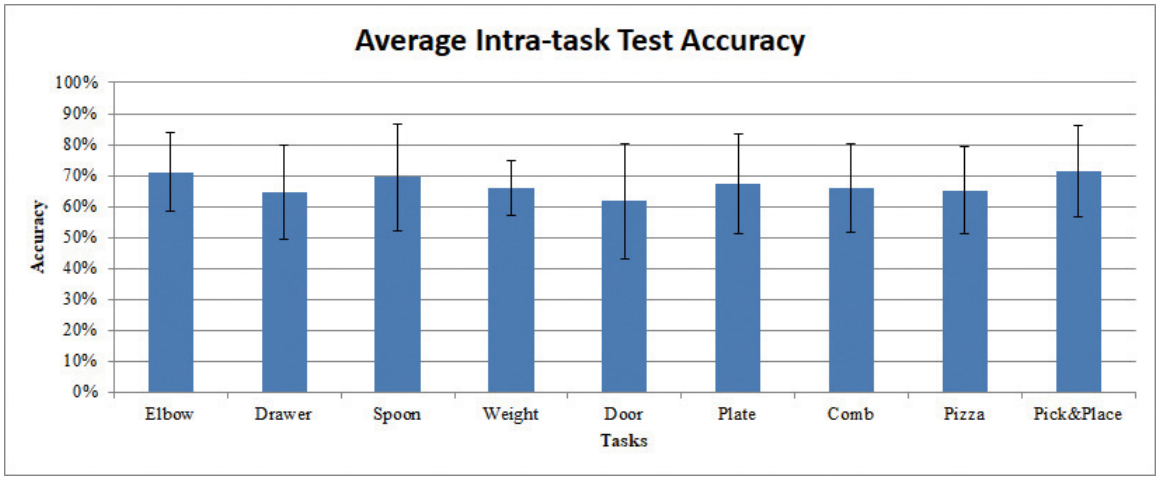

Figure 4.8 Average intra-task test accuracies for different motor imagery tasks.

As shown in Figure 4.8, the Pick&Place task had the highest average intra-task test accuracy (0.715±0.148) among all the motor imagery tasks, followed by Elbow task

(0.711±0.128). However, the difference between different tasks is not statistically significant (one-way ANOVA, p=0.817). The door task, on the other hand, had the lowest average intra-task test accuracy (0.618±0.186). The average intra-tasks testing result shows the test accuracy was significantly higher than random (accuracy higher than 0.6359, p=0.05 according to Muller-putz et al. [185]), except for the door task. All tasks showed higher accuracy than chance level (accuracy higher than 0.6141, p=0.1).

4.4. Discussion

All nine motor imagery tasks focused on upper extremity activities, centered around elbow joint movement. These tasks can arguably be divided into three main categories: i) simple joint tasks (SJM, i.e. Figure 4.2(b), Figure 4.2(c) and Figure 4.2(e)); ii) simple elbow joint that is commonly executed in everyday life and requires a relatively low level of synergy of other joints (DSJM, i.e. Figure 4.2(f), Figure 4.2(g) and Figure 4.2(h)); and iii) and goal-oriented tasks (GOM, i.e. Figure 4.2 (d), Figure 4.2(i) and Figure 4.2(j)), which require trajectory planning and multi-joint synergy.

The EEG performance varied across participants and the type of motor imagery task. GOM tasks such as Pick&Place Task and Pizza Task had a significantly higher accuracy compared to the SJM tasks. However, not all GOM tasks investigated in this study had higher cross-validation accuracy (e.g. Soup Task). In the Pizza Task and the Pick&Place Task, some activities were found from the F8 channel in lower frequency, which might be related to the motor planning activity [130], [186], [187]. More precise neural recordings would be needed to verify the brain region involved in order to confirm the activities in these tasks. However, it is surprising to see the Soup Task did not induce similar activities in the same frequency band (in Figure 4.6(c)). This phenomenon may be due to the task design. It can be observed from Figure 4.6(c) that the highest R^2 value is located in the O2 area, which suggests the Soup Task may be primarily related to vision/target related activity [80].

In the R^2 analysis, the peak R^2 value for the SJM tasks is generally smaller, and the contrast of the R^2 mapping is lower than DSJM and GOM tasks. The “low-contrast” feature may result in the lower accuracy in cross-validation and intra-task test for models generated from the SJM tasks. While the difference is not statistically significant, this

“low-contrast” feature might be a general pattern for upper extremity motor imagery. This could explain why the SJM tasks have higher inter-task test accuracy among all the other tasks (i.e. the EEG model generated from the SJM tasks are more versatile). For the SJM tasks, only the elbow joint was involved. All the three SJM tasks were similar. The only difference was the resistance feedback in these tasks. For example, in the Weight Task, because of the imagination of the weight, the Weight Task showed higher P3 activities than C3 activities. That might explain why the EEG model from the Weight Tasks exhibited higher versatility than DSJM and GOM tasks. For the Weight Task, there was only a 6% mean accuracy decrease between testing with data from its own task and the other tasks.

It is interesting to see how imagined interaction with other objects induces parietal lobe activities [188], such as the R^2 value mapping varies in Elbow Task and Weight Task. The movement is physically almost the same, however, by just imaging a dumbbell in the hand excites brain activities around the P3 area.

4.5. Chapter summary

In this chapter, the goals set by Objective 1 was investigated. We conclude that the possibility of using the BCI model generated with one type of MI task for multiple MI tasks is proven. EEG models generated from single joint movements motor imagery tasks show higher versatility (higher inter-task test accuracy) than other tasks. Among all the tested tasks, the Weight Task show a statistically higher inter-task test accuracy than the other tasks ($p<0.05$) with the average inter-task testing accuracy as 0.605 ± 0.022. Also, the other two single joint motor imagery tasks (i.e. Elbow Task and Drawer Task) show higher inter-task test accuracy compared to non-single joint tasks. However, the difference is not statistically significant ($p>0.05$). The inter-task testing accuracy for the Elbow Task and Drawer Tasks is 0.594 ± 0.022 and 0.590 ± 0.022, respectively. Among the single joint motor imagery tasks, the difference is not statistically significant (ANOVA, $p>0.05$). For applications like rehabilitation, it would be possible for individuals to go through an EEG training session that only involves the motor imagery of simple one-joint movements. The EEG model generated could then be re-used to classify other goal-oriented motor imagery tasks.

4.6. Contributions, limitations and future work

The content of this chapter addressed the repetitive EEG data acquisition and model generation problem in BCI involved rehabilitation training. In clinical practice, a complete rehabilitation protocol usually contains multiple training tasks designed for specific rehabilitation purposes. Therefore, the BCI system would need to be trained with those specific training tasks with repetitive data acquisition, which would require a lot of time and effort on the part of healthcare professionals and users. In order to address this problem, we proposed to train the EEG model on a “versatile” MI task, and reuse the EEG model for other different training tasks. This method effectively reduces the time for BCI involved rehabilitation setup, so that healthcare resources can be utilized in a better way. For end-users of the BCI system, a reduction in BCI setup time makes the technology easier to use and cheaper to access.

There were some limitations of the study included in this chapter. First, the quality of MI and limb movements were not monitored objectively, even though participants were pre-trained on how to perform kinesthetic imagination before the data acquisition, and were also monitored visually by the examiner during the data acquisition. Contamination of the EEG data was not strictly controlled. Second, one of the participants was left-handed, meaning that their EEG data were flipped between left and right hemispheres during the R^2 analysis. Although it is possible that the “flipping process” affected the results in the analysis, the impact is relatively low considering that results were summarized from all 12 participants. Third, the inter-task test accuracy was relatively low compared to the BCI studies in the literature, which was caused by the algorithms selected in this study. The goal of this study was to investigate the feasibility of the idea of versatile MI tasks. Selecting advanced feature/classifiers is computationally expensive. Therefore, only primitive features and algorithms were used. It is necessary for a future study to investigate MI tasks with more advanced features and algorithms to fully understand the role of machine learning algorithms used in this study.

In addition, it might be interesting to investigate why some MI tasks have higher versatility than other MI tasks. A study using imaging tools with higher spatial resolution

(e.g. MRI and MEG) could potentially give insight into the versatility difference of MI tasks.

Chapter 5.

Stroke rehabilitation with BCI – combining motor imagery training and physical training

This chapter is reproduced with permission from the following paper I co-authored:

Zhang, X., Elnady, A. M., Randhawa, B. K., Boyd, L. A., & Menon, C. (2018). Combining Mental Training and Physical Training with Goal-Oriented Protocols in Stroke Rehabilitation: A Feasibility Case Study. *Frontiers in Human Neuroscience*, *12*. https://doi.org/10.3389/fnhum.2018.00125

Some sections are adapted to fit within the scope and comply with the format of the thesis.

This chapter is included to address Objective 2, which is related to the design and development of a new rehabilitation training platform. The proposed rehabilitation training platform is designed to assist the users when both motor imagery and physical engagement were detected. The feasibility and potential efficacy of the proposed platform are also tested with multiple sessions on one case participant.

5.1. Introduction

Stroke has become one of the leading healthcare problems for the modern society [1], [2]. Even if the patients managed to survive from the stroke, they usually suffer from permanent disabilities for the rest of their lives [1], [2]. Studies suggest that rehabilitation is the key to early motor recovery for stroke survivors. However, conventional rehabilitation therapy is labor and cost intensive. Robotic and FES devices can provide a high dose of training repetitions and thus may serve as an alternative, or supplementary training method to conventional rehabilitation therapy [12], [13]. BCIs could potentially augment neuroplasticity by introducing active training [15], [16]. However, active training alone may not be sufficient. New studies suggest combining motor imagery with physical training could boost rehabilitation training outcomes [38].

In this chapter, the author was intended to address the goal set by Objective 4, by proposing a portable stroke rehabilitation platform that combines physical and active

motor imagery training for stroke rehabilitation. The proposed platform consisted of an electroencephalography (EEG) based BCI system for active motor imagery training and an elbow exoskeleton orthosis for physical training. Specifically, for the physical training, a force sensor embedded orthosis was used for elbow extension/flexion and a functional electrical stimulation (FES) unit was used for hand extension. To use this system, the participant was required to both imagine the designated task and move the forearm to the designated direction (flexion or extension depends on the context) to trigger the assistance of the orthosis (BCI and force sensor control: BF control for short). The BF control mechanism was designed specifically for combining motor imagery and physical training. A progressive functional training protocol with three increasing levels of difficulty was also developed, to support the proposed training platform. Motor improvements were assessed as clinical outcome measures using Wolf Motor Function Test (WMFT).

5.2. General system setup

The BF control method was designed to ensure the users' engagement in both motor imagery and physical training. EEG data were collected to assess mental engagement, while force information was collected to gauge motor output. The BF control flowchart is shown in Figure 5.1. BF control was used as basic blocks to complete the training tasks in the protocol. However, there were many different options to facilitate the proposed training protocol. For example, the training platform can be designed fully via functional electrical stimulation. However, Lew et al. reported that not all individuals with chronic stroke are able to use an FES unit for elbow position control [189]. Therefore, a full FES design was not applicable to this study. Stationary robotic designs were also rejected (such as Kinarm [8] or Harmony [190]), as the primary objective was to design a portable platform to promote flexibility in rehabilitation. Therefore, a unique design consisting of an elbow orthosis was introduced to facilitate movement together with an FES unit to activate object-releasing hand movement. The proposed stroke rehabilitation platform was built on top of the BF control method. Each step of the movement in the training was programmed to run the BF control to ensure the participant focus.

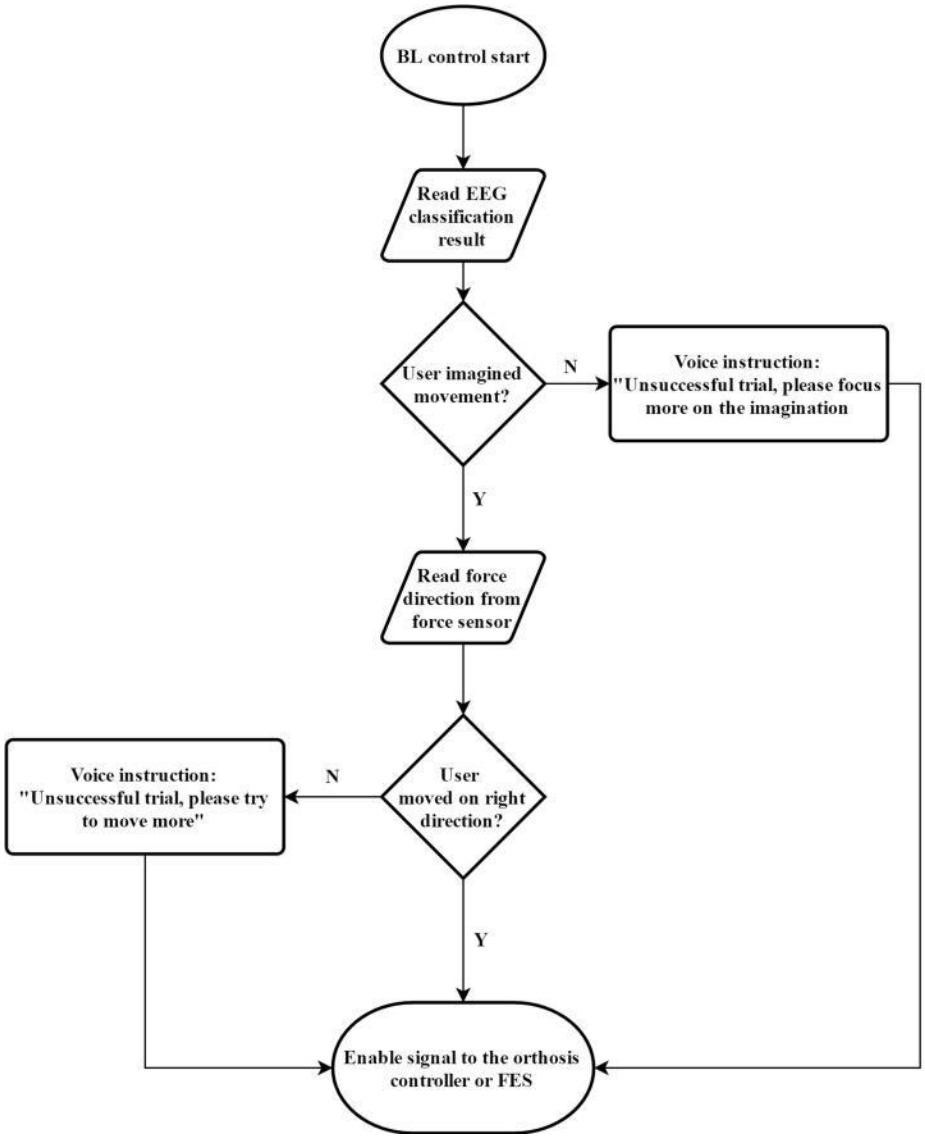

Figure 5.1 Flow chart for the BF control method, which was used in this chapter to combine active training together with physical training

As shown in the BF control diagram, the user was required to concentrate on MI of the rehabilitation task with the most impaired limb, then move that limb in the designated direction with the orthosis. If successful, the device assisted the participants in finishing the training with the designated protocol. If the participants failed in one part of the BF control, they would be informed of which part they failed (either “not enough focus on motor imagery” or “not enough movement in the designated direction”), and the proposed platform would passively move their limb according to the training protocol, to ensure minimal training was administered. The combination of mental and physical training was designed to put emphasis on the connection between MI and physical

movement, so that the participants could correlate thinking and moving during training, and consequently improve motor function.

5.2.1. Elbow Orthosis design and development

The elbow orthosis used in this chapter is an arm robot prototype developed in our lab, not by the author (see Figure 5.2). This elbow orthosis was modified across multiple versions [29], [191].

The elbow orthosis was fabricated from an off the shelf brace (Breg T scope Elbow Brace) with mechanical stops and active mechanical components that had one degree of freedom (DOF) for elbow flexion/extension. The orthosis is actuated via a brushless 24-Volts DC (BLDC) motor

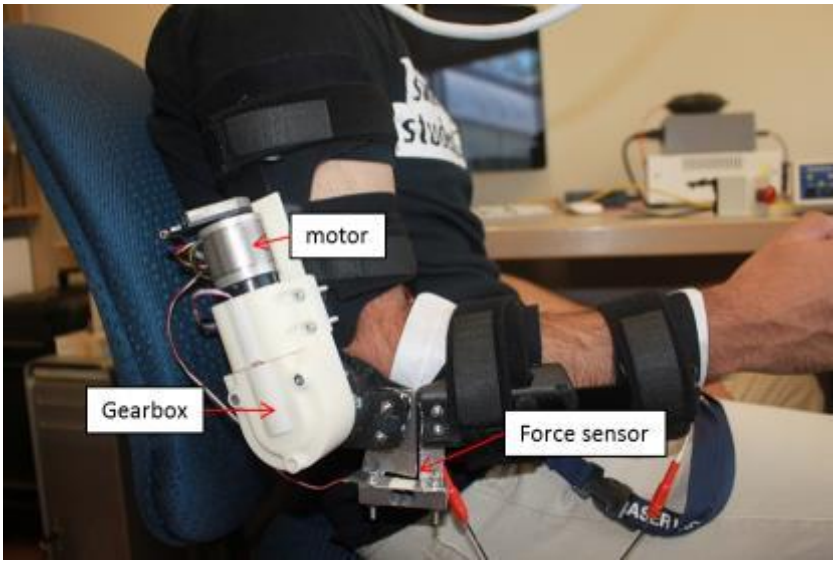

Figure 5.2 Orthosis used in this chapter [192]**.**

The angular position of the end effector of the orthosis was measured via a low-profile long life EVWAE Panasonic potentiometer. In addition, an encoder (HEDL 500 CPT with 3 channels) was mounted on the motor side as a redundant sensor for safety purposes. The orthosis was encapsulated in a custom-made casing. The casing was rapid-prototyped from acrylonitrile butadiene styrene (ABS) plastic to minimize the weight.

A micro force sensor (Phidgets 3133, 0-5 kg) was integrated at the end effector of the orthosis to measure the interaction forces between the user and the orthosis. The integrated micro load has a 0.05% precision, 0.05% Non-Linearity of the full scale (FS), 0.05% hysteresis of FS, and 0.1% Creep of FS (per 30 min). These features enable the accurate measurement of the human and the orthosis interaction forces. Theoretically, the orthosis has a total range of motion between 0° and 130°. The range of motion was limited to only 30° to 120° via the mechanical stops of the brace, for safety purposes.

5.2.2. Functional Electrical Stimulation

A functional electric stimulation (FES) unit (RehaStim, Hasomed Inc., Germany) was used in this chapter to assist wrist/hand extension. The FES unit generates symmetrical biphasic pulses, with a fixed frequency of 35Hz and peak duration of 150μs. The participant was required to wear two self-adhesive electrodes on the forearm of the impaired arm to aid wrist and finger flexion (grasp action). The stimulus amplitude of the FES was incrementally tested with the participant until the impaired hand is fully and comfortably extended.

5.2.3. EEG acquisition and classification

A 32-channel, EGI Geodesic N400 system (Electrical Geodesics Inc., USA) was used to record the EEG data from the participant. EEG acquisition and analysis were divided into a two-step process: 1) collect EEG data to obtain a BCI model of the participant; and 2) utilize the obtained model to classify the participant's intentions in real time.

For the EEG data acquisition process, the participant was using the theory derived from the research result presented in Chapter 4. Since this study involves multiple goal-oriented tasks centered with elbow activities, the motor imagery of Weight Task was used.

For a model generation, 'Stimulus Presentation' mode in BCI2000 [170] was used, where the EEG was recorded at 1kHz and filtered with a bandpass filter of 1-45 Hz. In this stimulus presentation mode, two different visual cues were displayed on the computer monitor. The first cue was a cross-sign in the middle of a white screen. During

the cross picture on the screen, the participant was asked to keep his eye on the cross and relax. The second cue was a picture of an elbow; the participant was asked to perform the kinesthetic motor imagery for elbow extension and flexion for at least two repetitions. Kinesthetic motor imagery means that the participant was asked to imagine himself performing the movement and focusing on the sensation of the movement [175]. Each Stimulus Presentation run consisted of 20 randomized cues (rest or elbow). Each cue was shown on the monitor for 4 seconds, followed by randomized intervals of 4-6 seconds (relax intervals). The participant was required to complete five runs of stimulus presentation. 50 trials of the participant's EEG data during motor imagery of elbow movement and 50 trials of rest were collected.

In order to obtain the BCI control model, the data were analyzed offline using BCILAB [176], a BCI toolbox based on Matlab (The MathWorks, Inc., USA). First, data were resampled at 250 Hz to reduce the system resource consumption. Then, a finite impulse response (FIR) band-pass filter was used to filter out the 6–35 Hz frequency band. This frequency band covers the mu and beta rhythms, which is reported to contain ERS and ERD activities during motor imagery [130].

The author exploited a searching method to search the EEG data from 0.5s to 3s after each visual cue, with 2s of window size and 0.5s of step size. For each EEG epoch, Band Power (BP) [179], Common Spatial Pattern (CSP) [134] and Filter Bank Common Spatial Pattern (FBCSP) [178] were independently used as feature extraction, and then a grid search for the best combination of the feature algorithm and classifiers was performed. In this study, Linear Discriminant Analysis (LDA), Dual Augmented Lagrangian (DAL) method and support vector machine (SVM) were used as potential searched classifiers. Detailed feature settings are shown in Table 5.1. Hyper-parameters of the classifiers, like regularization parameter and the kernel scaling parameter, were also included in the grid search, with a geometric progression from 2^{-15} to 2^{10} and 2 as the common ratio. The three feature extraction algorithms and three classifiers were tested with all possible 9 feature-classifier combinations with a 10x10 cross-validation.

Table 5.1 Feature settings during model training

Feature Algorithm	BP	CSP	FBCSP
Frequency Band	6-32Hz	6-32Hz	6-15Hz; 15-25Hz; 25-32Hz
Feature Dimension	17	6	18

During the offline data classification, 54 binary models were generated. The model with the highest cross-validation accuracy was saved for later use. During the online classification, the EEG signal was filtered with the same FIR 1-45Hz bandpass filter. Then the signal was streamed to a buffer and the pre-acquired model was applied on the buffered EEG signal.

For the online classification process, the participant was using the theory derived from the research result presented in Chapter 6.

Classification decisions were obtained once every 500ms with a sliding moving average buffer containing the latest 8 decisions. The BCI system output frequency was the same as with using the EEG model directly, as the buffer was configured to output synchronously with the EEG model prediction. If the average value was greater than the pre-set activity threshold, enable command would be sent to the orthosis control module. The activity threshold may vary among different sessions, due to the contacts of the EEG acquisition station was using saline solution. In order to get the proper activity threshold and to minimize false positive, the participant was asked to complete EEG data collection and analysis before the actual training. The participants were asked to rest without closing their eyes for 30 seconds, while the EEG data was collected, and the online classification was running (output every 500ms). The activity threshold was arbitrarily set as 0.1 higher than the max output value from the classifier in the online classification, so that the system had a good balance between sensitivity (ease to activate for the user) and stability (ability to resist interference). Through this process, the possibility of artifact contamination in the BCI control was minimized.

5.3. Inclusion criteria

The inclusion criteria included: 1) age range from 35 to 85 years, (2) post-stroke duration ≥ 6 months, (3) MoCA ≥ 25 [172] (4) shoulder active range of motion (ROM) in all directions of 10^{o}-15^{o}, (5) elbow passive extension and flexion ROM of 0-130^{o}, (6) wrist passive extension ROM of 0-15^{o}, and (7) passive full extension for fingers. Potential participants were excluded if they had; (1) other neurological conditions in addition to stroke, (2) unstable cardiovascular disease, or (3) other serious diseases that precluded them from undergoing the study (i.e. undergoing other studies, etc.). Next, participants were contacted by a healthcare professional to determine if they could commit to a 6-week intensive training protocol. Finally, a 37-year-old male with aphasia was recruited to, who was 11 years post-stroke.

5.4. Assessment tests

For pre-assessment, three baseline assessments (BLA) was administrated to the participant, each performed two weeks apart. During the training session, the participant went through a battery of tests again every two weeks. The primary outcome measure was the WMFT assessment. Other secondary outcome measures were: Fugl Meyer Motor Assessment (FMMA) and the success rate of triggering the device during each training day. The participant was required to complete the WMFT and FMA every other week as clinical outcome assessments by a “blind” test administrator, who was neither aware of, nor involved in, the study protocol.

5.5. Brain Symmetry index (BSI) of the Participant

The traditional questionnaire-based assessment method was used in this chapter. In addition, brain symmetry index (BSI) was also calculated in this study, in order to confirm with the feasibility of using EEG as an assessment of motor function.

In addition to the WMFT, we were also interested in understanding if the training outcome could be reflected in EEG. The BSI was originally designed to help visualize and quantitatively asses the quality of the EEG. The BSI is designed to quantitatively assess the temporal and spectral balance between left and right hemispheres. The

previous applications of the BSI include EEG monitoring during carotid endarterectomy, acute stroke operation, as well as seizure detection [193]. Other work showed that BSI is negatively correlated with participant's functional motor outcomes (i.e. the higher the BSI, the lower the FMA) [20], [23], [25], [193].

$$BSI(t) = \frac{1}{k}\sum_{n=1}^{k}\left|\frac{R_n^*(t) - L_n^*(t)}{R_n^*(t) + L_n^*(t)}\right| \qquad \textbf{Equation 5.1}$$

Where k is the number of discrete frequencies, and

$$R_n^*(t) = \frac{1}{m}\sum_{ch=1}^{m} a_n^2(ch,t) \qquad \textbf{Equation 5.2}$$

$R_n^*(t)$ is for the channels on the right hemisphere. A similar equation was used for the channels on left hemisphere ($L_n^*(t)$). In this equation, $a_n^2(ch,t)$is the Fourier coefficient with index n of channel ch, at time t, corresponding to a particular event epoch [t-T, t]. In this chapter, BSI was calculated with T = 4s, both at rest and during motor imagery.

5.6. Training protocol

The total training duration was 6 weeks. Each week consisted of 3 sessions of training sessions (approximately one and a half hour) on alternate days. WMFTs were administrated to the participant once every other week. Three sessions of baseline assessments were assigned two weeks before the training and one follow-up retention session was assigned to the participant four weeks after the training. The full study schedule is shown in Table 5.2.

Table 5.2 Training and testing schedule for the case study

	Baseline Assessment			Training weeks						Retention
Training Schedule	D1	D1+2W	D1+4W	TW1	TW2	TW3	TW4	TW5	TW6	TW6 + 4W
Assessments (WMFT, FM).	√	√	√	√	√		√		√	√
Stimulus presentation	√			√						
Training Protocol				Warm-up	Level1	Level1	Level2	Level2	Level3	

TW: training week, D: day, W: week.

5.6.1. Warm-up training (Training week 1)

During the warm-up training (Training week 1), three basic sessions (described below) were introduced to the participant. The aim of this warm-up training was to familiarize the participant with the orthosis system and the basic BCI control methods.

In warm-up training session 1, no engagement was required from the participant. This session involved passive movements of the elbow flexion-extension (using orthosis) and hand opening (using FES). The training lasted for 30 minutes for each movement (elbow and hand). Each movement was repeated 25 times. Session 1 was designed to familiarize the participant with the orthosis and ensure the participant's range of motion on the hemiparetic upper limb could tolerate the range of the orthosis.

In a warm-up training session 2, the participant was required to trigger the orthosis using only kinesthetic motor imagery. This session involved active movements of the elbow flexion-extension (using orthosis) and hand opening (using FES) controlled by the participant through EEG. If the participant was unable to trigger the device within the designated time, the device would passively move the participant's arm to receive minimal training. The training lasted for half an hour for each movement (elbow and hand). The minimum number of repetitions for each movement was 10 times if all trials were unsuccessful. Session 2 was designed to familiarize the participant with BCI control and obtain the activity threshold for the EEG online classification.

In a warm-up training session 3, the participant repeated the same movements as in session 2 using different control mechanism. For elbow movement, the participant was required to concentrate on imaging opening/closing elbow and then move his elbow towards the designated direction (BF control). For hand and wrist control, the participant was required to concentrate on imaging opening the hand to switch on the FES that assists in opening the hand, the FES was designed to switch off automatically after five seconds. Session 3 was designed to get the participant familiarized with the basic control components of the goal-oriented protocols proposed in the training sessions.

5.6.2. Goal-oriented training tasks (Training weeks 2-6)

The training from the second to the sixth week required the participant to complete 12 days in which four different goal-oriented tasks were practiced. Each task was assisted by the orthosis, which could be triggered by the BF control. The functional task was split into three levels of difficulty. Level 1 included only elbow movement, simple flexion/extension. Level 2 included: a task using both hands to improve bilateral control and coordination. Level 3 included: reach, grasp, place, and release an object.

Level 1 task, plate-cleaning task: the participant was requested to wear the orthosis and hold the plate in a horizontal position close to the trunk with the non-paretic arm (as shown in Figure 5.3(a)). Then the participant was required to place the paretic arm proximal to the trunk and above the plate. This was defined as the initial position. At the end of each training repetition, the device would return to this position. Vocal instructions from the device would instruct the participant to imagine the sensation of moving elbow to wash the plate and physically extend his elbow (to meet the criteria for BF control). If the participant successfully passed the BF control check, the orthosis would assist the participant to perform elbow extension (as shown in Figure 5.3(b)). If the participant failed to pass the BF control check within 10 seconds after vocal instructions, the device would automatically extend the participant's elbow and inform the participant this was an unsuccessful trial. After extending the participant's elbow, the device would ask the participant to flex his elbow to complete the task cycle (as shown in Figure 5.3(c)). Same BF control checking method was used to ensure the participant was engaged in the training.

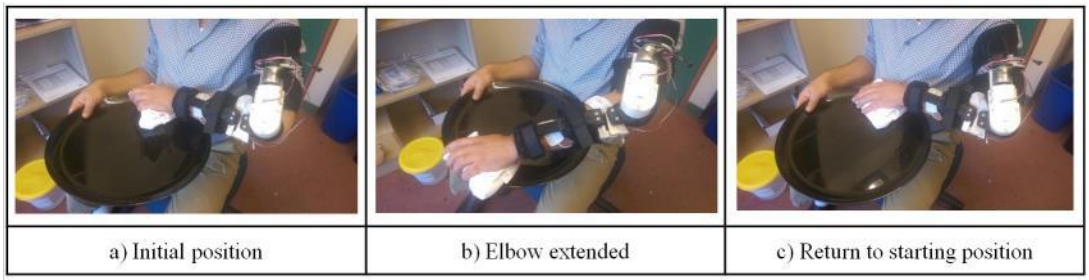

Figure 5.3 Illustration for level 1 training protocol: plate cleaning task

Level 2 involved lifting a bucket: the participant was requested to wear the orthosis, extend both of his arms and hold a bucket (as shown in Figure 5.4(a)). This was defined as the initial position. At the end of each training repetition, the device returned to this position. Same as in level 1, vocal instructions from the device instructed the participant to imagine the sensation of flex elbow to lift the bucket and physically flex his elbow. If the participant successfully passed the BF control check, the orthosis would assist the participant to perform elbow flexion to lift the bucket (as shown in Figure 5.4(b)). If the participant failed to pass the BF control check within 10 seconds after the vocal instructions, the device would automatically flex the participant's elbow and inform the participant this was an unsuccessful trial. After flexing the participant's elbow, the device would ask the participant to extend his elbow to put the bucket on the desk (as shown in Figure 5.4(c)). Same BF control checking method was used to ensure the participant was engaged in the training.

Figure 5.4 Illustration for level 2 training protocol: lifting and placing task

Level 3 involved a placing and releasing task: In this level, FES unit was added to assist with hand control. The participant wore the orthosis and FES electrode and held his paretic hand in front of his chest. This was defined as the initial position. At the end of each training repetition, the device returned to this position. As in level 1 and 2 vocal instructions from the device instructed the participant to imagine the sensation of

extending his elbow to reach and grab the target object and physically extend his elbow and open the hand. The FES unit would assist to open the participant's hand. The device would wait for three seconds, and the FES unit would be switched off so that the participant could hold the object (as shown in Figure 5.5(b)). If the participant failed to pass the BF control check within 10 seconds after the vocal instructions, the device would automatically extend the participant's elbow, open the hand, and inform the participant this was an unsuccessful trial. After grasping the object, the device would give vocal instruction to ask the participant to flex his elbow to pick up the ball from the desk (as shown in Figure 5.5(c)). The same BF control checking method was used to ensure the participant was thinking about the elbow movement and moving towards the correct direction. Then, the device would give vocal instructions to imagine elbow extension and physically extend his elbow to place the object down. If the participant successfully passed the BF control check, the orthosis would assist the participant to perform elbow extension. After the orthosis reached the designated extension angle, the FES unit switched on, so that the participant could release the object in his hand (as shown in Figure 5.5(d)). Again, the device asked the participant to imagine elbow flexion and physically flex his elbow to move his hand back to the initial position. BF control checking was also used in this phase (as shown in Figure 5.5(e)).

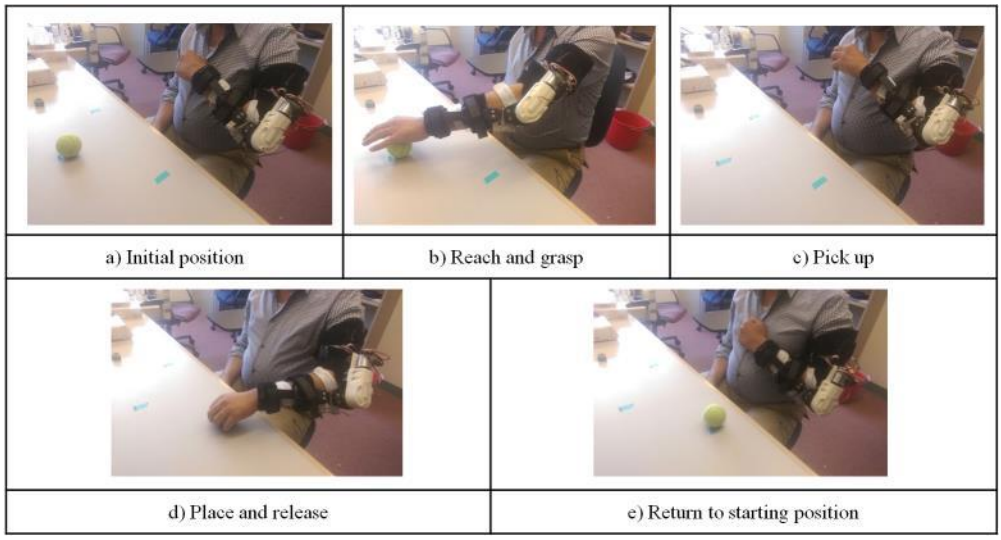

Figure 5.5 Illustration for level 3 training protocol: picking-up and placing task

During training, a trial was considered successful only if the participant was able to trigger both EEG system with motor imagery and bend the force sensor in the correct direction of the required movement of the elbow. If the participant for any reason did not

have a successful trial, the orthosis system would perform the required movement by moving the participant's limb passively to maintain a minimum number of delivered repetitions (10 repetitions).

5.7. Results

5.7.1. BCI performance

During the BCI model training (obtaining or generation), the EEG data collected was sent to three types of feature extraction algorithm and cross-validated with three types of classifiers. For the participant in this study, the CSP feature algorithm together with LDA classifier returned the highest cross-validation accuracy of 80.1%. The spatial filter obtained is shown in Figure 5.6. The colors indicate the weight values for the spatial filters, as shown in the Z axis in the figure. Clear event-related desynchronization (ERD) was captured by the CSP algorithm in Figure 5.6(b).

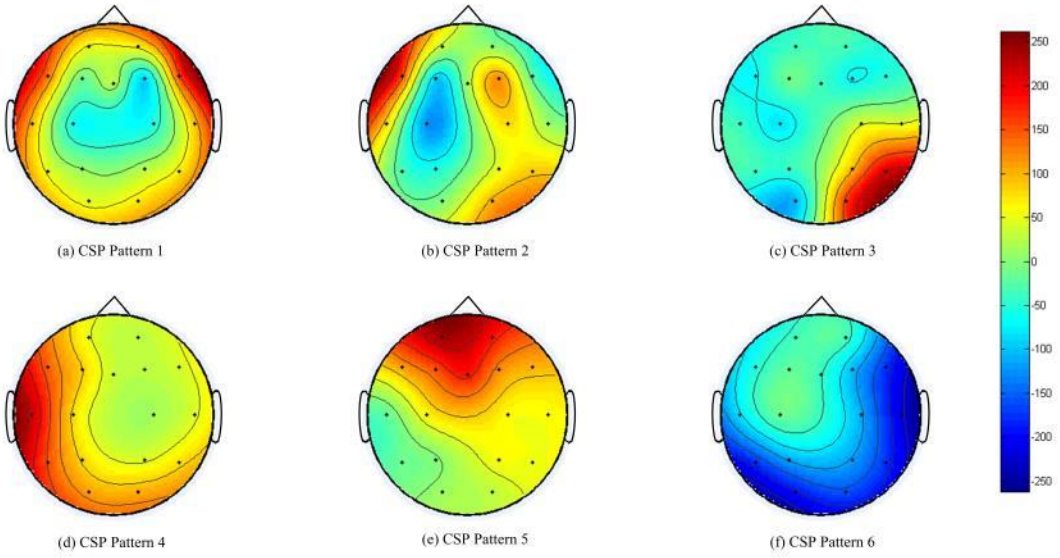

Figure 5.6 CSP model obtained for the participant. Although this is a participant with chronic stroke, Figure (b) exhibits a spatial pattern similar to ERD/ERS activity in healthy participants.

5.7.2. Success rate

According to the training protocol, the device can either facilitate active training (BCI or BF control) or passive training. The success rate was introduced to measure the control accuracy during the training. The success rate was calculated as the ratio of successfully controlled trials, by the participant, in the total training trials within one training day. For example, if the participant was missing one control clue during one trial, this trial was not counted as successful. The calculated success rate on each training day was averaged and summarized for each training week in Table 5.3.

Table 5.3 Success rate in triggering the system

	BCI success rate	BF control success rate
Week1	0.684±0.048	0.410
Week2	0.771±0.138	0.497±0.152
Week3	0.653±0.215	0.453±0.076
Week4	0.74±0.124	0.697±0.095
Week5	0.936±0.022	0.826±0.017
Week6	0.906±0.111	0.831±0.133

The participant was a BCI novice. In the first training week, the participant's success rate was 68.4% with BCI control, and his success rate for BF control was only 41.0%. However, after six weeks of training, the participant managed to achieve a success rate of 90.6% for BCI control and 83.1% for BF control.

5.7.3. WMFT and FMMA result

According to the inclusion criteria, the participant had shoulder active range of motion in all directions of 10°-15°. The participant was required to complete the WMFT and FMMA every other week by a "blind" test administrator, who was neither aware of, nor involved in, the study protocol. The first three sets of WMFT data were collected as baseline measurements without training involved.

Table 5.4 Wolf Motor scores of the participant

			Right Hand Assessment							
			Baseline			Assessment in training weeks				Retention
No.	Assessment Content	Unit	1	2	3	1	2	3	4	5
1	Forearm to table (side)	seconds	3.62	3.83	3.72	3.44	3.08	4.24	3.74	4.13
2	Forearm to box (side)	seconds	120.00	120.00	16.91	120.00	16.02	120.00	14.88	9.22
5	Hand to table (front)	seconds	2.17	5.01	3.49	2.23	3.205	4.55	4.69	2.58
6	Hand to box (front)	seconds	120.00	120.00	120.00	8.57	10.28	27.36	30.51	4.78
7	Weight to box (highest)	lbs	0.00	0.00	0.00	3	2	2	2	3
8	Reach and retrieve	seconds	6.36	4.17	3.26	7.04	2.80	2.98	4.13	16.81
14	Grip strength (mean)	kg	7.12	4.34	9.29	6.34	9.47	4.43	6.45	6.37
16	Fold Towel	seconds	120	82.56	120	120.00	89.22	71.81	120.00	120
17	Lift Basket	seconds	4.16	9.52	7.82	9.45	5.74	6.06	8.34	7.49

*The tasks which participant was not able to finish throughout the study, were not included in this table

WMFT scores are shown in Table 5.4. Data were omitted if the participant was not able to finish the task throughout the baseline measurement and the six weeks of training. The baseline assessment showed that the participant was not able to finish Extend-elbow (side), Extend-elbow (weight) and Hand-to-box (front). The participant was also not able to several fine motor movements including Lift-can, Lift-pencil, Lift-paper-clip, and Stack-checkers,

WMFT results show that participant was still not able to complete all the tasks, after the training. Therefore, he scored 120 seconds (max allowed time) for hand to box in the baseline and first practice sessions. Major improvements were observed for Forearm-to-Box (side) by 89%, Hand-to-Box (front) by 96% and Weight-to-Box. The participant also showed minor improvements in Hand-to-table (28%), when the retention score was compared to the baseline data (third session). The participant's score showed major fluctuations on Forearm-to-Box task and Fold-Towel task.

The detailed FMMA score is shown in Table 5.5. Only minor fluctuations were observed during and after the training of this study.

Table 5.5 Fugl Meyer Motor Assessment score of the participant

	Baseline Assessment			Assessment1	Assessment2	Assessment3	Assessment4	Retention
Right Arm	22	23	22	19	19	22	21	22
Left Arm	62	64	64	64	62	62	62	62

5.7.4. WMFT score regression analysis

In this section, all the items measuring time in the WMFT were taken and an average time of finishing one task of the WMFT was calculated. The baseline assessment session consisted of three assessments, therefore, standard deviations were shown in the baseline column of Figure 5.7. The remaining assessments were only one-time assessments. The average time in finishing each task of WMFT was summarized in Figure 5.7. After training, the participant managed to decrease his average time in finishing all items of the WMFT test by 12%, which was 11.17 seconds. The average time for WMFT tasks fit well into a monotonic decreasing natural logarithm function (r = 0.789). According to the linear hypothesis test, the result was statistically different (p= 0.0103).

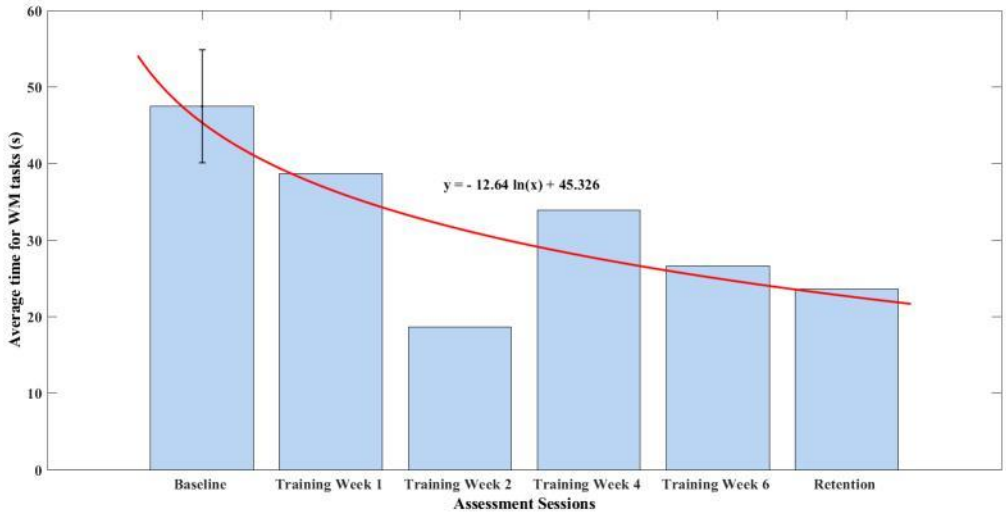

Figure 5.7 Summary for average time to finish WM tasks.

5.7.5. Correlation between BSI and WMFT score

In this chapter, the participant's BSIs were calculated both in resting state and motor imagery state according to Equation 5.1. Correlations between the WMFT and BSI during both rest and motor imagery states were investigated, to further assess the improvement in the WMFT data. The regression results are shown in Figure 5.8.

Figure 5.8(a) shows the regression correlation between averaged WMFT score and resting state BSI. Both Pearson's correlation (r = 0.2790, p = 0.6494) and Spearman's correlation (r = 0.3000, p = 0.6833) indicated very low correlation between the two. Figure 5.8(b) shows the correlation between averaged WMFT score and motor imagery state BSI. Both Pearson's correlation (r = 0.9568, p = 0.0107) and Spearman's correlation (r = 1.0000, p = 0.0167) indicated very high correlation. In addition, the MI state BSIs were also summarized throughout the six-week rehabilitation training in Figure 5.9, which shows a similar profile as the averaged WMFT data in Figure 5.7.

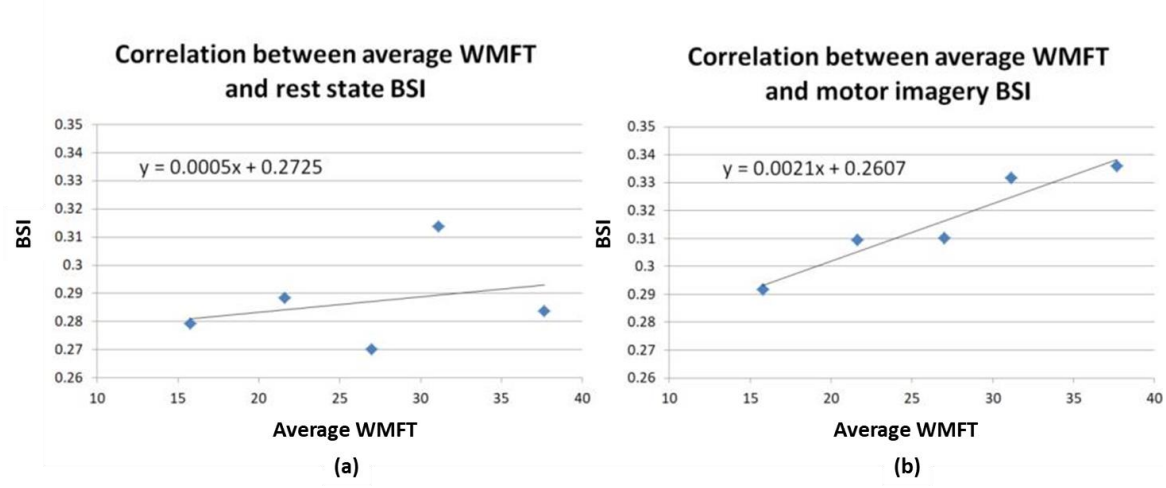

Figure 5.8 Correlation between the participant's average WMFT score and BSI

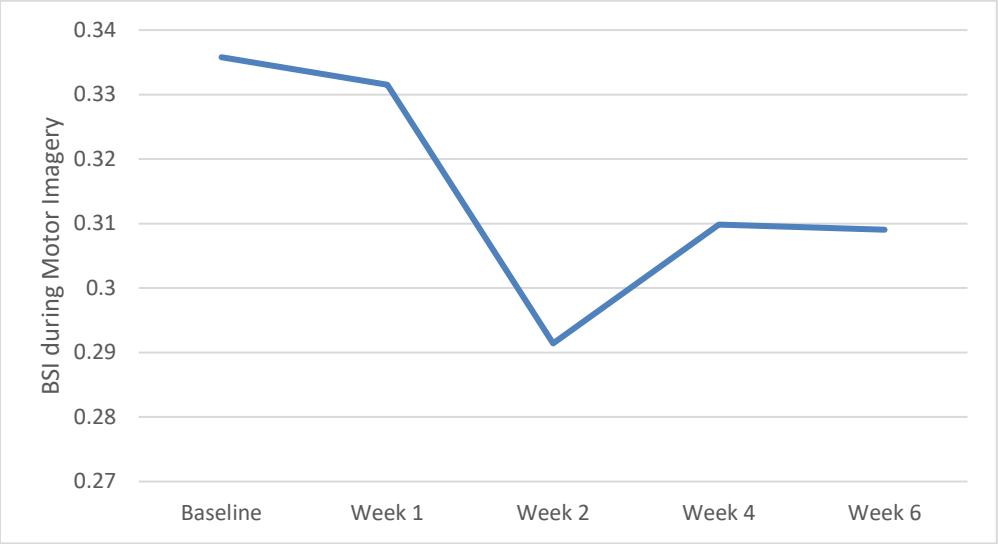

Figure 5.9 The BSI calculated from MI state, during the six-week rehabilitation training

5.8. Discussion

The current chapter focused on the feasibility of the proposed BCI training platform over six weeks of progressive training. The participant's left hemisphere was affected by a stroke. Therefore, in the stimulus presentation session, the participant was required to imagine movements of his right upper-limb. Based on the spatial patterns obtained from the offline analysis (Figure 5.6), it is clear that the BCI system is able to capture the ERD for motor imagery (Figure 5.6(b)). Considering the participant had no prior experience with BCI, the offline analysis accuracy (80.1%) was reasonable. The participant was actually able to control the device with motor imagery. During the training process, the training protocol was changed to level 2 and level 3 respectively in Week 3 and Week 5. The author also noted variability in the success rate decrease in some training weeks; for example, there was 11.8% decrease in BCI, 4.4% decrease in BF control for Week 3, and 3.0% decrease in BCI for Week 6. The success rate decrease was consistent with the training protocol changes, and the participant managed to quickly adapt to new challenges. The results strongly suggest that both device and protocol were well tolerated by the participant and that training with the proposed device is feasible.

Further, the proposed platform was successfully tested over six weeks of training. In the baseline assessments, the participant showed very limited ability to functionally use his arm as measured by the WMFT tasks. For example, the participant was not able to complete Hand-to-box (front) and Lift-can tasks. Over the intervention time frame, the participant showed major improvements in the primary outcome measure. The WMFT quantifies upper extremity motor function through timed movement tasks. In this study, the participant was able to improve both timing and strength in selected tasks. He improved most on the Hand-to-Box task and Weight-to-Box task on the stroke affected side, which suggested he had improved his control on the shoulder, elbow, and wrist joints of the affected side. Those improvements were clinically meaningful according to Lin et al. [194]. The participant showed minor improvements in other tasks that are strength based including Forearm-to-Box, Hand-to-Table, and Lift-Basket. However, there was no sign of improvement on fine motor tasks of his affected side. There could be several explanations for the low improvements on the impaired hand. One could be the BF control mechanism was mainly designed to work on the elbow joint. Therefore, the participant inherently gained more training in this joint. Another explanation could be distal digit functions are hard to rehabilitate, or that the participant needed a higher dose of the training. However, considering the participant was spending about one hour in each training session, and the participant was reporting fatigue both mentally and physically after each session, extending the length of the sessions may not be applicable. The fluctuations in the performance of other WMFT tasks for this chronic stroke survivor also suggests the participant was on “the margin” of completing those tasks within the required time, perhaps he could have continued to improve with more training. Finally, it is possible that the neural substrates that support fine motor movement (i.e. the corticospinal tract) was severely damaged by the stroke and not capable of supporting any recovery.

Additionally, BSIs were calculated from the participant’s EEG signal, both for the rest state and the motor imagery state. In the literature, BSI was negatively correlated with the functional outcomes (FMA) of the stroke survivors [25]. In this study, no correlation was found between the rest state BSI and averaged WMFT. This might be related to the participant’s relatively stable performance on the FMA score, as shown in Table 5.5. In Figure 5.8, a strong positive correlation was found between motor imagery state BSI and averaged WMFT score ($r = 0.9568$, $p=0.0107$). In theory, a low BSI score

suggests less symmetry on the EEG of two hemispheres. Although motor imagery in healthy should cause unbalanced activity between two hemispheres. However, other studies have suggested motor recovery comes with increased ipsilateral hemisphere movements [195]–[203]. Therefore, the positive correlation between motor imagery BSI could provide evidence that the participant had actual improvement during the training.

Based on these results, the author contends that the participant gained control, coordination, and strength in some of the shoulder, elbow, and forearm joint/muscles with repetitive goal-oriented training over a six-week period.

5.9. Chapter Summary

This chapter presented a new rehabilitation platform combining motor imagery and physical training for post-stroke rehabilitation. The proposed training platform together with its supporting training protocol were well tolerated by an individual with chronic stroke during six-weeks of training. By the end of the rehabilitation training, the participant was able to utilize EEG and force sensor to control the orthosis to finish the training tasks at a very high success rate (90.6% for the BCI control, 83.1% for the BF control). The participant improved his motor function after the training with reduced overall WMFT time. The preliminary results of this case study suggest combining motor imagery and physical training is feasible and possibly effective for patients with chronic stroke.

5.10. Contributions, limitations and future work

A challenge in the field of rehabilitation involving BCIs is that users may learn to control the rehabilitation device with reasonable accuracy, but show limited motor function improvement at the end of the training. This suggests that using only active training with the BCI might not be enough, as the users might find a way to control the rehabilitation device through compensatory movements or other strategies instead of through improvements in motor function. A combination of mental and physical training could help users correlate the motor imagery with the actual movement performed [38]. However, no such system has been designed or reported in the literature. In order to facilitate the idea of combining mental and physical training, a novel training platform

was designed and fabricated in this study by integrating BCI with force sensor feedback on an elbow orthosis. In order to test the feasibility of the proposed platform and the supporting protocol, one case participant with chronic stroke was recruited and went through six weeks of rehabilitation training. The proposed rehabilitation platform and supporting protocol address the challenge of combining mental and physical training, as identified in the pilot study in Chapter 3 and also proposed in [38].

The major limitation of the study was with the efficacy of the proposed platform and protocol. Although the participant improved during training, the platform and protocol were tested with only one case participant. Therefore, it is not possible to definitely determine the efficacy of the training platform and protocol. Although the efficacy of the platform and protocol was not the objective of this study, it would be of interest for future studies to investigate with a group of participants with chronic stroke. Secondly, the case participant did improve during the six weeks of rehabilitation training. However, whether the improvement was caused by motor learning or motor recovery is still unclear. In other words, the neuroscientific explanation for the motor function improvement is lacking. Therefore, a study using neuro-imaging tools with higher resolution (such as MRI and MEG) would be advised to investigate the mechanisms responsible for the participant's motor improvement. Thirdly, the training dose was chosen based on similar studies in the literature [15], [16]. A future study investigating the effect of training dose would be of interest.

Chapter 6.

Filtering EEG model predictions to improve BCI application performance

The goal set by Objective 3 is addressed in this chapter, by investigating two proposed methods of transferring an EEG offline analysis method into an online BCI application.

6.1. Introduction

Brain-computer interface (BCI) has been a popular research topic for decades [38], [40], [41], [84], [92]. Many new methods and algorithms have been developed to analyze the target signal in an offline paradigm in the last decade [41]. Currently, EEG offline analysis algorithms can reach 8-class classification with relatively high accuracy [44]. The transition of the offline analysis method to an online control scheme is another major factor that affects the BCI performance. Most of the BCIs in the literature apply the generated BCI model directly to the buffered streaming data, as can be seen in [45]–[51]. Given the performance of the BCI application was directly affected by the predictions of the BCI model, processing the predictions generated by the BCI model could potentially improve the online classification performance of the BCI applications. To the best of our knowledge, no study has been reported on such topic.

The major goal of the BCI online classification process is to increase the sensitivity of the classification while suppressing false positives. In applications that use BCI to control devices, the system is supposed to be configured to have less positive outputs (output 1) in order to make the system stable [204]. In other words, in binary classification situations between rest (output 0) and action (output 1), the BCI system should be biased towards to the rest state. In this case, the BCI users have to maintain a certain control signal with a certain intensity to activate the BCI system. Since Müller-putz et al. have reported a confidence interval of “randomness” in the process [185], the “bias level” could be derived directly from a Gaussian distribution model with the number of samples used in the model generation process.

The “occasional” misclassifications from a classifier could be minimized by simply applying a moving average on the BCI classification outputs with a window of a designated length. In this case, the BCI users have to maintain the control signal for a certain period to activate the BCI system.

In this chapter, the author focuses on the binary online BCI classification applications. Two methods of filtering the prediction of the BCI models were proposed and evaluated: Biased-classification and moving average method. The proposed two methods were introduced and evaluated for one participant with chronic stroke in six weeks of rehabilitation training. The proposed methods were shown to out-perform the method of directly applying the offline analysis model on buffered EEG data (referred to as non-special online classification in the following context), in the six weeks of rehabilitation training. Between these two methods, the moving average method showed higher accuracy, and the biased-classification method showed higher response speed.

6.2. Method

In this chapter, a 32-year-old individual with chronic stroke was recruited, whose data were also used in Chapter 5. He completed six weeks (18 sessions) of training with a stroke rehabilitation training platform introduced in [192]. During training in Chapter 5, the EEG data of the participant using the rehabilitation training platform were recorded. The system and training protocol was discussed explicitly in [192]. The protocol of this study was approved by the Office of Research Ethics at Simon Fraser University and the participant signed an informed consent form at the beginning of each training session.

6.2.1. EEG offline analysis and BCI Model generation

A 32-channel, EGI Geodesic N400 system (Electrical Geodesics Inc., USA) was used to record the EEG data from the participant. The EEG data were recorded at 1 kHz and filtered with a bandpass filter of 1-45 Hz. For the BCI model generation, we collected 50 trials of the participant’s EEG data when the participant was performing motor imagery of elbow movement and 50 trials when the participant was resting with eyes open.

In order to obtain the BCI model, the data collected from the baseline assessments were analyzed offline using BCILAB [176], which is a BCI toolbox based on Matlab (The MathWorks, Inc., USA). A grid searching method was used to search from 0.5 seconds to 3 seconds after the visual stimulation in data acquisition, with a two-second widow and 0.5 seconds as step size. During the model generation, Band Power (BP)[22], Common Spatial Pattern (CSP)[134] and Filter Bank Common Spatial Pattern (FBCSP)[178] were used as features independently from other features. And Linear Discriminant Analysis (LDA), Dual Augmented Lagrangian (DAL) method and support vector machine (SVM) were used as classifiers independently from other classifiers. Each type of features and each classifier were combined and evaluated independently to search for the best combination of features and classifiers with a 10×10 cross-validation. The detailed offline model analysis was described in [192].

6.2.2. Online biased-classification setup

In order to decrease the false positive output of a BCI application, the classifier can be tuned to be biased towards 0 outputs. The biased classification can be easily achieved by gating the loss function with a binominal distribution estimation, so that the risk for false positive outputs is minimized. In this section, the confidence interval (T_{biased}) of randomness was first determined according to [185].

For a binomial distribution with X=0.5 unbiased estimator μ was calculated as:

$$\mu = \frac{nX + 2}{n + 4} \qquad \text{Equation 6.1}$$

where n is the number of trial samples used in model generation.

The threshold (T_{biased}) of the biased classifier was then calculated as the upper-boundary of the randomness confidence interval (as mentioned in [185]):

$$T_{biased} = \mu + \sqrt{\frac{\mu(1-\mu)}{n+4}} Z_{1-\frac{\alpha}{2}} \qquad \text{Equation 6.2}$$

where n is the number of trials used in the model generation, $Z_{1-\frac{\alpha}{2}}$ is the $1-\frac{\alpha}{2}$ quantile of the standard normal distribution N(0,1) and α is the significance (typically, α= 0.05, or 0.1). In this chapter, α = 0.05 was used to calculated T_{biased}.

The output predictions (P_{biased}) of the classifier were configured based on the probability outputs of the classifier (p), which is a direct cut-off with the threshold of T_{biased}:

$$P_{biased} = \begin{cases} 0, & p \leq \mathrm{T}_{\mathrm{biased}} \\ 1, & p > \mathrm{T}_{\mathrm{biased}} \end{cases} \qquad \text{Equation 6.3}$$

A pseudo-online process was used to evaluate the performance of the proposed method in this chapter. During the pseudo-online classification analysis with biased-classification, Raw EEG data were streamed from the recorded data file. The raw EEG data were also streamed into a temporary buffer. The buffer length was determined by the model generation process specified in the previous chapter (Section 5.2.3), where the model was generated through grid-search of listed time-epochs, features and classifiers. The model with the highest cross-validation accuracy was used in the pseudo-online analysis. Raw EEG data were filtered with a predefined bandpass FIR filter with a passband of 1-45Hz. Predictions were produced every 0.064s, on the pseudo-streamed EEG data. The predictions were calculated with the biased-classification model on the buffered data.

6.2.3. Online moving average classification setup

In the time domain, the probability output of a binary classifier can be considered as a signal. The “occasional” misclassification would be considered as the noise caused by the environment or the user. Therefore, a simple moving-average filter could be adopted to minimize the impact of external noise. In addition, the moving average method would make the BCI system harder to activate and subsequently improve the stability of the system. Moreover, by comparing the moving-average value to a predefined threshold value obtained from resting EEG data at the beginning of the rehabilitation training, we can estimate the noise level of the training day and minimize

the variance caused by daily EEG acquisition system setup (or different sessions in the rehabilitation training).

In this chapter, a pseudo-online process was used. During the pseudo-online classification analysis, EEG data were streamed from the recorded data file and temporarily stored into a buffer. As with the biased classification method, the buffer length was determined by the model generation process (Section 5.2.3), where the BCI model was generated through grid-search of listed time-epochs, features and classifiers. The same offline analysis model from the previous section was used in this part of the analysis. The EEG data were filtered with a predefined bandpass FIR filter with a passband of 1-45Hz. Predictions were produced every 0.064s, on the pseudo-streaming EEG data. A sliding moving average window of the latest 8 classification outputs was used to calculate output (p). Due to the utilization of the sliding window, the decision rate of the BCI application was able to be set synchronously with the EEG model prediction, which was not limited by the moving average length. The length of the moving average only affects how much the BCI application is biased to "0" output.

A threshold (T_{ma}) was predefined at the beginning of each rehabilitation training session. The participant was asked to rest for 30s while the EEG acquisition system was set up. The 30 seconds were determined based on previous trials with healthy participants during the protocol design phase, which was a balance between BCI setup time and confidence of the noise level estimation. The max value of the classifier output was recorded during the 30s of the recording. T_{ma} was set to be 0.1 plus the max value of p during the 30s of recording. The prediction output (P_{ma}) of the process defined as:

$$P_{\text{thresh}} = \begin{cases} 0, & p \leq \mathrm{T}_{\text{thresh}} \\ 1, & p > \mathrm{T}_{\text{thresh}} \end{cases} \qquad \text{Equation 6.4}$$

6.2.4. Classification accuracy evaluation

The performance of the proposed methods was also evaluated in this chapter. During the data acquisition, the behavior of the rehabilitation platform was also recorded. The rehabilitation platform behavior was used to label the events in the EEG data for the performance evaluation. The detailed events were described in [192]. A four-second

window after the event label was used to minimize the effect of the user's response to the event labels.

The performance of the BCI application was also evaluated with accuracy, precision (true positives over total positive predictions), false positive rate (false positives over condition negatives). With the current design of the training protocol, the number of trials with each class is not balanced, therefore, F_1 score[205] was also calculated as:

$$\mathrm{F}_1 = \frac{2}{\frac{1}{precision} + \frac{1}{recall}} \qquad \text{Equation 6.5}$$

In Equation 6.5, the recall was calculated true positives over condition positives.

Cohen's kappa score [204] was also included in this chapter to evaluate the BCI application performance. In this chapter, Cohen's kappa score was calculated as:

$$k = \frac{p_o - p_e}{1 - p_e} \qquad \text{Equation 6.6}$$

where p_o is the classification accuracy and p_e is the hypothetical probability of change agreement. p_e was calculated with the number of total trials (N) and trial numbers of class k predicted as class i (n_{ki}). In the binary classification case (k is either 1 or 2), p_e was calculated as:

$$p_e = \frac{1}{N^2} \sum_{k=1}^{2} n_{k1} n_{k2} \qquad \text{Equation 6.7}$$

6.2.5. Classification delay evaluation

In the online classification application, the classification delay is a direct performance metric which evaluates how fast the BCI control responds. In this chapter, classification delay was also used as a measure to evaluate the response speed of the online BCI application. The participant was instructed by event labels (vocal commands) from the rehabilitation platform to start performing motor imagery. In this part of the analysis, the classification delay was defined as the time elapse between the vocal

command label from the exoskeleton and the first “1” output from the BCI. If the user missed one event label in the BCI application, the outputs of the BCI in this trial would not be analyzed in the delay analysis. In this case, the delay analysis would be independent from the impact of Type II error.

The Kolmogorov-Smirnov goodness-of-fit hypothesis test was used to test the normality of the delay time on the two proposed filtering methods. Considering that the number of successful trials may be different for the two methods, Wilcoxon rank sum test was used to test if the delay time for the two methods were statistically different.

6.3. Result

6.3.1. Classification accuracy result

The EEG data recorded from the baseline assessments were used to generate the EEG classification model used in this study. EEG data collected in the six-week BCI involved rehabilitation training were used to test the performance of the two proposed filtering methods in a simulated online paradigm. According to the rehabilitation training protocol, the participant was required to start as resting state and follow the vocal commands from the rehabilitation platform. Therefore, in each EEG recording from one training trial, one rest state trial of EEG data and multiple motor imagery state trials of EEG data were recorded. In order to balance the number of two classes of the BCI, only the first trial of motor imagery recording in each training trial was used in the evaluation. In this part of the chapter, 273 trials of EEG from motor imagery state and 273 trials of EEG from rest state were extracted from the six weeks of rehabilitation training. The receiver operating characteristic (ROC) curve of the obtained EEG model is shown in Figure 6.1.

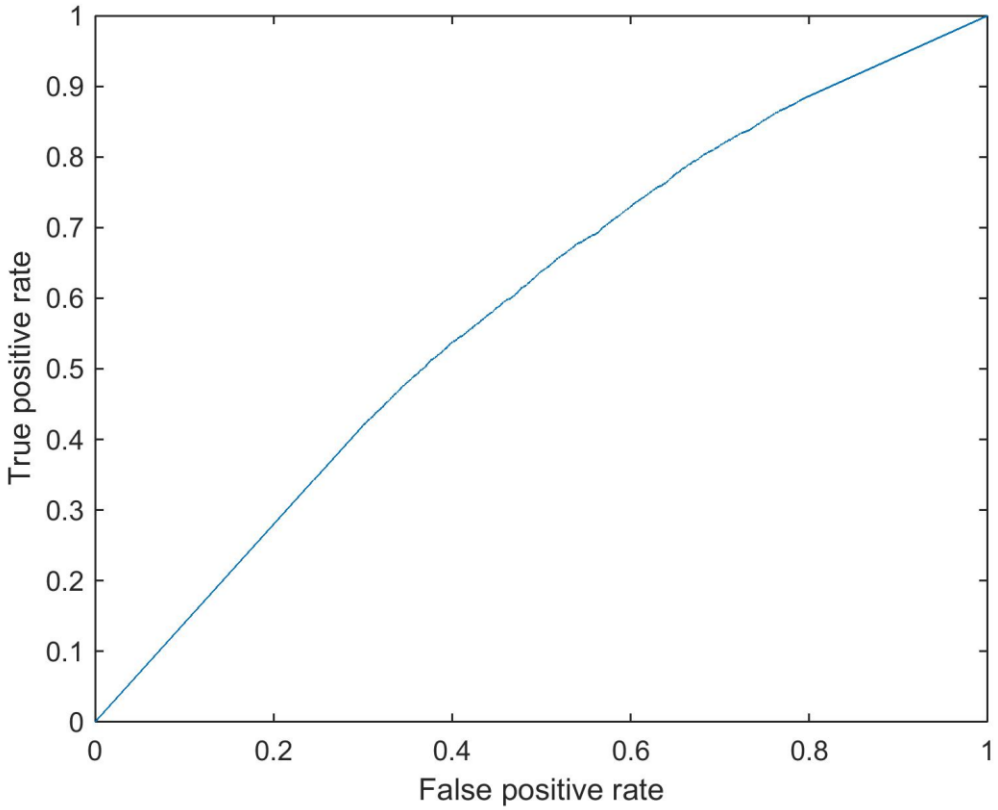

Figure 6.1 The receiver operating characteristics of the BCI model used in this study

For the biased-classification method, T_{biased} was determined by the number of training trials during the model generation. In the model generation process, 100 trials of EEG data with equal trials of two classes (motor imagery and rest) were used. According to Equation 6.2, T_{biased} = 0.5961 was calculated. Additionally, T_{biased}=0.5 was also included to compare as a non-special online classification method (i.e. directly applying the BCI model on the buffered EEG data).

For the moving average online classification method, T_{ma} was predefined at the beginning of each rehabilitation training session, with 30s of rest EEG data.

The online classification was evaluated with a pseudo-online classification analysis process, as described in the method section. The EEG data were collected during six weeks of BCI involved rehabilitation training with one case participant (baseline data were not included in the six weeks). The result was summarized in Figure 6.2.According to the pseudo-online classification result in Figure 6.2, both proposed

filtering methods had higher accuracy than directly applying BCI model to the buffered data. However, the biased-classification accuracy was not statistically higher than randomness according to [185]. The moving average method achieved an average accuracy of 59.89% across the six weeks of rehabilitation training, which is statistically higher than randomness. Considering the fact that participant is novice to BCIs at the beginning of the rehabilitation training, the model accuracy is satisfactory. In terms of the false positive rate, the moving average method is higher than the biased-classification method. However, the moving average method outperforms the biased-classification method in all the other accuracy-equivalent evaluations.

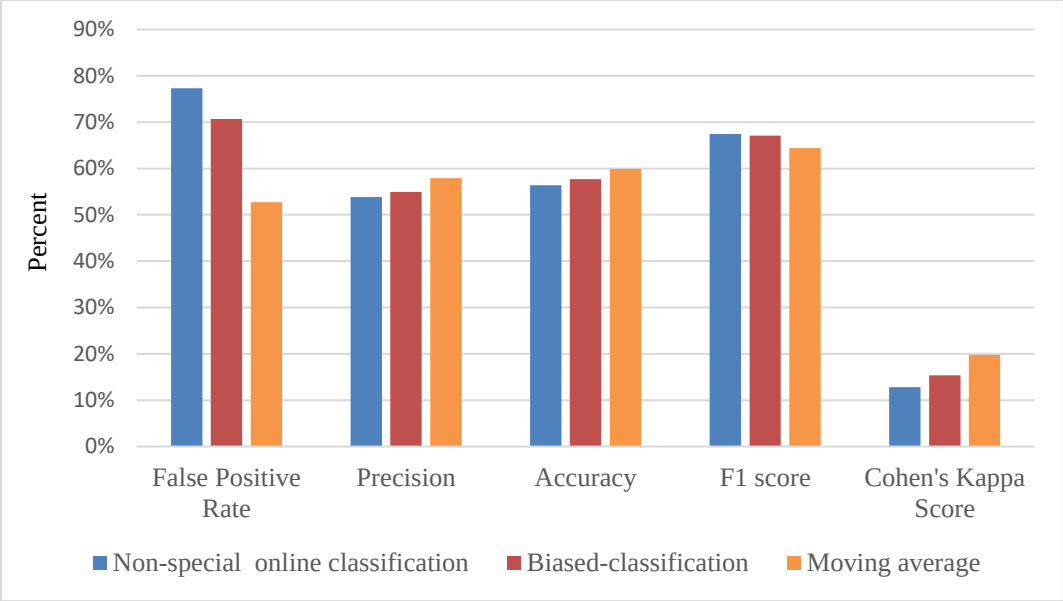

Figure 6.2 Classification performance evaluation on the proposed biased-classification and moving average method.

6.3.2. Online classification delay result

The classification delay result was summarized and shown in Figure 6.3. On average the moving average method showed lower classification delay than the biased-classification method. According to the Kolmogorov-Smirnov goodness-of-fit hypothesis test, the distribution of delay time on the moving average method was not normally distributed (n=443, P= 1.07×10^{-107}). Wilcoxon rank sum test showed the delay time of the two online classification method was significantly different (n_1 = 443, n_2 = 560, P = 8.56×10^{-6}). The biased-classification method responds than the moving average method.

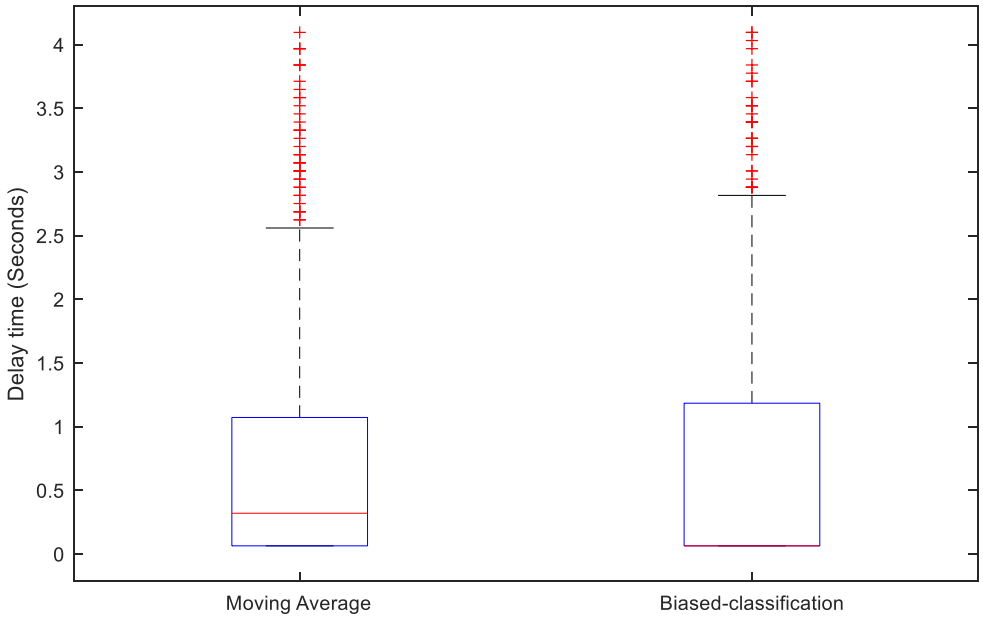

Figure 6.3 Classification delay summary for moving average classification and biased classification

6.4. Discussion

In this chapter, two prediction filtering methods were proposed and evaluated with EEG data in a pseudo-online way. EEG data collected from six weeks of BCI involved rehabilitation training from one case participant were used. In the first method, a threshold value was calculated depending on the training sample size, and a biased-classification method was then built utilizing the threshold value. In the second method, a moving average method was proposed to process the probability output of the classifier, to filter out the “classification noise”. The two prediction filtering methods were also evaluated in this chapter with EEG data from one case participant with chronic stroke during six weeks of rehabilitation training.

Although the highest cross-validation accuracy was 80.1% for the model generation[192], which utilized the EEG data collected in the three baseline assessments, the overall average pseudo-online classification accuracy during six weeks of training barely surpassed the randomness level, with the EEG data collected in the six weeks of BCI involved rehabilitation training. The daily EEG acquisition setups

did introduce a lot of influence, which resulted in the variation between the training set for model generation and the actual rehabilitation training. However, the participant was able to learn how to use the training system very effectively. It only takes a few sessions before the participant learns how to use the training system. In the last week of the case study, the participant was able to control the BCI with very high accuracy (average 90.6%), using the moving average method proposed in this chapter [192].

Based on the evaluation results, both of the proposed prediction filtering methods outperformed the non-specific online classification method in all evaluations except F_1 score. However, the F_1 score does not take the true negatives into account [205], and Cohen's kappa score was suggested to be a better measure [204]. The result on Cohen's kappa score suggested that the moving average method had better performance. In addition, the moving average method had the lowest false positive accuracy, which is crucial in a binary online classification for applications like rehabilitation. Lower false positive would decrease the possibility of triggering assistance by mistake and ensure the participants' focus on the training protocol.

Since the proposed biased classification used the same number of data points with the non-specific online classification method, the delays caused by the BCI algorithm should be intrinsically the same with these two methods. Considering the moving average method requires 8 recent predictions to calculate the mean, the moving average method should require more time to respond. This initial hypothesis has been supported by Figure 6.3, where the response delay for biased-classification method is significantly shorter than the moving average method.

The relatively low accuracy of online classification is still an issue for the application of BCIs. The two prediction filtering methods proposed in this study are still simple and naïve. More sophisticated algorithms should be developed to minimize the variations between the training set for model generation and the actual online application. Also, the result of this study has been limited by the population of the participants. The possibility of generalizing the result and conclusion of the proposed methods with a large population is still unknown. A future study with more participants should be conducted to investigate this potential problem.

6.5. Chapter Summary

The goal set by Objective 2 was addressed in this chapter, by investigating the two prediction filtering methods in an online BCI application. The scope of this chapter was to introduce and evaluate two prediction filtering methods for long-term BCI applications like rehabilitation. Two naïve prediction filtering methods were first proposed in this chapter. In the biased classification method, a threshold value was calculated depending on the training sample size, and a biased-classification method was then built utilizing the calculated threshold value. A moving-average method was proposed to process the probability output of the classifier, to filter out the "classification noise" and calibrate the online classification process with respect to the variation introduced by the EEG acquisition set-up. The performance of two prediction filtering methods was also evaluated in this chapter with EEG data from one case participant with chronic stroke during six weeks of rehabilitation training. Both of the proposed two prediction filtering methods outperformed the method of directly applying the BCI model on the buffered EEG data. Between the two proposed methods, the moving-average method achieved significantly higher classification accuracy than the biased classification method, yet the biased classification method showed a significantly faster response than the moving-average method.

6.6. Contributions, limitations and future work

This chapter evaluated two methods of improving the BCI application performance by filtering the classification output of the EEG model. Although the offline EEG analysis methods have been extensively researched, the performance of the online BCI application is still not satisfactory, especially for users with chronic stroke, as discussed in Chapter 3. Therefore, the process of configuring the BCI application using the EEG model generated from offline analysis requires further investigation and improvement.

The two methods of filtering the classification results of the EEG model presented in this study contribute to filling in the gap between the offline EEG analysis and practical BCI application. With the same offline analysis method, the performance of the BCI application can be improved. This study also benefits the healthcare community

and the users of the BCI system, as it contributes to the reliability of the current BCI technology, making it less demanding for rehabilitation applications.

Although the two proposed methods were investigated with EEG data collected from six weeks of BCI involved rehabilitation training, only one participant with chronic stroke was recruited. This limits the generalizability of the results obtained in this study. A future study involving more participants with chronic stroke is necessary to consolidate the results of the two proposed methods. In addition, the threshold value for the moving average method was calculated using 30 seconds of resting state EEG data, which were determined based on previous studies with healthy participants and participants with chronic stroke. A study investigating the impact of such hyperparameters in the future will help better understand the roles of hyperparameters in the methods proposed in this chapter, as well as develop new methods to improve the performance of the BCI.

Chapter 7.

Quantifying motor function with EEG

This chapter is reproduced with permission from the following paper I co-authored:

Zhang, X., D'Arcy, R & Menon, C. (2019). Scoring upper-extremity motor function from EEG with artificial neural networks: a preliminary study, accepted manuscript on Journal of Neural Engineering.

Some sections are adapted to fit within the scope and comply with the format of the thesis.

This chapter is included to address Objective 4, by investigating the possibility of translating EEG data into an accurate and reliable motor function assessment.

7.1. Introduction

In stroke-related research, assessment of the stroke survivors' motor function plays an important role [27]. Currently, assessment deficit and residual motor function of stroke survivors rely on individual sessions between the healthcare professional and the patient, with standardized assessments. For example, the Medical Research Council (MRC) 0-to-5 scale muscle power assessment tool is one of the most ubiquitous tools for motor power assessment in the clinical field [206], which aids to the investigation of peripheral nerve injuries. Other standardized assessments are also commonly used in the research field. For instance, the Functional Independence Measurement (FIM) was developed to offer a uniform system of measurement for disability [54]. Wolf Motor Function Test (WMFT) was designed to assess functional motor abilities via testing how much time the examinee spends on specifically designed motor tasks [53]. Fugl–Meyer Assessment (FMA) was designed to assess the ability of patients in terms of motor function, balance, cutaneous and joint sensation. The tasks can be sub-divided into several sections, and the examiner can select the sub-sections he/she is interested in [52]. However, those score systems are neither completely objective nor easy to administrate. The examiners' professional experience and skills are essential for the proper administration of those scoring methods.

Electroencephalography (EEG) is a well-established tool in clinical practice. Evidence indicates that EEG changes during the stroke rehabilitation process are able to predict motor recovery post-ischaemic stroke [19], [24], [127]. Literature has suggested band power shifts of EEG data correlates with motor function change. For instance, the intensity of event-related desynchronization/synchronization (ERD/ERS) signal has been reported to correlate with motor function both in healthy and stroke [22], [128]–[130]. Delta-alpha ratio (DAR) calculate from rest state EEG signal was reported to correlate with functional recovery in post-acute traumatic brain injury [26]. Brain symmetry indexes (BSI) have also been reported in several studies to correlate with the functional performance of the stroke survivors [23], [25]. Recently, Large-Scale Phase Synchrony (LPS) has been researched as a prognosis and possible assessment tool in [28]. However, the correlations between the EEG scores in the previous works and the motor functions scores are relatively low ($r<0.8$), and the scores calculated from EEG in the previous works are neither accurate nor reliable enough to be considered as an assessment tool. All the previous works investigated participants with acute/subacute stroke and the feasibility of using EEG data to quantify motor function for chronic stroke remains unknown.

With advancements in electronic technology, temporal resolution and channel numbers of modern EEG acquisition systems keep increasing, and there is abundant information collected from EEG. Although it is difficult to investigate all possible feature algorithms in EEG analysis, modern artificial neural network algorithms are very suitable for such applications with an end to end learning paradigm, which is learning from data without any prior feature selection [56], [57]. There are two major artificial neural network approaches in EEG applications: restricted Boltzmann machine (RBM) and the convolutional neural network (CNN) [165]. The artificial neural networks have been investigated extensively in EEG application in the recent year. For example, RBMs have been used to classify motor imagery of EEG by Lu et. al [207]. Deep Belief Networks (DBNs), which is considered as a special type of RBMs [165], has found their applications in detecting abnormal EEG signals [208], classifying sleep stages [209], and extraction of motion-onset visual evoked potentials [210]. The convolutional neural network (CNN) is an artificial neural network that can learn local patterns in data by using convolutions as its key component. Recent researches have proven that CNNs could be able to be used in motor imagery of EEG analysis with superior performance

[211]. Other applications for CNNs in EEG analysis include epilepsy detection [212]–[216], event-related potentials [217]–[220], and music rhythm retrieval [221], [222]. To the best of our knowledge, there is no previous study using an artificial neural network with EEG data to estimate the users' motor function.

The primary goal for this chapter is to address the goal set by Objective 3, by investigating the possibility of utilizing EEG as a stable and objective measurement for motor function assessment. In this study, a CNN based method for processing EEG data was introduced to automatically score motor function of participants with chronic stroke. Considering the motor function is a broad concept, this study would primarily focus on the motor function of the upper extremity. According to the literature, the FMA is a well-designed, feasible and efficient clinical examination method that has been tested widely in the stroke population [223]. FMA has been widely used in stroke rehabilitation studies as an outcome measure [10], [11], [28], [117], [224]. Its upper extremity motor scale section only takes approximately 20 minutes to complete. Additionally, FMA has been reported to correlate with LPS of EEG for acute/subacute stroke survivors [16]. Therefore, FMA was selected as the standard motor function score. In this chapter, the proposed CNN was regressed on the upper-extremity FMA score of the participants. The performance of the prediction was also evaluated with within-participant testing and cross participant testing.

7.1.1. Demographics

The protocol for this study was approved by the Office of Research Ethics at Simon Fraser University and all participants gave informed consent before participating.

During the recruitment, the inclusion criteria were set as follows: 1) age range from 35 to 85 years; (2) post-stroke duration ≥ 6 months; (3) MoCA score greater or equal to 23 [172][225]; (4) able to click a computer-mouse-like button. Potential participants were excluded if they had; (1) other neurological conditions in addition to stroke; (2) unstable cardiovascular disease; or (3) other serious diseases that precluded them from undergoing the study (i.e. undergoing other assessments or recordings in this study, etc.). Fifteen participants with chronic stroke were recruited to join the study. One

was excluded due to his inability to go through MoCA. The demographic data of participants with chronic stroke were shown in Table 7.1.

Table 7.1 the demographic data for the participants with chronic stroke

Participant ID	Gender	Age	More affected hand	Years after stroke	MoCA	FMA score
P1	Male	70	Left	6	23	51
P2	Female	41	Left	0.5	27	10
P3	Male	68	Left	1	29	38
P4	Male	63	Left	10	28	14
P5	Male	73	Left	6	28	37
P6	Male	67	Left	2	28	36
P7	Female	62	Right	5	26	41
P8	Male	64	Left	6	24	47
P9	Male	80	Right	11	23	39
P10	Female	50	Right	6	23	46
P11	Male	63	Right	1	--	18
P12	Male	39	Right	11	15	6
P13	Male	64	Left	3	27	45
P14	Male	75	Right	1	25	49
P15	Male	64	Left	0.5	23	24

Participant 11 was not able to complete the MoCA test, and therefore, was excluded from the study. Participant 12 was aphasia. Although he only scored 15 in MoCA, he was evaluated by a professional physical therapist to be able to give consent and follow the instructions in this study.

In addition, twelve healthy participants were also recruited to participate in the study. Their detailed information is shown in Table 7.2.

Table 7.2 The demographic data for the healthy participants

Participant ID	Gender	Age	Dominant Hand
H1	Male	22	Right
H2	Male	27	Right
H3	Male	30	Right
H4	Male	24	Right
H5	Female	29	Right
H6	Male	23	Right
H7	Female	29	Right
H8	Female	28	Right
H9	Female	28	Right
H10	Female	27	Right
H11	Female	71	Left
H12	Male	76	Right

7.1.2. Data acquisition

EEG data were acquired from 12 healthy participants and 14 participants with chronic stroke. Figure 7.1 shows the EEG acquisition setup. A 32-channel g.Nautilus system was used to stream and record the EEG data at 500Hz. The montage (shown in Figure 7.2) is a standard 10-20 system with reference on the right earlobe and the common ground is in the midpoint of the line segment between FpZ and FZ.

Evidence from the literature suggests motor function could be reflected in the features of ERD/ERS signals [224], [226]. In this chapter, the EEG data was recorded when the participants were performing button clicking movement, once every self-estimated 10 seconds, as shown in Figure 7.1. The 10 seconds interval was used to clearly separate the EEG activities induced by adjacent clicks [21], [22], [128]–[130], [227]. For the healthy participants, EEG data were collected by clicking with the dominant hand. For the participants with chronic stroke, EEG data were collected by clicking with the more affected hand. The upper-extremity motor function assessment part of FMA was also administrated on the same day as the EEG data collection. During the FMA, the examiner assessed the motor function of the participant as instructed in the FMA protocol. For example, one of the assessments tests the participant's volitional movement with synergies. The examiner asks the participant to move his/her hand from contralateral knee to ipsilateral ear, and the examiner scores the participant on individual joint movement quality (none joint movement scores 0; partial joint movement scores 1;

full joint movement scores 2). Since FMA has a strong ceiling effect [223], [228], [229], full scores of FMA (66) were assigned for the healthy participants in the later processes.

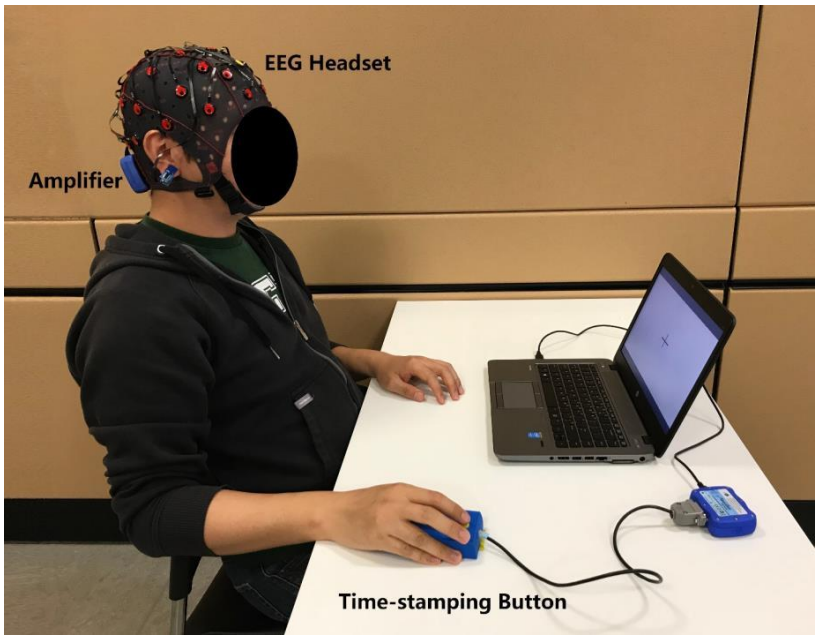

Figure 7.1 EEG acquisition system setup

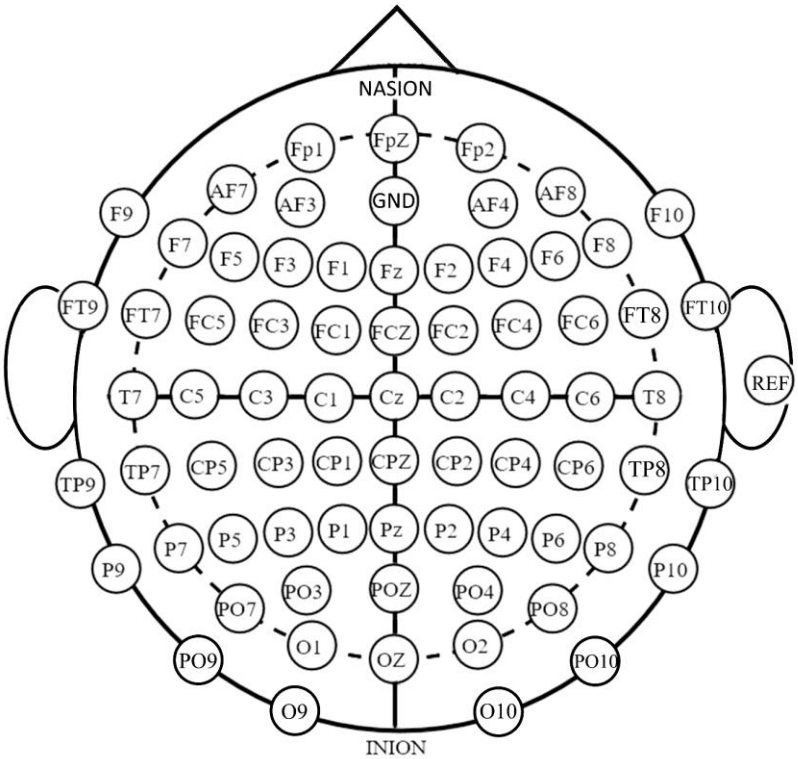

Figure 7.2 The g.Nautilus system montage for EEG acquisition channels

7.1.3. Data pre-processing

Firstly, the EEG data were recorded while the participants were performing dominant/impaired side button clicking. For later process purposes, if the data recordings were performed while the participant was clicking with his/her left hand, the recording channels were swapped between the corresponding left and right hemisphere channels in the pre-process. For example, if one participant was using his/her left hand during the data recording, his EEG data from C3 and C4 channel would be swapped, the same between Fp1 and Fp2, P3, and P4 etc.

The whole EEG data pre-process is shown in Figure 7.3. The EEG data were firstly filtered using a 1-45 Hz bandpass FIR filter. And all following data process was done within 1-45 Hz of the original EEG data. According to the literature, ERD/ERS signal may last for 8-9 seconds [21], [22], [128]–[130], [227]. Therefore, in order to include the ERD/ERS information, clicking events with interspace shorter than 9 seconds were removed from the following process steps, based on the clicking timestamps in the recorded EEG data. Event epochs were extracted from a time window of 4 seconds before the clicking till 2 seconds after. The EEG data were then normalized in each trial to minimize the data acquisition variation. In order to expand the dataset size, a multiple-epoch extraction method was adopted. For every actual clicking time stamp, five trials were extracted. 100ms delay was applied for each of the five trials. This method has been proven to be valid in other neural network training applications [211], [230], [231]. In total, 170 trials of EEG data were extracted for each participant. For each extracted epoch, Fast Fourier Transform (FFT) was performed on each channel of the EEG data and the power spectrum density (PSD) and the phase response were calculated accordingly. Since the EEG data have been filtered through a 1-45 Hz bandpass filter, the power and phase data from greater than 45 Hz has been discarded. With 500Hz as the sampling frequency and 6 seconds as the signal length, frequency components below 45Hz are thus calculated as the first 270 elements after FFT. Through the EEG pre-process, each trial of the EEG data has been converted into a three-dimensional matrix of 270×32×2, where 32 is the number of EEG channels, 2 stands for the PSD and phase response.

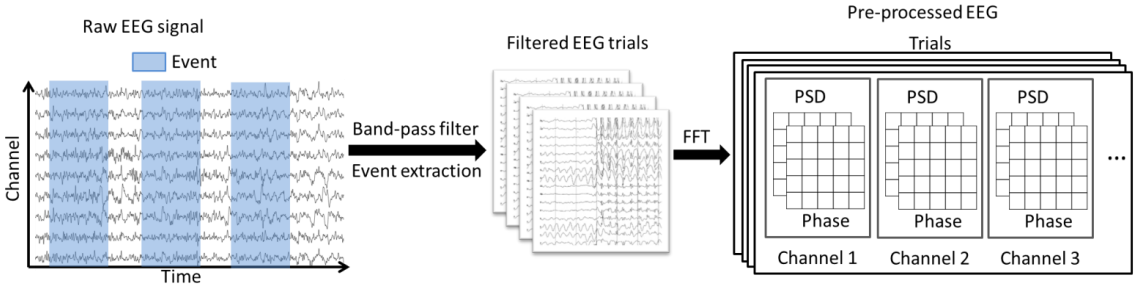

Figure 7.3 Flow chart of EEG pre-process and reshaping

7.1.4. Neural network model configuration and hyperparameter tuning

In this chapter, Keras[232] together with tensorflow[233] were used to build the neural network models. Apache Spark[234] was used to facilitate the model generation process in a computer cluster maintained by Compute Canada.

An artificial neural network consisting of two layers of convolutional layers and four layers of fully connected layers is proposed. Exponential linear unit [235] was used as activation functions for the first six layers and linear activation was used as the activation function for the output layer. The overall network configuration is shown in Figure 7.4. The last layer was a fully connective layer of one neuron with linear activation. According to the network configuration, when the model was trained, a regression model with linear activation will be generated. In this chapter, the regression model was generated on the participants' FMA score. Mean square errors were used as loss function to calculate the gradient and update the weights of the model. The train and test datasets were divided according to the test modality, i.e. either within-participant testing or cross-participant testing, which was introduced in Section 7.1.5 and 7.1.6 respectively. In the within-participant testing, 140 trials of EEG data from each participant were used in the model generation, then extra 30 trials of EEG data were used to test the model performance. In the cross-participant testing, the proposed method was evaluated with a leaving-one-out-cross-validation method, where the models were generated with EEG data from 25 participants and tested with the remaining one participant's EEG data.

All the data were randomized and divided into batches to feed into the model training process.

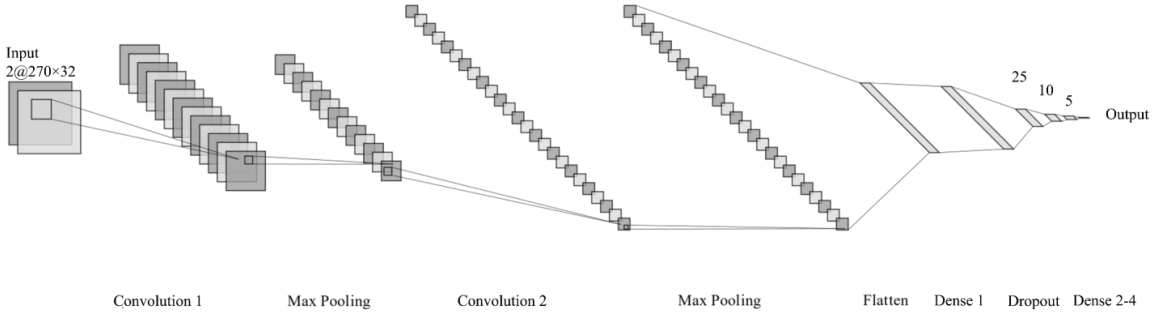

Figure 7.4 Neural network structural configuration.

In order to get the best performance for the proposed convolutional neural network, hyperparameters of the model were searched with a given range for optimal configurations, as shown in Table 7.3.

Table 7.3 Hyperparameter tuning table

Parameter name	Searched range	Number of iterations caused by the parameter searching
Kernel size	(2,2) to (10,10), with step size of 2 on each dimension	25
Convolution 1 layer number of neurons	25, 50 and 100	3
Convolution 2 layer number of neurons	25, 50 and 100	3
Dropout layer	0 to 1 with 0.05 step size	21
Dense 1 layer number of neurons	25, 50 and 100	3
Batch size	64 and 128	2
Number of iterations	50, 100, 200	3

Firstly, the input kernel size of the first convolutional neural network layer was grid-searched from 2-10 with a step size of 2, in order to understand the optimal spatial-frequency combination of the convolution input layer. Then the hyperparameters were grid-searched on the main layers. According to Table 7.3, in order to acquire one optimal model, 81050 models need to be generated. This is too much computation resource requirement even for high-performance clusters. Therefore, in this chapter, a Tree-structured Parzen Estimator (TPE) solver [236] was used to find the optimal hyperparameter. The solver was set to run hyperparameter search for 100 steps to reduce the high volume of computation induced by model generation. For the hyperparameter optimization, models were generated with 140 trials from each

participant and tested with 30 trials of EEG data from each participant. The models with the lowest mean square error were returned for later analysis.

Also, in order to investigate the necessity of using deep neural networks, a two-layer shallow CNN was constructed to compare the performance with a six-layer CNN. 140 trials of each participant's data were used during training. The configuration of the shallow neural network is shown in Figure 7.5. Hyper-parameters as batch size and the number of iterations were searched as described in Table 7.3.

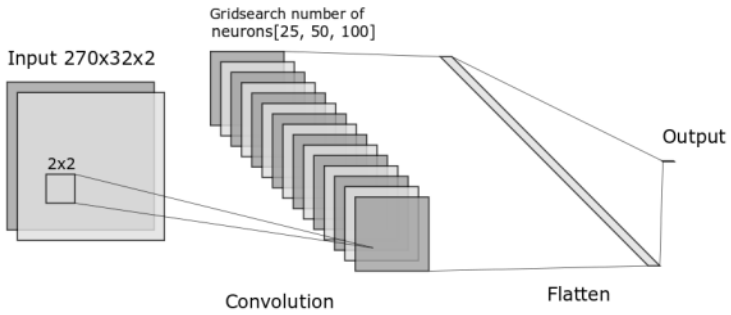

Figure 7.5 A shallow neural network configuration to compare

7.1.5. Within-participant testing

As mentioned previously, 140 trials of EEG data from each participant were used as a training set to obtain the CNN model. With the fine-tuned CNN model, 30 extra trials for each participant, which were not involved in the model generation process, were used to test the model. Since in the EEG data pre-processing, five trials were extracted from one actual clicking event, the authors have paid special attention to make sure the EEG data trials extracted from the same event stayed in one subset. The result was referred to as within-participant testing in this chapter.

7.1.6. Cross-participant testing

Since the author is trying to introduce a method to quantify the upper-extremity functionality, it is important to test the prediction accuracy for participants, whose data were not involved in the model generation process. Due to the limit of our participant

pool, we exploited a leaving-one-out test scheme as our cross-participant testing method to test the prediction performance of the proposed method. During the cross-participant testing, one participant's EEG data will be removed from the training process. The model will be hyperparameter--tuned and trained using 140 trials of EEG data from the remaining participants, with the same hyperparameter optimization process. The obtained model will be evaluated with the removed participant's EEG data (140 trials). The cross-participant testing process will loop through each participant in our participant pool.

7.2. Result

7.2.1. Test result for within-participant testing

In the within-participant testing section, 140 trials of each participant's EEG data during clicking were involved in the model training. The hyperparameters were firstly optimized. Models with the lowest mean square error were returned after hyperparameter optimization. The returned hyperparameters were summarized in Table 7.4. Due to the optimization method used in this part of the thesis, the hyperparameters were tuned jointly using a TPE optimizer. The result shown in Table 7.4 is just one local optimal hyperparameter combination. The proposed CNN configuration converged well with regression on the participants' EEG data in the model generation process as shown in Figure 7.6. With the optimized hyperparameter, the mean square error reached 6.411 at the end of the training process.

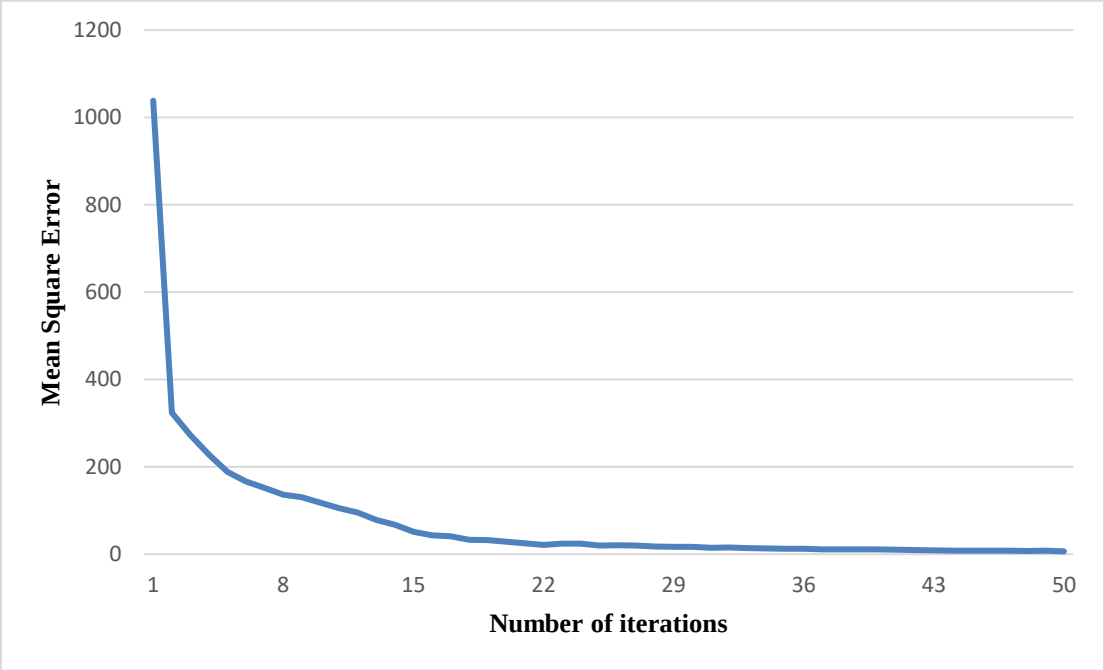

Figure 7.6 **The training loss change with the number of training iterations.**

Table 7.4 **The result for hyperparameter optimization in within-participant testing**

Parameter name	Returned best value
Convolution 1 layer Kernel size	[10,10]
Convolution 1 layer number of neurons	25
Convolution 2 layer number of neurons	50
Dropout layer	0.05
Dense 1 layer number of neurons	50
Batch size	128
Number of iterations	50

With only the EEG data collected from stroke survivors, one model was obtained through the hyperparameter optimization and model generation process (EEG data from

14 participants with chronic stroke were included). With the within-participant test method, the average prediction and standard deviation value are shown in Figure 7.7. The average prediction from the trained neural network model with only EEG data from stroke survivors also achieved very high linear correlation with the participants' FMA scores in within-participant testing (n=14, r=0.9899, p = 1.4653×10^{-11}).

With the hyperparameters returned from the hyper-parameter optimization, one model was also generated with EEG data from both participants with chronic stroke and healthy (EEG data from all 26 participants were included). The model was tested with 30 trials of EEG data which were not involved in the model generation. Predictions were averaged for each individual participant. The result was summarized in Figure 7.8. In order to keep the correlation analysis consistent, the prediction results for the healthy participants were removed from the correlation analysis. The average prediction from the trained neural network model achieved very high linear correlation with the FMA scores from participants with chronic stroke, in within-participant testing (n =14, r = 0.9921, p = 3.3907×10^{-12}).

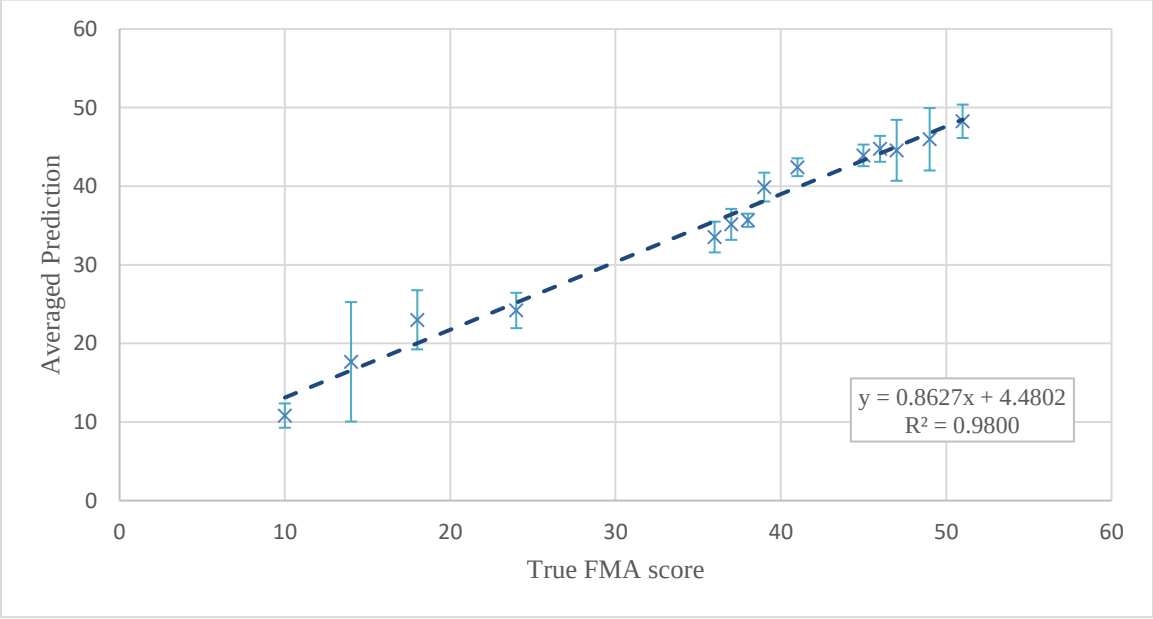

Figure 7.7 **Correlation between the FMA score and averaged prediction score for the within-participant testing. EEG data from 14 participants with chronic stroke were involved in the model generation.**

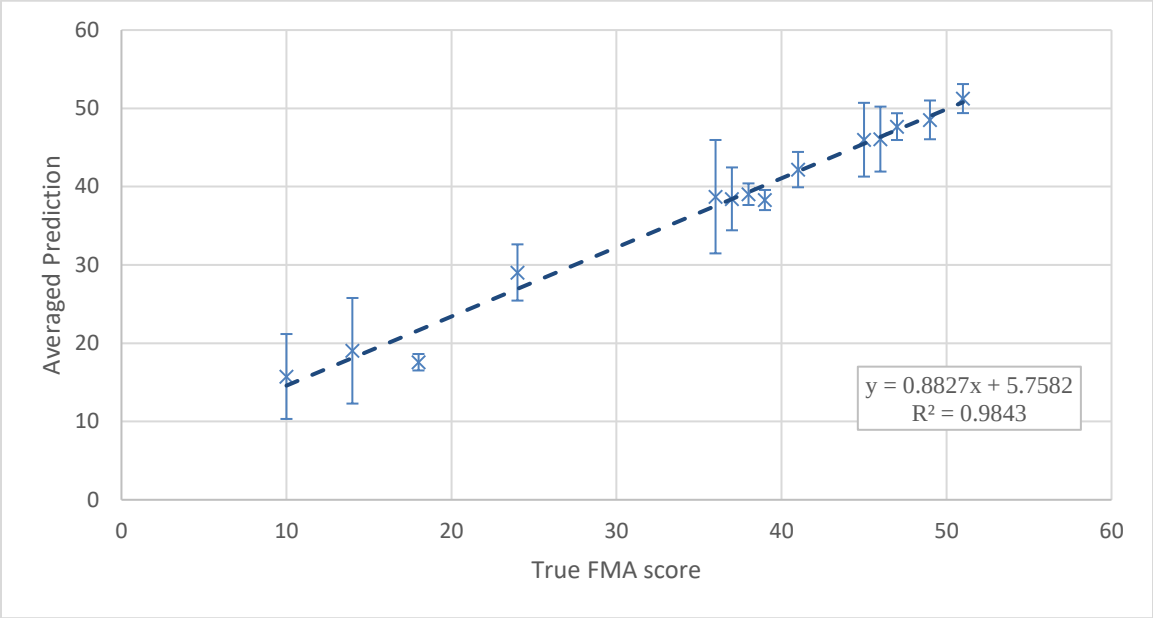

Figure 7.8 Correlation between the FMA score and averaged prediction score for the within-participant testing, EEG data from 26 participants (including both healthy and stroke survivors) were involved in the model generation. Healthy participants' motor function predictions were not included in the correlation analysis.

7.2.2. Shallow convolutional neural network result

In order to investigate the possibility of achieving the same performance with a shallow neural network, a two-layer neural network was also proposed and evaluated. The two-layer neural network model was generated and tested with the same process as described in section 6.1.3 and 6.1.4. EEG data from all 26 participants were included in the hyperparameter optimization and model generation process. The shallow also converged during the training. We also used the within-participant testing method to test the model performance. The test result is presented in Figure 7.9.

Figure 7.9 Shallow neural network test performance for within-participant testing setup. EEG data from 26 participants (including both healthy and stroke survivors) were involved in the model generation. Healthy participants' motor function predictions were not included in the correlation analysis.

Since the predictions were obtained from each trial of EEG data, the predictions of 30 trials of EEG data were also averaged, mean and standard deviation value are also shown in Figure 7.9. The average prediction from the trained neural network model achieved very high linear correlation with the participants' FMA scores in within-participant testing (n =14, r = 0.9069, p = 7.6955×10^{-06}, healthy participants' motor function prediction result was not included in the correlation analysis).

7.2.3. Test result for cross-participants testing

The proposed neural network model was also evaluated with a leave-one-out test scheme. The models were generated through the same hyperparameters tuning process as described in Section 2.3. This left-out participant's EEG data will be only used in the model testing process, not involving the model generation process. The left-out participant was looped through all the participants in this study. With only the EEG data collected from stroke survivors, models were obtained through the hyperparameter optimization process. EEG data from 14 participants with chronic stroke were included in

the hyperparameter optimization and model generation. With the cross-participant test method, the average prediction and standard deviation value are shown in Figure 7.10. The average prediction from the trained neural network model with only EEG data from stroke survivors also showed a relatively low linear correlation with the participants' FMA scores in cross-participant testing (n=14, r= 0.6836, p = 0.0070).

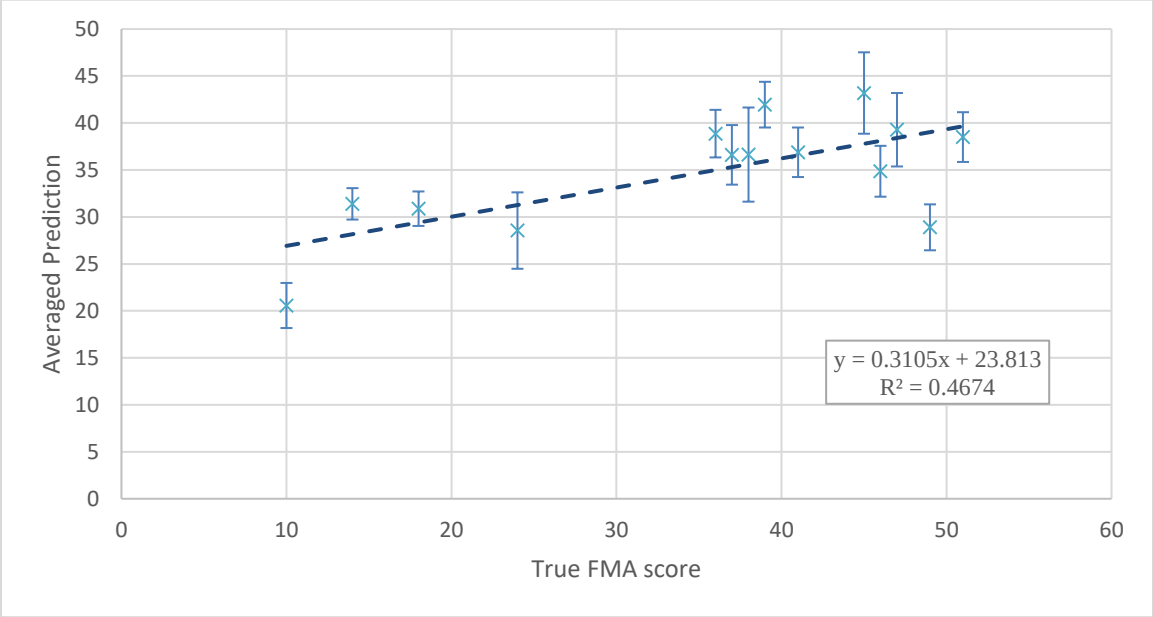

Figure 7.10 The correlation between the FMA score and averaged prediction score for the cross-participant testing, EEG data from 14 participants with chronic stroke were involved in the model generation.

Additionally, with the EEG data collected from the healthy participants involved in the model generation, EEG data from all 26 participants were included in the hyperparameter optimization and model generation. The testing result was summarized in Figure 7.11. Since the predictions were obtained from each trial of EEG data, the predictions of 140 trials of EEG data were also averaged, mean and standard deviation value are also shown in Figure 7.11. In order to keep the correlation analysis consistent, the prediction results for the healthy participants were removed from the correlation analysis. The average prediction from the trained neural network model achieved a very high linear correlation with the participants' FMA scores in within-participant testing (n= 14, r = 0.9867, p = 7.9342×10^{-11}).

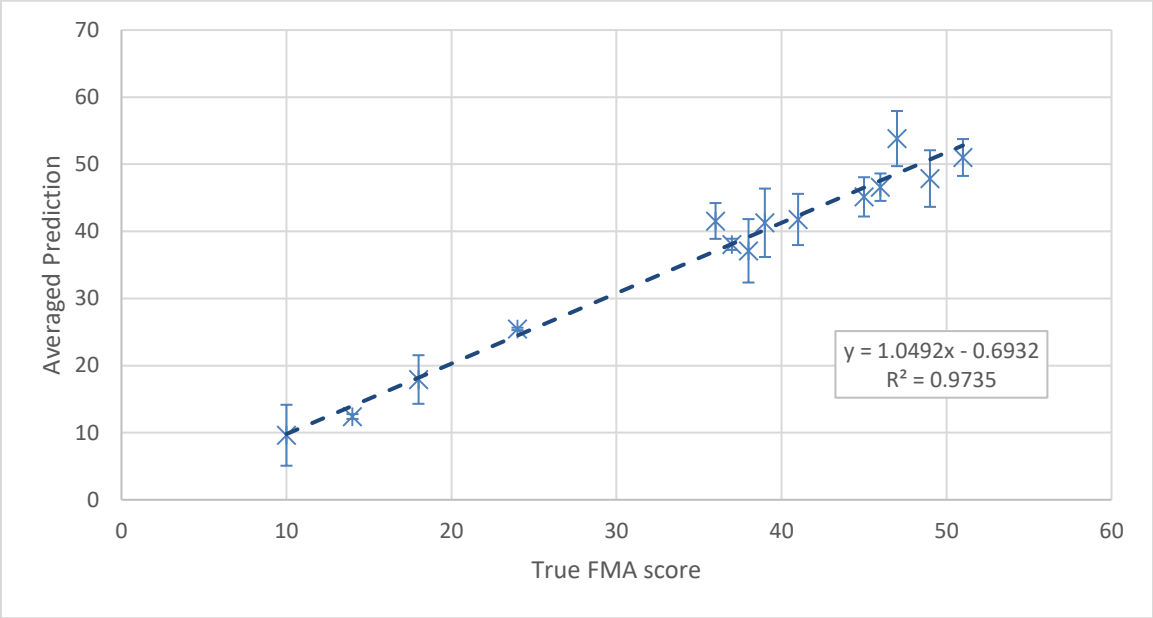

Figure 7.11 The correlation between predictions and FMA scores for the cross-participant testing, where the proposed method was tested with a leaving-one-participant-out-cross-validation method. EEG data from 26 participants (both healthy and stroke survivors) were included in the model generation. Healthy participants' motor function predictions were not included in the correlation analysis.

7.2.4. Increasing EEG data with healthy participant

The objective of this chapter is to create a model that can best estimate motor function in cross-participant testing in participants with stroke. The following figure shows the prediction in cross-participant testing in participants with chronic stroke, in three different cases, i.e. when, in addition to data from stroke participants, data from 0, 10, and 12 healthy individuals were respectively used in the model generation (i.e. training). Figure 7.12 shows that prediction accuracy of the obtained model (i.e. cross-participant testing result for participants with stroke only) increases progressively by increasing the number of healthy participants' EEG data used in the model generation. This result shows that a better model for participants with stroke can be generated when EEG data of healthy participants were also included in the model generation. The results shown in Figure 10 are important, as they provide evidence that the performance of the proposed method has a high potential to improve by increasing the number of participants.

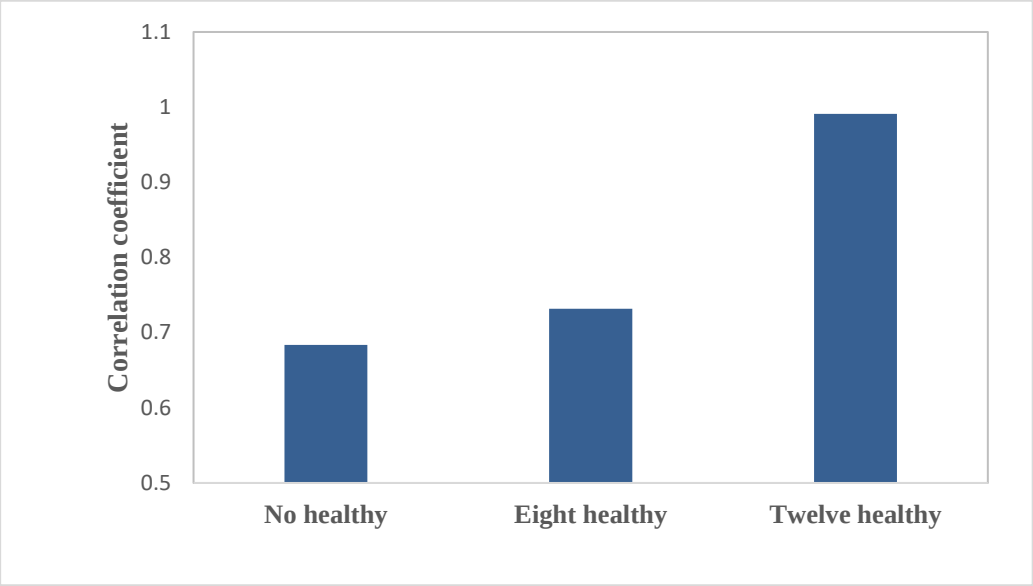

Figure 7.12 Correlation coefficient with an increased number of healthy participants, predictions of healthy participants were not included in the correlation analysis.

7.3. Discussion

In this chapter, the authors described a method of assessing upper-extremity motor function for participants with chronic stroke, using EEG data. In this method, a configuration of a seven-layer neural network was introduced. During the model generation process, the model converged well. For the hyperparameter optimization, TPE was introduced to reduce the amount of computation that was needed. Although 100 steps of optimization were set arbitrarily, the outcome in the testing sections showed 100 steps were sufficient.

In order to investigate the performance of the proposed method, two test methods were introduced in this study (i.e. within-participant testing and cross-participant testing).

In references [22], [23], [25], [26], [28], [128]–[130], the motor function predictions were generated with all the participants EEG data simultaneously. Therefore, the results presented in these papers should not be considered as “across-participant” test results. In order to compare our results with the results in the literature, the within-participant testing was included in this chapter. In the within-participant test section, the accuracy of

the proposed method was investigated.140 trials of EEG data from all the participants' data were used in the model generation, and the remaining data (30 trials) were used in testing. The result suggested the proposed method is very accurate with the test dataset ($n = 14$, $r = 0.9921$, $p = 3.3907 \times 10^{-12}$, predictions from healthy participants were not included in the correlation analysis). The proposed method showed higher accuracy than the methods reported in the literature.

Combining the results in Table 7.1, Figure 7.7 and Figure 7.8, the participants' FMA scores can be roughly grouped into two groups, with FMA score 10-24 and 35-51 respectively. And for the prediction close to the edge of the groups, larger prediction variation and error can be observed. The same feature can also be consistently found in Figure 7.9 and Figure 7.11. This should be caused by the intrinsic FMA score distribution of the participants recruited for this study. For example, the research in this chapter was not able to recruit participants with low FMA score participants (close to 0), middle FMA score (with FMA score ranged from 25-34) and high FMA score participants (close to the full score, 66). And thus, this phenomenon suggests the performance of the proposed method can be further optimized with a larger population, whose FMA score distribution could cover the "blank areas" in this study. However, it is generally hard to recruit people with FMA scores in the "blank areas". For example, with FMA score close to the full score, participants will be less interested in participating study targeting chronic stroke survivors. And with low FMA score close to 0, it will be difficult for those participants to move out of the house or follow the study protocol.

Comparing the within-participant testing results of the proposed CNN and the results with the shallow neural network, the proposed CNN shows higher accuracy than the shallow neural network. However, the proposed CNN required 8 hours of 256 CPUs and 16 GPUs to obtain results. In contrast, the shallow neural network only required 40 mins of 8 CPUs to get results. Therefore, the shallow neural network has the potential to be used with relatively smaller systems with limited system resources and limited data, where the model needs to be re-trained frequently.

The proposed method also exhibited very good reliability even when the participant's EEG data has not been involved in the model generation. With a very reliable performance for the cross-participant testing, the proposed method may not

need to re-train the model when a new participant joins the testing. This is very crucial for this method to be used in practical applications. With only 26 participants' EEG data, the proposed method is already able to predict upper-extremity motor function reliably. The proposed method showed its potential to be used widely in research and clinical applications.

Adding healthy participants' EEG data in the model generation process has practical value in clinical applications. Generally, recruitment of participants with chronic stroke is more difficult than healthy. Therefore, it is more convenient and efficient to recruit some healthy participants and use their EEG data in the model generation, if the EEG data could also improve the model performance. With only EEG data from participants with chronic stroke, the proposed method managed to achieve very high prediction accuracy and reliability in with-in participant testing ($n=14$, $r=0.9899$, $p = 1.4653\times10^{-11}$), as shown in Figure 7.7. With only 14 participants' EEG data, the proposed method outperformed the results in [22], [23], [25], [26], [28], [128]–[130]. Although the cross-participant testing results with data from only participants with chronic stroke was not very satisfactory, the correlation from cross participant testing results is still strong ($n=14$, $r= 0.6836$, $p = 0.0070$). With only EEG data from participants with chronic stroke, the result in cross-participant testing showed very good reliability ($n = 14$, $r = 0.9867$, $p = 7.9342\times10^{-11}$, predictions from healthy participants were not included in the correlation analysis).

Since this chapter is a preliminary study for proofing the concept of using EEG and CNN as an upper-extremity motor function assessment tool, there are four major limitations in this study. Firstly, only 26 participants were recruited and only 14 of them were chronic stroke survivors. The performance of the proposed method was constrained by the number of participants that the authors were able to recruit. If we want to obtain a model for general clinical applications, a clinical trial with a large population is necessary. The performance of the proposed method was greatly improved when healthy participants' EEG data were included in the model generation process (as discussed in Section 7.2.4). This phenomenon could be caused either by the "data hungry" nature of the CNN method [237], or the healthy participant's EEG data completed some form of distribution gaps in the training dataset. At this point, the author is unable to draw any conclusion on this point. Elaborated investigations of this

phenomenon is beyond the scope of this chapter. It could be of interest for future researches. Secondly, the study was done with same-day EEG data acquisition, so the long-term prediction performance of the proposed method has not been validated. A longitudinal study is needed to prove the long-term reliability of the proposed method. Thirdly, the current results were an investigation with FMA scores. The primary goal of this chapter was to prove the concept of using EEG as an upper-extremity motor function assessment tool. FMA is a well-recognized and relatively easy-to-administer motor function assessment in the stroke rehabilitation field. Additionally, FMA has been reported to correlate with LPS of EEG for acute/subacute stroke survivors [28]. Therefore, FMA was selected as the standard motor function score in this study. The EEG data can potentially be regressed on assessments that are more sensitive to motor function changes, e.g. WMFT, to investigate the sensitivity of the proposed method for measuring upper-extremity functionality. Fourthly, the protocol requires the participant to click on a button, which limited the population, as some participants were not able to follow the study protocol. Therefore, protocols with fewer limitations can be investigated to make the proposed method applicable to everyone, for example, sleeping or consciously resting state can be investigated as potential protocols, as suggested in a previous study [28].

7.4. Chapter summary

The goal set by Objective 3 was addressed in this chapter by introducing a method of utilizing a specific CNN model to score upper-extremity function using EEG data. Twelve healthy participants and fourteen chronic stroke survivors participated in this study. EEG data were recorded while the participants were clicking on a computer mouse-like button. CNN models were trained based on the participants' Fugl Meyer motor assessment score. The result showed that the proposed method achieved high prediction accuracy both within ($n = 14$, $r = 0.9921$, $p = 3.3907\times10^{-12}$) and cross ($n = 14$, $r = 0.9867$, $p = 7.9342\times10^{-11}$) participant testing. Based on the result, the proposed method yields high accuracy and robustness in predicting the users' motor function. This evidence suggested that it is possible to use EEG as an accurate and reliable motor function assessment score. In this study, the proposed assessment method can score motor function in individuals with stroke autonomously, which could therefore effectively streamline the assessment procedures in clinical practice.

7.5. Contributions, limitations and future work

The content of this chapter addressed the problem that questionnaire-based motor function assessments are partially subjective and require prior training of the examiner. It has been reported in the literature that some features of EEG data correlate with motor function performance. EEG was thus selected to generate an objective motor function score in this chapter. However, the correlations between results from reported algorithms (utilizing basic EEG features such as band power [24] [26] and phase information [20]) and motor function performance are usually moderate, with correlation coefficients less than 0.8. In addition, those studies were only done with correlation analysis. Whether those correlations could be generalized with untested participants is still unknown. In this chapter, ANN technology was used to enable end-to-end learning on hidden features of EEG data. Some recent papers suggested that CNN has superior performance in EEG analysis focused on event-related potentials with limited number of training data [57], [211], [217]–[220]. Therefore, a seven-layer CNN was proposed and evaluated in this chapter to translate the EEG data into motor function scores.

The study in this chapter contributes to the scientific community by showing that EEG data is able to estimate motor function with good accuracy and reliability. In addition, the proposed ANN method contributes to the field of stroke rehabilitation research by providing an automated, reliable and objective method to quantify motor function, which can assist healthcare professionals in precisely tailoring treatments for their patients.

The primary limitation of the study is the size of the population. The proposed ANN method was investigated with 26 participants and only 12 of them were participants with chronic stroke. In the future, a large-scale study would be advised to address concerns about the clinical significance of the proposed ANN method. Secondly, the data acquisition protocols between healthy participants and participants with chronic stroke were not exactly the same, as healthy participants were required to click with the dominant hand, while participants with chronic stroke were required to click with the most impaired hand. The hand dominance of the participants with chronic stroke may have affected the performance of the ANN model. Although hand dominance or the most impaired side were pre-processed by flipping their EEG data between the right and left

hemispheres for all EEG data collected on the left side (for consistency), a study specifically investigating the importance of hand dominance and side of the stroke impairment is needed to address this limitation. Thirdly, the role of healthy participants' data is still unclear. Although this concern has been partially addressed by the results presented in Section 7.2.4, a future study could be conducted by setting the total amount of the training data constant while varying the portion of healthy participants to fully investigate the role of EEG data from healthy participants. Another limitation of the study was that the ANN method was selected without comparing its performance with other machine learning methods. In the future, a study systematically investigating other types of machine learning methods would be of interest. A longitudinal study investigating the long-term robustness of the proposed method would also be suggested.

Chapter 8.

Conclusions and future work

8.1. Conclusions

In this thesis, the author discussed EEG applications in stroke rehabilitation. This thesis started with a preliminary pilot study to identify the possible challenges. The author identified the following four objectives following the pilot study, which are listed below.

- Objective 1: Reduce the time for repetitive raw data acquisition by investigating the possibility of using one MI to generate the BCI model and classify other MIs.
- Objective 2: Design and develop a rehabilitation training platform, which assists the user when both mental and physical engagement were detected. The feasibility of the proposed platform over multiple sessions will also be investigated.
- Objective 3: Investigate methods to improve online classification performance using biased-classification and moving-average.
- Objective 4: Investigate the feasibility of translating EEG data into an accurate and reliable motor function assessment.

Objective 1 was addressed in Chapter 4. The general model approach method was proposed to deal with the repetitive EEG data acquisition and model generation problem when applying BCI during rehabilitation training. By studying the versatility of the motor imagery tasks during EEG data acquisition, the general rules of selecting MI with higher versatility were determined. As the author mentioned in the previous chapters, higher versatility of MIs refers to higher test accuracy when the model was generated from one type of MI and tested with other similar but different types of MIs. In that chapter, 12 healthy participants were included in the study. Nine MI tasks centered on upper-extremity were investigated. Among all nine MI tasks, MIs of single joint movements showed higher versatility than the rest. The performance difference among the single joint MI tasks was not significant (ANOVA $p>0.05$). Among the three single joint movements investigated in the chapter (i.e. Elbow Task, Weight Task, and Drawer Task), Weight Task showed the highest inter-task test accuracy and the difference was

significant among all nine selected MI tasks ($p<0.05$). This piece of evidence suggests that the Weight Task is the most versatile MI task in the MI tasks investigated. For future studies with BCI applications in rehabilitation training, single joint MI tasks should be considered to avoid repetitive EEG data acquisition for different goal-oriented tasks. For future studies with BCI applications in rehabilitation training of upper-extremity specifically, Weigh Task is recommended.

Objective 2 was addressed in Chapter 5. It is suggested in the literature that combining motor imagery and physical training might further boost motor function recovery. A portable rehabilitation training platform was designed and fabricated to fulfill this need. The proposed rehabilitation training platform consisted of three major sub-systems: a BCI control system, a robotic orthosis, and an FES system. The BCI control system was incorporated to ensure the user's focus on the rehabilitation protocol. A force sensor was embedded in the robotic orthosis to monitor the interaction force between the user and the device. The FES system was used for hand opening when the user had limited control of his/her fingers. To use the proposed rehabilitation platform, the user was required to perform pre-defined MI to activate the assistance from the BCI control system. Then, the user was required to move his/her stroke-impaired elbow in the designated direction to activate the assistance from the robotic orthosis. A three-level progressive rehabilitation training protocol was also proposed to support the rehabilitation training platform. The feasibility of the proposed system was investigated with one participant with chronic stroke during six weeks of rehabilitation training. WMFT was performed every other week to monitor possible motor function improvement. The participant learned how to use the proposed system within the first training session. At the end of the six weeks of training, the user was able to control the proposed rehabilitation training platform with very high accuracy (90.6% for the BCI control, 83.1% for the BF control). The proposed rehabilitation training platform, which combines motor imagery and physical training, has been proven to be feasible for patients with chronic stroke. In addition, the participant showed improvement in WMFT (12% improvement), which supported the potential efficacy of the proposed rehabilitation training platform. The strong correlation between the BSI and the WMFT also suggested motor function improvement. However, since only one participant was recruited for this study, the efficacy of the proposed rehabilitation training platform cannot be concluded.

Objective 3 was addressed in Chapter 6. In that chapter, in order to deal with the low accuracy problem with the BCI online classification, two methods of filtering the probability prediction output of online BCI applications were introduced. One of the methods was proposed based on machine learning theory, which was a biased-classification method toward resting state, with decision thresholds calculated from a normal distribution assumption. The other method was proposed based on signal processing theory, which utilized a moving-average method to smooth the classification output, with decision thresholds observed from 30 seconds of rest state EEG data at the beginning of each training day. The proposed methods were evaluated with a pseudo online analysis based on EEG recordings of one participant with chronic stroke during six weeks of rehabilitation training with BCI. Performance measures like accuracy, false positive rate and response delay were summarized to evaluate the two proposed methods. The performance of the proposed methods was also compared with the non-filtering method. It was concluded that both proposed methods showed superior performance than the traditional non-filtering method. Between the two proposed methods, the moving average method showed better performance with lower false positive rate (0.5275), higher precision (0.5789), higher accuracy (0.5989) and higher Cohen's Kappa Score (0.1978). The biased-classification method had a significantly lower delay (Wilcoxon rank sum test, $n_1 = 443$, $n_2 = 560$, $P = 8.56\times10^{-6}$). In BCI applications for stroke rehabilitation, where response delay is not a major issue, the moving average method is recommended.

Objective 4 was addressed in Chapter 7. The primary objective was to deal with the problems in the questionnaire-based motor function assessment methods. In that chapter of the thesis, a CNN configuration for generating a motor function score from EEG was proposed and evaluated with within-participant testing and cross-participant testing. Fourteen participants with chronic stroke and twelve healthy participants were recruited in this part of the study. EEG data were recorded while the participants were performing button clicking once every self-estimated 10 seconds. The proposed CNN was trained with regression on the FMA scores, which were collected on the same day as the EEG data acquisition. The within-participant testing results suggested that the model converged well during the training, and the resulted prediction score outperformed the scores proposed in the literature ($r = 0.9931$, $p = 8.0751\times10^{-24}$). The cross-participant testing results suggested that the prediction scores were still accurate and reliable, even

if the participants' EEG data were not involved in the model generation ($r = 0.9590$, $p = 1.2098\times10^{-14}$). The cross-participant testing results was a crucial piece of evidence suggesting the proposed method would potentially have reliable performance in actual clinical applications when the majority of the users' EEG data were not involved in the model generation.

In conclusion, all four objectives proposed at the beginning of this thesis were successfully addressed. Future research paths may involve investigating advances specific to the methods proposed in this thesis. Alternatively, non-approach specific related modifications of the research methods may also be investigated with respect to the challenges of EEG applications in stroke rehabilitation.

8.2. Future works

For the study presented in Chapter 4, limitations were mainly related to the methodology. In that part of the thesis, a limited number of MI tasks were investigated. Due to the lack of expertise in neuroscience, the conclusion was drawn only with the test accuracy of the MI tasks investigated in the study, without specific explanations based on the neuro-scientific theories. For better understanding of the performance variation of the MI tasks, a study utilizing neuro-imaging tools with high spatial resolution is necessary. In addition, the study in Chapter 4 focused on upper-extremity only. Whether the conclusions in this study can be used for other joints remains unclear.

For the study introduced in Chapter 5, a portable rehabilitation platform together with a special supporting protocol were proposed to fulfill the need of combining motor imagery and physical training in the rehabilitation field. The proposed platform and protocol were evaluated during six weeks of rehabilitation training with one participant with chronic stroke. Limitations of the study in that chapter were mainly related to the fact that only one individual participated, which limited conclusions about the possible efficacy of the proposed platform. The efficacy of the proposed platform needs to be investigated in a controlled clinical study with a larger population with stroke.

For the study presented in Chapter 6, the major limitation was also related to the number of participants. Although the data were collected for a relatively long time (six weeks), the data were recorded from only one participant with chronic stroke. Therefore,

the conclusions of that chapter are still preliminary. In order to further consolidate the conclusions, a group of participants with chronic stroke in a long-term rehabilitation training is necessary. The two methods proposed in this chapter are simple and straightforward, there is still plenty of room for improvement in the performance. More complex processing/filtering methods can be further investigated to improve the BCI application accuracy.

For the CNN model proposed in Chapter 7, although the configuration was reliable and accurate in the cross-participant testing, the performance can be further improved with a larger population. For example, a training dataset without gaps in the distribution of the motor function scores would definitely improve the performance of the proposed CNN model. The detailed CNN configuration and parameters can also be further investigated with a larger population. In addition, the sensitivity and longitudinal effect of the proposed method were not investigated thoroughly. A long-term clinical study with repetitive EEG data acquisition and motor function assessments is needed for such purpose. The EEG data protocol of mouse clicking is hard for some patients with severe chronic stroke. Possible protocols that are less constraining should be explored (for instance: eyes-closed, or resting state with eyes open etc.). At last, it would be interesting to investigate which features of the PSD and phase information contributed to the motor function score. This is a limitation of the CNN method. As the features are highly abstracted with neural networks, it is difficult to determine the key features from the trained CNN models. Some literature suggested the input-maximization approach could be a possible method, which might be an interesting topic for future studies.

References

[1] D. Mozaffarian *et al.*, “Heart disease and stroke statistics-2016 update a report from the American Heart Association,” *Circulation*, vol. 133, no. 4. pp. e38–e48, 2016.

[2] H. Igo Krebs, N. Hogan, M. L. Aisen, and B. T. Volpe, “Robot-aided neurorehabilitation,” *IEEE Trans. Rehabil. Eng.*, vol. 6, no. 1, pp. 75–87, 1998.

[3] G. Kwakkel, R. C. Wagenaar, T. W. Koelman, G. J. Lankhorst, and J. C. Koetsier, “Effects of Intensity of Rehabilitation After Stroke : A Research Synthesis,” *Stroke*, vol. 28, no. 8, pp. 1550–1556, 1997.

[4] N. Hogan *et al.*, “Motions or muscles? Some behavioral factors underlying robotic assistance of motor recovery.,” *J. Rehabil. Res. Dev.*, vol. 43, no. 5, pp. 605–618, 2006.

[5] K. Wing, J. V Lynskey, and P. R. Bosch, “Whole-body intensive rehabilitation is feasible and effective in chronic stroke survivors: a retrospective data analysis.,” *Top. Stroke Rehabil.*, vol. 15, no. 3, pp. 247–55, 2008.

[6] H. I. Krebs, B. Volpe, and N. Hogan, “A working model of stroke recovery from rehabilitation robotics practitioners,” *J. Neuroeng. Rehabil.*, vol. 6, no. 1, p. 6, 2009.

[7] G. Herrnstadt, N. Alavi, B. K. Randhawa, L. A. Boyd, and C. Menon, “Bimanual Elbow Robotic Orthoses: Preliminary Investigations on an Impairment Force-Feedback Rehabilitation Method,” *Front. Hum. Neurosci.*, vol. 9, 2015.

[8] R. J. Sanchez *et al.*, “A pneumatic robot for re-training arm movement after stroke: Rationale and mechanical design,” in *Proceedings of the 2005 IEEE 9th International Conference on Rehabilitation Robotics*, 2005, vol. 2005, pp. 500–504.

[9] Y. Ren, S. H. Kang, H. S. Park, Y. N. Wu, and L. Q. Zhang, “Developing a multi-joint upper limb exoskeleton robot for diagnosis, therapy, and outcome evaluation in neurorehabilitation,” *IEEE Trans. Neural Syst. Rehabil. Eng.*, vol. 21, no. 3, pp. 490–499, 2013.

[10] R. C. V Loureiro, W. S. Harwin, K. Nagai, and M. Johnson, “Advances in upper limb stroke rehabilitation: A technology push,” *Med. Biol. Eng. Comput.*, vol. 49, no. 10, pp. 1103–1118, 2011.

[11] T. Proietti and V. Crocher, “Upper-Limb Robotic Exoskeletons for Neurorehabilitation : A Review on Control Strategies,” vol. 9, pp. 4–14, 2016.

[12] C. T. Freeman, A. M. Hughes, J. H. Burridge, P. H. Chappell, P. L. Lewin, and E. Rogers, “A robotic workstation for stroke rehabilitation of the upper extremity using FES,” *Med. Eng. Phys.*, vol. 31, no. 3, pp. 364–373, 2009.

[13] P. Poli, G. Morone, G. Rosati, and S. Masiero, “Robotic technologies and rehabilitation: New tools for stroke patients’ therapy,” *BioMed Research International*, vol. 2013. 2013.

[14] H. S. Lo and S. Q. Xie, “Exoskeleton robots for upper-limb rehabilitation: State of the art and future prospects,” *Med. Eng. Phys.*, vol. 34, no. 3, pp. 261–268, 2012.

[15] J. R. Wolpaw, N. Birbaumer, D. J. McFarland, G. Pfurtscheller, and T. M. Vaughan, “Brain–computer interfaces for communication and control,” *Clin. Neurophysiol.*, vol. 113, no. 6, pp. 767–791, Jun. 2002.

[16] J. J. Daly and J. R. Wolpaw, “Brain-computer interfaces in neurological rehabilitation,” *The Lancet Neurology*, vol. 7, no. 11. pp. 1032–1043, 2008.

[17] R. Gentili, C. Papaxanthis, and T. Pozzo, “Improvement and generalization of arm motor performance through motor imagery practice,” *Neuroscience*, vol. 137, no. 3, pp. 761–772, 2006.

[18] S. P. Finnigan, M. Walsh, S. E. Rose, and J. B. Chalk, “Quantitative EEG indices of sub-acute ischaemic stroke correlate with clinical outcomes,” *Clin. Neurophysiol.*, vol. 118, no. 11, pp. 2525–2532, 2007.

[19] M. Gandolfi *et al.*, “Quantification of Upper Limb Motor Recovery and EEG Power Changes after Robot-Assisted Bilateral Arm Training in Chronic Stroke Patients : A Prospective Pilot Study,” vol. 2018, 2018.

[20] M. J. A. M. Van Putten, J. M. Peters, S. M. Mulder, J. A. M. De Haas, C. M. A. Bruijninckx, and D. L. J. Tavy, “A brain symmetry index (BSI) for online EEG monitoring in carotid endarterectomy,” *Clin. Neurophysiol.*, vol. 115, no. 5, pp. 1189–1194, 2004.

[21] L. Gao, J. Wang, and L. Chen, “Event-related desynchronization and synchronization quantification in motor-related EEG by Kolmogorov entropy.,” *J. Neural Eng.*, vol. 10, no. 3, p. 036023, 2013.

[22] C. Neuper and G. Pfurtscheller, “Event-related dynamics of cortical rhythms: Frequency-specific features and functional correlates,” *Int. J. Psychophysiol.*, vol. 43, no. 1, pp. 41–58, 2001.

[23] M. J. A. M. Van Putten and D. L. J. Tavy, “Continuous quantitative EEG monitoring in hemispheric stroke patients using the brain symmetry index,” *Stroke*, vol. 35, no. 11, pp. 2489–2492, 2004.

[24] S. Finnigan and M. J. A. M. van Putten, “EEG in ischaemic stroke: Quantitative EEG can uniquely inform (sub-)acute prognoses and clinical management,” *Clinical Neurophysiology*, vol. 124, no. 1. pp. 10–19, 2013.

[25] A. A. Anastasi, O. Falzon, K. Camilleri, M. Vella, and R. Muscat, “Brain Symmetry Index in Healthy and Stroke Patients for Assessment and Prognosis,” vol. 2017, 2017.

[26] J. Leon-Carrion, J. F. Martin-Rodriguez, J. Damas-Lopez, J. M. Barroso y Martin, and M. R. Dominguez-Morales, “Delta-alpha ratio correlates with level of recovery after neurorehabilitation in patients with acquired brain injury,” *Clin. Neurophysiol.*, vol. 120, no. 6, pp. 1039–1045, 2009.

[27] C. M. Stinear, “Prediction of motor recovery after stroke: advances in biomarkers,” *Lancet Neurol.*, vol. 16, no. 10, pp. 826–836, 2017.

[28] T. Kawano *et al.*, “Large-Scale Phase Synchrony Reflects Clinical Status after Stroke: An EEG Study,” *Neurorehabil. Neural Repair*, vol. 31, no. 6, pp. 561–570, 2017.

[29] A. M. Elnady *et al.*, “A Single-Session Preliminary Evaluation of an Affordable BCI-Controlled Arm Exoskeleton and Motor-Proprioception Platform.,” *Front. Hum. Neurosci.*, vol. 9, no. March, p. 168, 2015.

[30] A. Frisoli *et al.*, “A new gaze-BCI-driven control of an upper limb exoskeleton for rehabilitation in real-world tasks,” *IEEE Trans. Syst. Man Cybern. Part C Appl. Rev.*, vol. 42, no. 6, pp. 1169–1179, Nov. 2012.

[31] C. Wang *et al.*, “A feasibility study of non-invasive motor-imagery BCI-based robotic rehabilitation for stroke patients,” in *2009 4th International IEEE/EMBS Conference on Neural Engineering, NER ’09*, 2009, pp. 271–274.

[32] M. Y. Pang, J. E. Harris, and J. J. Eng, “A community-based upper-extremity group exercise program improves motor function and performance of functional activities in chronic stroke: A randomized controlled trial,” *Arch. Phys. Med. Rehabil.*, 2006.

[33] B. Z. Allison *et al.*, “Toward smarter BCIs: extending BCIs through hybridization and intelligent control,” *J. Neural Eng.*, vol. 9, no. 1, p. 013001, 2012.

[34] G. Pfurtscheller, “The hybrid BCI,” *Front. Neurosci.*, 2010.

[35] S. Amiri, A. Rabbi, L. Azinfar, R. Fazel-Rezai, and V. Asadpour, “A Review of P300, SSVEP, and Hybrid P300 / SSVEP Brain- Computer Interface Systems,” *Brain-Computer Interface Syst. - Recent Prog. Futur. Prospect.*, vol. 2013, pp. 1–8, 2013.

[36] R. Scherer, A. Schloegl, F. Lee, H. Bischof, J. Janša, and G. Pfurtscheller, “The self-paced graz brain-computer interface: Methods and applications,” *Comput. Intell. Neurosci.*, vol. 2007, 2007.

[37] R. Scherer, G. R. Muller-Putz, and G. Pfurtscheller, “Self-initiation of EEG-based brain-computer communication using the heart rate response,” *J. Neural Eng.*, vol. 4, no. 4, pp. L23–L29, 2007.

[38] U. Chaudhary, N. Birbaumer, and A. Ramos-Murguialday, “Brain–computer interfaces for communication and rehabilitation,” *Nat. Rev. Neurol.*, vol. 12, no. 9, pp. 513–525, Aug. 2016.

[39] E. A. Curran and M. J. Stokes, “Learning to control brain activity: A review of the production and control of EEG components for driving brain–computer interface (BCI) systems,” *Brain Cogn.*, vol. 51, no. 3, pp. 326–336, 2003.

[40] S. Silvoni *et al.*, “Brain-Computer Interface in Stroke: A Review of Progress,” *Clin. EEG Neurosci.*, vol. 42, no. 4, pp. 245–252, 2011.

[41] F. Lotte, M. Congedo, A. Lécuyer, F. Lamarche, and B. Arnaldi, “A review of classification algorithms for EEG-based brain–computer interfaces,” *J. Neural Eng.*, vol. 4, no. 2, pp. R1–R13, 2007.

[42] D. J. McFarland and J. R. Wolpaw, “Brain-Computer Interfaces for Communication and Control,” *Commun. ACM*, vol. 54, no. 5, pp. 60–66, 2011.

[43] I. Choi, I. Rhiu, Y. Lee, M. H. Yun, and C. S. Nam, *A systematic review of hybrid brain-computer interfaces: Taxonomy and usability perspectives*. 2017.

[44] B. J. Edelman, B. Baxter, and B. He, “EEG source imaging enhances the decoding of complex right-hand motor imagery tasks,” *IEEE Trans. Biomed. Eng.*, vol. 63, no. 1, pp. 4–14, 2016.

[45] A. Lenhardt, M. Kaper, and H. J. Ritter, “An adaptive P300-based online brain-computer interface,” *IEEE Trans. Neural Syst. Rehabil. Eng.*, 2008.

[46] M. Spüler, W. Rosenstiel, and M. Bogdan, “Online Adaptation of a c-VEP Brain-Computer Interface(BCI) Based on Error-Related Potentials and Unsupervised Learning,” *PLoS One*, 2012.

[47] H. Yuan, A. Doud, A. Gururajan, and B. He, “Cortical imaging of event-related (de)synchronization during online control of brain-computer interface using minimum-norm estimates in frequency domain,” *IEEE Trans. Neural Syst. Rehabil. Eng.*, 2008.

[48] J. J. Wilson and R. Palaniappan, “Analogue mouse pointer control via an online steady state visual evoked potential (SSVEP) brain-computer interface,” in *Journal of Neural Engineering*, 2011.

[49] C. Brunner, R. Scherer, B. Graimann, G. Supp, and G. Pfurtscheller, “Online control of a brain-computer interface using phase synchronization,” *IEEE Trans. Biomed. Eng.*, 2006.

[50] M. K. Hazrati and A. Erfanian, “An online EEG-based brain-computer interface for controlling hand grasp using an adaptive probabilistic neural network,” *Med. Eng. Phys.*, vol. 32, no. 7, pp. 730–739, 2010.

[51] B. Koo *et al.*, “A hybrid NIRS-EEG system for self-paced brain computer interface with online motor imagery,” *J. Neurosci. Methods*, 2015.

[52] A. R. Fugl-Meyer, L. Jääskö, I. Leyman, S. Olsson, and S. Steglind, “The post-stroke hemiplegic patient. 1. a method for evaluation of physical performance.,”

Scand. J. Rehabil. Med., vol. 7, no. 1, pp. 13–31, 1975.

[53] S. L. Wolf *et al.*, “The EXCITE trial: Attributes of the Wolf Motor Function Test in patients with subacute stroke,” *Neurorehabil. Neural Repair*, 2005.

[54] R. Keith, C. Granger, B. Hamilton, and F. Sherwin, “The functional independence measure: a new tool for rehabilitation,” *Adv. Clin. Rehabil.*, vol. 1, no. 2, pp. 6–18, 1987.

[55] L. K. Kwah and J. Diong, “National Institutes of Health Stroke Scale (NIHSS),” *Journal of Physiotherapy*. 2014.

[56] Y. LeCun, Y. Bengio, G. Hinton, L. Y., B. Y., and H. G., “Deep learning,” *Nature*, vol. 521, no. 7553, pp. 436–444, 2015.

[57] J. Schmidhuber, “Deep Learning in neural networks: An overview,” *Neural Networks*, vol. 61. pp. 85–117, 2015.

[58] Stroke Association, “What is a stroke ?,” 2014.

[59] G. A. Donnan, M. Fisher, M. Macleod, S. M. Davis, S. Royal, and U. K. M. Macleod, “Stroke.,” *Lancet*, 2008.

[60] National Institute of Neurological Disorders and Stroke, “Stroke: Hope Through Research,” 2018. [Online]. Available: https://www.ninds.nih.gov/Disorders/Patient-Caregiver-Education/Hope-Through-Research/Stroke-Hope-Through-Research.

[61] R. Bonita, S. Mendis, T. Truelsen, J. Bogousslavsky, J. Toole, and F. Yatsu, “The global stroke initiative,” *Lancet Neurology*. 2004.

[62] P. Langhorne, J. Bernhardt, and G. Kwakkel, “Stroke Care 2 Stroke rehabilitation,” *Lancet*, vol. 377, no. 9778, pp. 1693–1702, 2011.

[63] C. Warlow, J. Van Gijn, and M. Dennis, “Stroke: Practical Management,” *N. Engl. J. Med.*, 2008.

[64] J. G. Broeks, G. J. Lankhorst, K. Rumping, and A. J. Prevo, “The long-term outcome of arm function after stroke: results of a follow-up study.,” *Disabil. Rehabil.*, 1999.

[65] G. Kwakkel, B. Kollen, and E. Lindeman, “Understanding the pattern of functional recovery after stroke: facts and theories,” *Restor. Neurol. Neurosci.*, 2004.

[66] M. F. Levin, J. A. Kleim, and S. L. Wolf, “What Do Motor ‘Recovery’ and ‘Compensation’ Mean in Patients Following Stroke?,” *Neurorehabil. Neural Repair*, 2009.

[67] E. Hunt, “Illustration of the two main categories of strokes,” 2018. [Online]. Available: https://en.wikipedia.org/wiki/Stroke#/media/File:Ischemic_Stroke.svg.

[68] P. Langhorne, F. Coupar, and A. Pollock, “Motor recovery after stroke: a

systematic review," *The Lancet Neurology*. 2009.

[69] T. H. Murphy and D. Corbett, "Plasticity during stroke recovery: From synapse to behaviour," *Nature Reviews Neuroscience*. 2009.

[70] P. Langhorne, J. Bernhardt, and G. Kwakkel, "Stroke rehabilitation," *Lancet*, vol. 377, no. 9778, pp. 1693–1702, 2011.

[71] R. M. D. Caton, "Electrical Currents of the Brain," *Chicago J. Nerv. Ment. Dis.*, 1875.

[72] A. Coenen, E. Fine, and O. Zayachkivska, "Adolf beck: A forgotten pioneer in electroencephalography," *Journal of the History of the Neurosciences*. 2014.

[73] D. Leigh, "A history of the electrical activity of the brain. The first half-century," *J. Psychosom. Res.*, 2012.

[74] H. L F, "'Hans Berger (1873-1941), Richard Caton (1842-1926), and electroencephalography,'" *J. Neurol. Neurosurg. Psychiatry*, 2003.

[75] F. A. Gibbs, H. Davis, and W. G. Lennox, "The electro-encephalogram in epilepsy and in conditions of impaired consciousness," *Arch. Neurol. Psychiatry*, 1935.

[76] S. Bozinovski, M. Sestakov, and L. Bozinovska, "Using EEG alpha rhythm to control a mobile robot," 2003.

[77] S. Baillet, J. C. Mosher, and R. M. Leahy, "Electromagnetic brain mapping," *IEEE Signal Process. Mag.*, vol. 18, no. 6, pp. 14–30, 2001.

[78] W. O. Tatum, "Ellen R. grass lecture: Extraordinary EEG," *Neurodiagn. J.*, vol. 54, no. 1, pp. 3–21, 2014.

[79] S. Shahid, R. K. Sinha, and G. Prasad, "Mu and beta rhythm modulations in motor imagery related post-stroke EEG: a study under BCI framework for post-stroke rehabilitation," *BMC Neurosci.*, vol. 11, no. Suppl 1, p. P127, 2010.

[80] E. R. Kandel, J. H. Schwartz, T. M. Jessell, S. A. Siegelbaum, and A. J. Hudspeth, *Principles of Neural Science, Fifth Edition*, vol. 3. 2014.

[81] T. Hanakawa, M. A. Dimyan, and M. Hallett, "Motor planning, imagery, and execution in the distributed motor network: A time-course study with functional MRI," *Cereb. Cortex*, vol. 18, no. 12, pp. 2775–2788, 2008.

[82] J. B. Ochoa, *EEG Signal Classification for Brain Computer Interface Applications*. 2002.

[83] J. R. Wolpaw, "Brain-computer interfaces as new brain output pathways.," *J. Physiol.*, vol. 579, no. Pt 3, pp. 613–619, 2007.

[84] L. F. Nicolas-Alonso and J. Gomez-Gil, "Brain computer interfaces, a review," *Sensors (Basel)*, vol. 12, no. 2, pp. 1211–1279, 2012.

[85] A. Remsik *et al.*, “A review of the progression and future implications of brain-computer interface therapies for restoration of distal upper extremity motor function after stroke,” *Expert Rev. Med. Devices*, vol. 4440, no. April, p. 17434440.2016.1174572, 2016.

[86] E. W. Sellers, T. M. Vaughan, and J. R. Wolpaw, “A brain-computer interface for long-term independent home use.,” *Amyotroph. Lateral Scler.*, vol. 11, no. 5, pp. 449–455, 2010.

[87] G. R. Müller-Putz and G. Pfurtscheller, “Control of an electrical prosthesis with an SSVEP-based BCI,” *IEEE Trans. Biomed. Eng.*, vol. 55, no. 1, pp. 361–364, 2008.

[88] H. Wang, T. Li, and Z. Huang, “Remote control of an electrical car with SSVEP-Based BCI,” in *Proceedings 2010 IEEE International Conference on Information Theory and Information Security, ICITIS 2010*, 2010, pp. 837–840.

[89] J. Meng, S. Zhang, A. Bekyo, J. Olsoe, B. Baxter, and B. He, “Noninvasive Electroencephalogram Based Control of a Robotic Arm for Reach and Grasp Tasks,” *Sci. Rep.*, vol. 6, no. 1, p. 38565, 2016.

[90] S. M. T. Müller, T. F. Bastos, and M. S. Filho, “Proposal of a SSVEP-BCI to command a robotic wheelchair,” *J. Control. Autom. Electr. Syst.*, vol. 24, no. 1–2, pp. 97–105, 2013.

[91] X. Yong and C. Menon, “EEG Classification of Different Imaginary Movements within the Same Limb,” *PLoS One*, vol. 10, no. 4, p. e0121896, 2015.

[92] K. K. Ang and C. Guan, “Brain-Computer Interface in Stroke Rehabilitation,” *J. Comput. Sci. Eng.*, vol. 7, no. 2, pp. 139–146, 2013.

[93] B. He, B. Baxter, B. J. Edelman, C. C. Cline, and W. W. Ye, “Noninvasive brain-computer interfaces based on sensorimotor rhythms,” *Proc. IEEE*, vol. 103, no. 6, pp. 907–925, 2015.

[94] I. J. Hubbard, M. W. Parsons, C. Neilson, and L. M. Carey, “Task-specific training: Evidence for and translation to clinical practice,” *Occupational Therapy International*, vol. 16, no. 3–4. pp. 175–189, Jan-2009.

[95] L. A. Boyd, E. D. Vidoni, and B. D. Wessel, “Motor learning after stroke: Is skill acquisition a prerequisite for contralesional neuroplastic change?,” *Neurosci. Lett.*, vol. 482, no. 1, pp. 21–25, Sep. 2010.

[96] A. S. Royer and B. He, “Goal selection versus process control in a brain-computer interface based on sensorimotor rhythms.,” *J. Neural Eng.*, vol. 6, no. 1, p. 016005, 2009.

[97] B. K. Min, R. Chavarriaga, and J. del R. Millan, “Harnessing Prefrontal Cognitive Signals for Brain-Machine Interfaces,” *Trends in Biotechnology*, 2017.

[98] X. Zhang, X. Yong, and C. Menon, “Evaluating the versatility of EEG models

generated from motor imagery tasks: An exploratory investigation on upper-limb elbow-centered motor imagery tasks," *PLoS One*, vol. 12, no. 11, 2017.

[99] J. R. Wolpaw and D. J. McFarland, "Control of a two-dimensional movement signal by a noninvasive brain-computer interface in humans," *Proc. Natl. Acad. Sci. U. S. A.*, vol. 101, no. 51, pp. 17849–17854, 2004.

[100] F. Meng *et al.*, "BCI-FES training system design and implementation for rehabilitation of stroke patients," *, 2008. Ijcnn 2008.*, pp. 4103–4106, 2008.

[101] E. Buch *et al.*, "Think to move: A neuromagnetic brain-computer interface (BCI) system for chronic stroke," *Stroke*, vol. 39, no. 3, pp. 910–917, 2008.

[102] J. J. Daly, R. Cheng, J. Rogers, K. Litinas, K. Hrovat, and M. Dohring, "Feasibility of a new application of noninvasive Brain Computer Interface (BCI): a case study of training for recovery of volitional motor control after stroke," *J Neurol Phys Ther*, vol. 33(4), no. 4, pp. 203–211, 2009.

[103] Y. Gu, K. Dremstrup, and D. Farina, "Single-trial discrimination of type and speed of wrist movements from EEG recordings," *Clin. Neurophysiol.*, vol. 120, no. 8, pp. 1596–1600, 2009.

[104] G. Prasad, P. Herman, D. Coyle, S. McDonough, and J. Crosbie, "Applying a brain-computer interface to support motor imagery practice in people with stroke for upper limb recovery: a feasibility study," *J. Neuroeng. Rehabil.*, vol. 7, no. 1, p. 60, 2010.

[105] H. G. Tan, K. H. Kong, C. Y. Shee, C. C. Wang, C. T. Guan, and W. T. Ang, "Post-acute stroke patients use brain-computer interface to activate electrical stimulation," in *2010 Annual International Conference of the IEEE Engineering in Medicine and Biology Society, EMBC'10*, 2010, pp. 4234–4237.

[106] K. K. Ang *et al.*, "Clinical study of neurorehabilitation in stroke using EEG-based motor imagery brain-computer interface with robotic feedback," in *2010 Annual International Conference of the IEEE Engineering in Medicine and Biology Society, EMBC'10*, 2010, pp. 5549–5552.

[107] D. Broetz, C. Braun, C. Weber, S. R. Soekadar, A. Caria, and N. Birbaumer, "Combination of Brain-Computer Interface Training and Goal-Directed Physical Therapy in Chronic Stroke: A Case Report," *Neurorehabil. Neural Repair*, vol. 24, no. 7, pp. 674–679, 2010.

[108] W. K. Tam, K. Y. Tong, F. Meng, and S. Gao, "A minimal set of electrodes for motor imagery BCI to control an assistive device in chronic stroke subjects: A multi-session study," *IEEE Trans. Neural Syst. Rehabil. Eng.*, vol. 19, no. 6, pp. 617–627, 2011.

[109] M. Gomez-Rodriguez, J. Peterst, J. Hin, B. Schölkopf, A. Gharabaghi, and M. Grosse-Wentrup, "Closing the sensorimotor loop: Haptic feedback facilitates decoding of arm movement imagery," in *Conference Proceedings - IEEE*

International Conference on Systems, Man and Cybernetics, 2010, pp. 121–126.

[110] K. Shindo *et al.*, “Effects of neurofeedback training with an electroencephalogram-based brain-computer interface for hand paralysis in patients with chronic stroke: A preliminary case series study,” *J. Rehabil. Med.*, vol. 43, no. 10, pp. 951–957, 2011.

[111] R. Ortner, D.-C. Irimia, J. Scharinger, and C. Guger, “A motor imagery based brain-computer interface for stroke rehabilitation.,” *Stud. Health Technol. Inform.*, vol. 181, pp. 319–23, 2012.

[112] V. Kaiser, A. Kreilinger, G. R. Müller-Putz, and C. Neuper, “First steps toward a motor imagery based stroke BCI: New strategy to set up a classifier,” *Front. Neurosci.*, no. JUL, 2011.

[113] F. Cincotti *et al.*, “EEG-based brain-computer interface to support post-stroke motor rehabilitation of the upper limb,” in *Proceedings of the Annual International Conference of the IEEE Engineering in Medicine and Biology Society, EMBS*, 2012, pp. 4112–4115.

[114] A. Vuckovic and F. Sepulveda, “A two-stage four-class BCI based on imaginary movements of the left and the right wrist,” *Med. Eng. Phys.*, vol. 34, no. 7, pp. 964–971, 2012.

[115] A. Ramos-Murguialday *et al.*, “Brain-machine interface in chronic stroke rehabilitation: A controlled study,” *Ann. Neurol.*, vol. 74, no. 1, pp. 100–108, 2013.

[116] B. M. Young, J. Williams, and V. Prabhakaran, “BCI-FES: could a new rehabilitation device hold fresh promise for stroke patients?,” *Expert Rev. Med. Devices*, vol. 11, no. 6, pp. 537–9, 2014.

[117] K. K. Ang *et al.*, “A Randomized Controlled Trial of EEG-Based Motor Imagery Brain-Computer Interface Robotic Rehabilitation for Stroke,” *Clin. EEG Neurosci.*, vol. 46, no. 4, pp. 310–320, 2015.

[118] R. D. Pinto and H. A. Ferreira, “Development of a Non-invasive Brain Computer Interface for Neurorehabilitation,” *Proceedings of the 3rd 2015 Workshop on ICTs for improving Patients Rehabilitation Research Techniques*. ACM, Lisbon, Portugal, pp. 126–130, 2015.

[119] J. Ibáñez, J. I. Serrano, M. D. Del Castillo, E. Monge, F. Molina, and J. L. Pons, “Heterogeneous BCI-Triggered Functional Electrical Stimulation Intervention for the Upper-Limb Rehabiliation of Stroke Patients,” in *Brain-Computer Interface Research*, C. Guger, G. Müller-Putz, and B. Allison, Eds. Springer International Publishing, 2015, pp. 67–77.

[120] B. Z. Allison, E. W. Wolpaw, and J. R. Wolpaw, “Brain–computer interface systems: progress and prospects,” *Expert Rev. Med. Devices*, vol. 4, no. 4, pp. 463–474, 2007.

[121] J. R. Wolpaw, *Brain-computer interfaces*, vol. 110, no. Journal Article PG-67-74. 2013.

[122] T. Trakoolwilaiwan, J. Lee, and J. Choi, “Convolutional neural network for high-accuracy functional near- infrared spectroscopy in a brain – computer interface : three-class classification of rest , right- , and left- hand motor execution functional near-infrared spectroscopy in,” vol. 5, no. 1, 2017.

[123] A. Chowdhury, H. Raza, Y. K. Meena, A. Dutta, and G. Prasad, “Online Covariate Shift Detection based Adaptive Brain-Computer Interface to Trigger Hand Exoskeleton Feedback for Neuro-Rehabilitation,” *IEEE Trans. Cogn. Dev. Syst.*, vol. XX, no. XX, pp. 1–11, 2017.

[124] J. Faller, C. Vidaurre, T. Solis-Escalante, C. Neuper, and R. Scherer, “Autocalibration and recurrent adaptation: Towards a plug and play online ERD-BCI,” *IEEE Trans. Neural Syst. Rehabil. Eng.*, vol. 20, no. 3, pp. 313–319, 2012.

[125] B. Blankertz, F. Losch, M. Krauledat, G. Dornhege, G. Curio, and K.-R. Muller, “The Berlin Brain–Computer Interface: Accurate Performance From First-Session in BCI-Na #x00CF;ve Subjects,” *IEEE Trans. Biomed. Eng.*, vol. 55, no. 10, pp. 2452–2462, 2008.

[126] C. Vidaurre, C. Sannelli, K. R. Müller, and B. Blankertz, “Machine-learning-based coadaptive calibration for Brain-computer interfaces,” *Neural Computation*. 2011.

[127] P. Nicolo, S. Rizk, C. Magnin, M. Di Pietro, A. Schnider, and A. G. Guggisberg, “Coherent neural oscillations predict future motor and language improvement after stroke,” *Brain*, vol. 138, no. 10, pp. 3048–3060, 2015.

[128] G. Pfurtscheller and C. Neuper, “Simultaneous EEG 10 Hz desynchronization and 40 Hz synchronization during finger movements.,” *Neuroreport*, vol. 3, no. 12. pp. 1057–60, 1992.

[129] A. Stancák and G. Pfurtscheller, “Event-related desynchronisation of central beta-rhythms during brisk and slow self-paced finger movements of dominant and nondominant hand,” *Cogn. Brain Res.*, vol. 4, no. 3, pp. 171–183, 1996.

[130] G. Pfurtscheller and F. H. Lopes Da Silva, “Event-related EEG/MEG synchronization and desynchronization: Basic principles,” *Clinical Neurophysiology*, vol. 110, no. 11. pp. 1842–1857, 1999.

[131] J. Muller-Gerking, G. Pfurtscheller, H. Flyvbjerg, J. Müller-Gerking, G. Pfurtscheller, and H. Flyvbjerg, “Designing optimal spatial fiters for single-trial EEG classification in a movement task,” *Clin. Neurophysiol.*, vol. 110, no. 5, pp. 787–798, 1999.

[132] B. Blankertz, R. Tomioka, S. Lemm, M. Kawanabe, and K. R. Müller, “Optimizing spatial filters for robust EEG single-trial analysis,” *IEEE Signal Process. Mag.*, vol. 25, no. 1, pp. 41–56, 2008.

[133] Y. Wang, S. Gao, and X. Gao, “Common spatial pattern method for channel selelction in motor imagery based brain-computer interface,” in *Engineering in Medicine and Biology Society, 2005. IEEE-EMBS 2005. 27th Annual International Conference of the*, 2006, pp. 5392–5395.

[134] H. Ramoser, J. Müller-Gerking, and G. Pfurtscheller, “Optimal spatial filtering of single trial EEG during imagined hand movement,” *IEEE Trans. Rehabil. Eng.*, vol. 8, no. 4, pp. 441–446, 2000.

[135] M. Grosse-Wentrup and M. Buss, “Multiclass common spatial patterns and information theoretic feature extraction,” *IEEE Trans. Biomed. Eng.*, 2008.

[136] S. Lemm, B. Blankertz, G. Curio, and K. R. Müller, “Spatio-spectral filters for improving the classification of single trial EEG,” *IEEE Trans. Biomed. Eng.*, 2005.

[137] G. Dornhege, B. Blankertz, M. Krauledat, F. Losch, G. Curio, and K. R. Müller, “Combined optimization of spatial and temporal filters for improving brain-computer interfacing,” *IEEE Trans. Biomed. Eng.*, 2006.

[138] G. Dornhege, B. Blankertz, M. Krauledat, F. Losch, G. Curio, and K.-R. Müller, “Optimizing spatio-temporal filters for improving brain-computer interfacing.”

[139] Z. J. Koles, M. S. Lazar, and S. Z. Zhou, “Spatial patterns underlying population differences in the background EEG,” *Brain Topogr.*, vol. 2, no. 4, pp. 275–284, 1990.

[140] “Common spatial pattern,” *Wikipedia*, 2017. [Online]. Available: https://en.wikipedia.org/wiki/Common_spatial_pattern#cite_note-1.

[141] C. M. Bishop, *Pattern Recognition And Machine Learning*. 2006.

[142] “Support vector machine,” *Wikipedia*, 2018. [Online]. Available: https://en.wikipedia.org/wiki/Support_vector_machine.

[143] I. Goodfellow, Y. Bengio, and A. Courville, “Deep Learning,” *Nat. Methods*, vol. 13, no. 1, pp. 35–35, 2015.

[144] M. Matsugu, K. Mori, Y. Mitari, and Y. Kaneda, “Subject independent facial expression recognition with robust face detection using a convolutional neural network.,” *Neural Netw.*, 2003.

[145] Y. LeCun, L. Bottou, Y. Bengio, and P. Haffner, “Gradient-based learning applied to document recognition,” *Proc. IEEE*, 1998.

[146] C. Szegedy, S. Ioffe, V. Vanhoucke, and A. A. Alemi, “Inception-v4, inception-ResNet and the impact of residual connections on learning,” in *31st AAAI Conference on Artificial Intelligence, AAAI 2017*, 2017.

[147] T. Elbert, C. Pantev, C. Wienbruch, B. Rockstroh, and E. Taub, “Increased Cortical Representation of the Fingers of the Left Hand in String Players,” *Science*

(80-.)., vol. 270, no. 5234, pp. 305–307, 1975.

[148] M. A. Lebedev, G. Mirabella, I. Erchova, and M. E. Diamond, “Experience-dependent Plasticity of Rat Barrel Cortex : Redistribution of Activity across Barrel-columns,” *Cereb. CORTEX*, vol. 10, no. 1, pp. 23–31, 2000.

[149] R. Chen, L. G. Cohen, and M. Hallett, “Nervous system reorganization following injury,” *Neuroscience*, vol. 111, no. 4, pp. 761–773, Jun. 2002.

[150] L. Wang *et al.*, “Dynamic functional reorganization of the motor execution network after stroke.,” *Brain*, vol. 133, no. Pt 4, pp. 1224–38, Apr. 2010.

[151] R. Colombo *et al.*, “Robotic techniques for upper limb evaluation and rehabilitation of stroke patients.,” *IEEE Trans. Neural Syst. Rehabil. Eng.*, vol. 13, no. 3, pp. 311–24, Sep. 2005.

[152] G. Fazekas, M. Horvath, and A. Toth, “A novel robot training system designed to supplement upper limb physiotherapy of patients with spastic hemiparesis.,” *Int. J. Rehabil. Res.*, vol. 29, no. 3, pp. 251–4, Sep. 2006.

[153] G. Fazekas, M. Horvath, T. Troznai, and A. Toth, “Robot-mediated upper limb physiotherapy for patients with spastic hemiparesis: a preliminary study.,” *J. Rehabil. Med.*, vol. 39, no. 7, pp. 580–2, Sep. 2007.

[154] A. C. Lo *et al.*, “Robot-Assisted Therapy for Long-Term Upper-Limb Impairment after Stroke,” *N. Engl. J. Med.*, vol. 362, no. 19, pp. 1772–1783, 2010.

[155] E. Formaggio *et al.*, “Modulation of event-related desynchronization in robot-assisted hand performance: brain oscillatory changes in active, passive and imagined movements.,” *J. Neuroeng. Rehabil.*, vol. 10, no. 1, p. 24, Jan. 2013.

[156] S. V Adamovich *et al.*, “A virtual reality based exercise system for hand rehabilitation post-stroke: transfer to function.,” *Conf. Proc. IEEE Eng. Med. Biol. Soc.*, vol. 7, no. 2, pp. 4936–4939, 2004.

[157] K. K. Ang *et al.*, “A clinical study of motor imagery-based brain-computer interface for upper limb robotic rehabilitation,” in *Engineering in Medicine and Biology Society, 2009. EMBC 2009. Annual International Conference of the IEEE*, 2009, pp. 5981–5984.

[158] M. Grosse-Wentrup, D. Mattia, and K. Oweiss, “Using brain-computer interfaces to induce neural plasticity and restore function.,” *J. Neural Eng.*, vol. 8, no. 2, p. 025004, Apr. 2011.

[159] J. Webb, Z. G. Xiao, K. P. Aschenbrenner, G. Herrnstadt, and C. Menon, “Towards a Portable Assistive Arm Exoskeleton foe stroke patient Rehabilitation Controlled Through a Brain Computer Interface,” in *The Fourth IEEE RAS/EMBS International Conference on Biomedical Robotics and Biomechatronics*, 2012, pp. 1299–1304.

[160] A. Ramos-Murguialday *et al.*, “Proprioceptive Feedback and Brain Computer Interface (BCI) Based Neuroprostheses,” *PLoS One*, vol. 7, no. 10, p. e47048, 2012.

[161] A. Caria *et al.*, “Chronic stroke recovery after combined BCI training and physiotherapy: a case report.,” *Psychophysiology*, vol. 48, no. 4, pp. 578–82, Apr. 2011.

[162] K. O. Babalola, “Brain-Computer Interfaces for Inducing Brain Plasticity and Motor Learning : Implications for Brain-Injury Rehabilitation,” Georgia Institute of Technology, Atlanta, Georgia, 2011.

[163] O. Falzon, K. P. Camilleri, and J. Muscat, “The analytic common spatial patterns method for EEG-based BCI data,” *J. Neural Eng.*, vol. 9, p. 045009, 2012.

[164] F. Lotte *et al.*, “A review of classification algorithms for EEG-based brain-computer interfaces: A 10 year update,” *J. Neural Eng.*, vol. 15, no. 3, p. 031005, Jun. 2018.

[165] F. Lotte *et al.*, “A Review of Classification Algorithms for EEG-based Brain-Computer Interfaces: A 10-year Update,” *J. Neural Eng.*, pp. 0–20, 2018.

[166] A. Kachenoura, L. Albera, L. Senhadji, and P. Comon, “Ica: a potential tool for bci systems,” *IEEE Signal Process. Mag.*, 2008.

[167] K. K. Ang, Z. Y. Chin, C. Wang, C. Guan, and H. Zhang, “Filter bank common spatial pattern algorithm on BCI competition IV datasets 2a and 2b,” *Front. Neurosci.*, vol. 6, no. MAR, pp. 1–9, 2012.

[168] I. Koprinska, “Feature Selection for Brain-Computer Interfaces,” in *Pacific-Asia conference on knowledge discovery and data mining.*, 2009, pp. 106–117.

[169] “American Electroencephalographic Society Guidelines for Standard Electrode Position Nomenclature1,” *J. Clin. Neurophysiol.*, 1991.

[170] G. Schalk, D. J. McFarland, T. Hinterberger, N. Birbaumer, and J. R. Wolpaw, “BCI2000: a general-purpose brain-computer interface (BCI) system,” *Biomed. Eng. IEEE Trans.*, vol. 51, no. 6, pp. 1034–1043, 2004.

[171] A. Delorme *et al.*, “EEGLAB, SIFT, NFT, BCILAB, and ERICA: new tools for advanced EEG processing.,” *Comput. Intell. Neurosci.*, vol. 2011, p. 130714, Jan. 2011.

[172] A. Aggarwal, “Comparison of the Folstein Mini Mental State Examination (MMSE) to the Montreal Cognitive Assessment (MoCA) as a Cognitive Screening Tool in an Inpatient Rehabilitation Setting,” *Neurosci. Med.*, vol. 01, no. 02, pp. 39–42, 2010.

[173] D. A. Jones, B. Bigland-Ritchie, and R. H. T. Edwards, “Excitation frequency and muscle fatigue: Mechanical responses during voluntary and stimulated

contractions," *Exp. Neurol.*, vol. 64, no. 2, pp. 401–413, 1979.

[174] K. K. Ang *et al.*, "A Large Clinical Study on the Ability of Stroke Patients to Use an EEG-Based Motor Imagery Brain-Computer Interface," *Clin. EEG Neurosci.*, vol. 42, no. 4, pp. 253–258, 2011.

[175] C. Neuper, R. Scherer, M. Reiner, and G. Pfurtscheller, "Imagery of motor actions: Differential effects of kinesthetic and visual–motor mode of imagery in single-trial EEG," *Cogn. Brain Res.*, vol. 25, no. 3, pp. 668–677, 2005.

[176] K. Christian Andreas and M. Scott, "BCILAB: a platform for brain–computer interface development," *J. Neural Eng.*, vol. 10, no. 5, p. 56014, 2013.

[177] G. Pfurtscheller and C. Neuper, "Motor imagery and direct brain- computer communication," *Proc. IEEE*, vol. 89, no. 7, pp. 1123–1134, 2001.

[178] Kai Keng Ang, Zheng Yang Chin, Haihong Zhang, and Cuntai Guan, "Filter Bank Common Spatial Pattern (FBCSP) in Brain-Computer Interface," in *2008 IEEE International Joint Conference on Neural Networks (IEEE World Congress on Computational Intelligence)*, 2008, pp. 2390–2397.

[179] G. Pfurtscheller and C. Neuper, "Motor imagery and direct brain-computer communication," *Proc. IEEE*, vol. 89, no. 7, pp. 1123–1134, 2001.

[180] R. Tomioka and M. Sugiyama, "Dual-augmented lagrangian method for efficient sparse reconstruction," *IEEE Signal Process. Lett.*, 2009.

[181] R. Tomioka and K. R. Müller, "A regularized discriminative framework for EEG analysis with application to brain-computer interface," *Neuroimage*, 2010.

[182] J. Schäfer and K. Strimmer, "A Shrinkage Approach to Large-Scale Covariance Matrix Estimation and Implications for Functional Genomics," *Stat. Appl. Genet. Mol. Biol.*, vol. 4, no. 1, 2005.

[183] R. Tomioka and K. R. Müller, "A regularized discriminative framework for EEG analysis with application to brain-computer interface," *Neuroimage*, vol. 49, no. 1, pp. 415–432, 2010.

[184] Y. Hochberg and A. C. Tamhane, "Multiple Comparison Procedures," *Wiley Ser. Probab. Stat.*, vol. 312, no. 5, pp. 2014–2015, 1987.

[185] G. R. Müller-putz, R. Scherer, C. Brunner, R. Leeb, and G. Pfurtscheller, "Better than random ? A closer look on BCI results," *Int. Jouranl Bioelectromagn.*, vol. 10, no. 1, pp. 52–55, 2008.

[186] M. Jeannerod, "Mental imagery in the motor context," *Neuropsychologia*, vol. 33, no. 11, pp. 1419–1432, 1995.

[187] E. B. Plow, P. Arora, M. A. Pline, M. T. Binenstock, and J. R. Carey, "Within-limb somatotopy in primary motor cortex - revealed using fMRI," *Cortex*, vol. 46, no. 3,

pp. 310–321, 2010.

[188] L. Fogassi and G. Luppino, “Motor functions of the parietal lobe,” *Current Opinion in Neurobiology*, vol. 15, no. 6. pp. 626–631, 2005.

[189] B. Lew, N. Alavi, B. K. Randhawa, and C. Menon, “An Exploratory Investigation on the Use of Closed-Loop Electrical Stimulation to Assist Individuals with Stroke to Perform Fine Movements with Their Hemiparetic Arm.,” *Front. Bioeng. Biotechnol.*, vol. 4, no. March, p. 20, 2016.

[190] B. Kim and A. D. Deshpande, “An upper-body rehabilitation exoskeleton Harmony with an anatomical shoulder mechanism: Design, modeling, control, and performance evaluation,” *Int. J. Rob. Res.*, vol. 36, no. 4, pp. 414–435, 2017.

[191] Z. G. Xiao, A. M. Elnady, J. Webb, and C. Menon, “Towards a brain computer interface driven exoskeleton for upper extremity rehabilitation,” in *5th IEEE RAS/EMBS International Conference on Biomedical Robotics and Biomechatronics*, 2014, pp. 432–437.

[192] X. Zhang, A. M. Elnady, B. K. Randhawa, L. A. Boyd, and C. Menon, “Combining Mental Training and Physical Training With Goal-Oriented Protocols in Stroke Rehabilitation: A Feasibility Case Study,” *Front. Hum. Neurosci.*, vol. 12, 2018.

[193] M. J. A. M. van Putten, “The revised brain symmetry index,” *Clin. Neurophysiol.*, vol. 118, no. 11, pp. 2362–2367, 2007.

[194] K. Lin, Y. Hsieh, C. Wu, C. Chen, Y. Jang, and J. Liu, “Minimal Detectable Change and Clinically Important Difference of the Wolf Motor Function Test in Stroke Patients,” *Neurorehabil. Neural Repair*, vol. 23, no. 5, pp. 429–434, 2009.

[195] F. Chollet, V. DiPiero, R. J. Wise, D. J. Brooks, R. J. Dolan, and R. S. Frackowiak, “The functional anatomy of motor recovery after stroke in humans: a study with positron emission tomography.,” *Ann. Neurol.*, vol. 29, no. 1, pp. 63–71, 1991.

[196] C. Weiller, F. Chollet, K. J. Friston, R. J. S. Wise, and R. S. J. Frackowiak, “Functional reorganization of the brain in recovery from striatocapsular infarction in man,” *Ann. Neurol.*, vol. 31, no. 5, pp. 463–472, 1992.

[197] M. D. Caramia, C. Iani, and G. Bernardi, “Cerebral plasticity after stroke as revealed by ipsilateral responses to magnetic stimulation,” *Neuroreport*, vol. 7, no. 11, pp. 1756–1760, 1996.

[198] M. Honda, T. Nagamine, H. Fukuyama, Y. Yonekura, J. Kimura, and H. Shibasaki, “Movement-related cortical potentials and regional cerebral blood flow change in patients with stroke after motor recovery,” *J. Neurol. Sci.*, vol. 146, no. 2, pp. 117–126, 1997.

[199] S. C. Cramer *et al.*, “A Functional MRI Study of Subjects Recovered From Hemiparetic Stroke,” *Stroke*, vol. 28, no. 12, pp. 2518–2527, 1997.

[200] Y. Cao, L. D'Olhaberriague, E. M. Vikingstad, S. R. Levine, and K. M. A. Welch, "Pilot study of functional MRI to assess cerebral activation of motor function after poststroke hemiparesis," *Stroke*, vol. 29, no. 1, pp. 112–122, 1998.

[201] M. L. Cuadrado, J. a Egido, J. L. González-Gutiérrez, and E. Varela-De-Seijas, "Bihemispheric contribution to motor recovery after stroke: A longitudinal study with transcranial doppler ultrasonography.," *Cerebrovasc. Dis.*, vol. 9, no. 6, pp. 337–44, 1999.

[202] D. M. Morris, G. Uswatte, J. E. Crago, E. W. Cook, and E. Taub, "The reliability of the wolf motor function test for assessing upper extremity function after stroke," *Arch. Phys. Med. Rehabil.*, vol. 82, no. 6, pp. 750–755, 2001.

[203] P. Belardinelli, L. Laer, E. Ortiz, C. Braun, and A. Gharabaghi, "Plasticity of premotor cortico-muscular coherence in severely impaired stroke patients with hand paralysis," *NeuroImage Clin.*, vol. 14, pp. 726–733, 2017.

[204] D. M. W. POWERS, "Evaluation: From Precision, Recall and F-Measure To Roc, Informedness, Markedness & Correlation," *J. Mach. Learn. Technol.*, 2011.

[205] Y. Sasaki, "The truth of the F-measure," *Teach Tutor mater*, 2007.

[206] E. K. Vanhoutte *et al.*, "Modifying the Medical Research Council grading system through Rasch analyses," *Brain*, vol. 135, no. 5, pp. 1639–1649, 2012.

[207] N. Lu, T. Li, X. Ren, and H. Miao, "A Deep Learning Scheme for Motor Imagery Classification based on Restricted Boltzmann Machines," *IEEE Trans. Neural Syst. Rehabil. Eng.*, vol. 25, no. 6, pp. 566–576, 2017.

[208] D. F. Wulsin, J. R. Gupta, R. Mani, J. A. Blanco, and B. Litt, "Modeling electroencephalography waveforms with semi-supervised deep belief nets: fast classification and anomaly measurement.," *J. Neural Eng.*, vol. 8, no. 3, p. 036015, 2011.

[209] M. Längkvist, L. Karlsson, and A. Loutfi, "Sleep Stage Classification Using Unsupervised Feature Learning," *Adv. Artif. Neural Syst.*, 2012.

[210] T. Ma *et al.*, "The extraction of motion-onset VEP BCI features based on deep learning and compressed sensing," *J. Neurosci. Methods*, 2017.

[211] R. T. Schirrmeister *et al.*, "Deep learning with convolutional neural networks for brain mapping and decoding of movement-related information from the human EEG," *arXiv*, 2017.

[212] P. Mirowski, D. Madhavan, Y. LeCun, and R. Kuzniecky, "Classification of patterns of EEG synchronization for seizure prediction," *Clin. Neurophysiol.*, 2009.

[213] P. Thodoroff, J. Pineau, and A. Lim, "Learning Robust Features using Deep Learning for Automatic Seizure Detection," Jul. 2016.

[214] A. Page, C. Shea, and T. Mohsenin, “Wearable seizure detection using convolutional neural networks with transfer learning,” in *Proceedings - IEEE International Symposium on Circuits and Systems*, 2016.

[215] J. Liang, R. Lu, C. Zhang, and F. Wang, “Predicting Seizures from Electroencephalography Recordings: A Knowledge Transfer Strategy,” in *Proceedings - 2016 IEEE International Conference on Healthcare Informatics, ICHI 2016*, 2016.

[216] A. Antoniades, L. Spyrou, C. C. Took, and S. Sanei, “Deep learning for epileptic intracranial EEG data,” in *IEEE International Workshop on Machine Learning for Signal Processing, MLSP*, 2016.

[217] H. Cecotti and A. Gräser, “Convolutional neural networks for P300 detection with application to brain-computer interfaces,” *IEEE Trans. Pattern Anal. Mach. Intell.*, 2011.

[218] H. Cecotti, M. P. Eckstein, and B. Giesbrecht, “Single-trial classification of event-related potentials in rapid serial visual presentation tasks using supervised spatial filtering,” *IEEE Trans. Neural Networks Learn. Syst.*, 2014.

[219] R. Manor and A. B. Geva, “Convolutional Neural Network for Multi-Category Rapid Serial Visual Presentation BCI,” *Front. Comput. Neurosci.*, 2015.

[220] J. Shamwell, H. Lee, H. Kwon, A. R. Marathe, V. Lawhern, and W. Nothwang, “Single-trial EEG RSVP classification using convolutional neural networks,” in *Micro- and Nanotechnology Sensors, Systems, and Applications VIII*, 2016.

[221] S. Stober, D. J. Cameron, and J. a Grahn, “Using Convolutional Neural Networks to Recognize Rhythm Stimuli from Electroencephalography Recordings,” *Neural Inf. Process. Syst. 2014*, 2014.

[222] S. Stober, A. Sternin, A. M. Owen, and J. A. Grahn, “Deep Feature Learning for EEG Recordings,” Nov. 2015.

[223] D. J. Gladstone, C. J. Danells, and S. E. Black, “The Fugl-Meyer Assessment of Motor Recovery after Stroke: A Critical Review of Its Measurement Properties,” *Neurorehabilitation and Neural Repair*, vol. 16, no. 3. pp. 232–240, 2002.

[224] S. Kim, J. Lee, and L. Kim, “ERS differences between stroke patients and healthy controls after hand movement,” *4th Int. Winter Conf. Brain-Computer Interface, BCI 2016*, 2016.

[225] N. Carson, L. Leach, and K. J. Murphy, “A re-examination of Montreal Cognitive Assessment (MoCA) cutoff scores,” *Int. J. Geriatr. Psychiatry*, 2017.

[226] V. Kaiser, I. Daly, F. Pichiorri, D. Mattia, G. R. Müller-Putz, and C. Neuper, “Relationship between electrical brain responses to motor imagery and motor impairment in stroke,” *Stroke*, vol. 43, no. 10, pp. 2735–2740, 2012.

[227] G. Pfurtscheller, C. Brunner, A. Schlögl, and F. H. Lopes da Silva, “Mu rhythm (de)synchronization and EEG single-trial classification of different motor imagery tasks,” *Neuroimage*, vol. 31, no. 1, pp. 153–159, 2006.

[228] M. Alt Murphy, C. Willén, and K. S. Sunnerhagen, “Relationships between kinematics of upper extremity movements and impairment severity as well activity limitations after stroke,” *Physiother. (United Kingdom)*, vol. 97, pp. eS63–eS64, 2011.

[229] M. L. Woodbury, C. A. Velozo, L. G. Richards, and P. W. Duncan, “Rasch analysis staging methodology to classify upper extremity movement impairment after stroke,” *Arch. Phys. Med. Rehabil.*, vol. 94, no. 8, pp. 1527–1533, 2013.

[230] K. He, X. Zhang, S. Ren, and J. Sun, “Deep Residual Learning for Image Recognition,” *2016 IEEE Conf. Comput. Vis. Pattern Recognit.*, pp. 770–778, 2016.

[231] C. Szegedy, V. Vanhoucke, S. Ioffe, J. Shlens, and Z. Wojna, “Rethinking the Inception Architecture for Computer Vision,” 2015.

[232] F. Chollet, “Keras,” *GitHub Repos.*, 2015.

[233] Tensorflow, “TensorFlow,” *2018*. 2018.

[234] Apache Spark, “Apache Spark™ - Lightning-Fast Cluster Computing,” *Spark.Apache.Org*, 2015. [Online]. Available: http://spark.apache.org/.

[235] D.-A. D.-A. Clevert, T. Unterthiner, and S. Hochreiter, “Fast and Accurate Deep Network Learning by Exponential Linear Units (ELUs),” *arXiv*, pp. 1–14, Nov. 2015.

[236] J. Bergstra, R. Bardenet, Y. Bengio, and B. Kégl, “Algorithms for Hyper-Parameter Optimization,” in *Advances in Neural Information Processing Systems (NIPS)*, 2011, pp. 2546–2554.

[237] C. C. Aggarwal, *Neural networks and deep learning : a textbook*. 2018.